KU LEUVEN

FACULTEIT INGENIEURSWETENSCHAPPEN

Quantifying the Flexibility of Residential Electricity Demand in 2050 Through Price Elasticities: a Bottom-up Approach

Jonas Engels
Dries Guldentops

Thesis voorgedragen tot het behalen van de graad van Master of Science in de ingenieurswetenschappen: energie

Promotor:
Prof. dr. ir. Geert Deconinck

Assessoren:
Prof. dr. ir. Ronnie Belmans
Prof. dr. ir. Gerrit Jan Schaeffer

Begeleider:
ir. Arne van Stiphout

Academiejaar 2013 – 2014

Preface

A sustainable energy supply is something that concerns all of us. However, an enormous change in mentality will be needed in order to succeed. Technically, there are a lot of possibilities that facilitate this, but the question of cost remains. With this thesis we hope to be able to contribute at least slightly to this objective.

We are proud to present our thesis as the final step in our career at the KU Leuven. We would like to thank our promotor, prof. dr. ir. Geert Deconinck and our mentor ir. Arne van Stiphout. Their insights and valuable input have been a great help to our thesis research. Making this thesis under their supervision has been a pleasure to us. We would like to thank ir. Sandro Iacovella for providing the necessary data and models and ir. Benjamin Dupont for his useful comments on the statistics in this thesis text. We thank Veronica Lucia Ortega for providing the necessary licenses and access to several servers.

We would like to thank our assessors, prof. dr. ir. Ronnie Belmans and prof. dr. ir. Gerrit Jan Schaeffer for their presence at the presentations and for reading our thesis text.

Next, we would like to thank those close to us. I thank my girlfriend, Elise, for her unconditional support. Furthermore, we thank our good friends and family.

Finally, we would like to thank the KU Leuven for these wonderful past five years. Especially, we want to thank EBIB Leuven for its facilities, where we spent many hours developing the content of this thesis text.

Jonas Engels
Dries Guldentops

Contents

Abstract

Global warming leads to a growing awareness that greenhouse gas emissions should be strongly reduced. To accomplish this, an increasing share of intermittent renewables is being integrated in the electricity network. The intermittent character of these sources demands a high degree of flexibility of the power system. With the advent of smart grids a new form of flexibility becomes available, namely the active participation of the demand side. A major challenge for the power system operator is to schedule this new flexibility ex-ante in the market. To be able to do this, this flexibility has to be quantified. In this thesis, a method is developed to quantify this flexibility for the residential sector through price elasticities, using a bottom-up approach. This is applied to Belgium, for a fully electrified, de-carbonized society in 2050.

Three types of flexible devices are considered: heating (heat pumps and electric heaters), electric vehicles and wet appliances (washing machine, dishwasher and tumble dryer). These appliances are grouped into houses according to their expected penetration rates. A household receives a varying price signal and automatically optimizes the energy consumption of its flexible devices towards minimal electricity cost, with regard to user constraints. In order to correctly represent the population structure and the penetration rates of the devices, houses are grouped together in neighbourhoods. Regarding such a neighbourhood, each price signal yields a corresponding electricity consumption pattern. In this thesis, a linear relationship is determined between a relative change of a price signal and a relative change in electricity consumption regarding a reference scenario. This yields price elasticities for a specific neighbourhood. A selective regression is applied which enables to determine the time interval in which price changes have an influence on the demand. By performing a Monte Carlo simulation, the characteristics of an average neighbourhood can be determined. This allows to scale up the results to the level of a country. The Monte Carlo simulation is performed for the four different seasons and both weekdays and weekends to assess their influence on the flexibility.

The annual electricity consumption that results from our model increases by a factor of 2 compared to the current one, due to the full electrification. The peak power consumption can increase by a factor 5 to 8 (depending on the season) due to load syncing and the new loads (heat pumps and EVs). The elasticity matrices point out that the most flexibility is available in winter and the least in summer. The maximum time that demand is shifted is found to be seven hours. Most flexibility originates from the heaters. EVs mainly provide flexibility at night, while wet appliances do not contribute much to the available flexibility.

Samenvatting

De opwarming van de aarde leidt tot een groeiende bewustwording dat de uitstoot van broeikasgassen sterk verminderd moet worden om de globale temperatuurstijging te beperken. Dit zorgt ervoor dat het aandeel van fluctuerende hernieuwbare energiebronnen in de elektriciteitsproductie toeneemt. Opdat het elektriciteitssysteem zou kunnen omgaan met deze onvoorspelbare, variërende energiebronnen heeft het een grote graad van flexibiliteit nodig. Door het ontwikkelen van nieuwe concepten als *slimme elektriciteitsnetwerken* ontstaan er nieuwe manieren om in deze nood aan flexibiliteit te voorzien, zoals de actieve deelname van de vraagzijde op de elektriciteitsmarkt. De netwerkbeheerder staat hier voor de grote uitdaging om deze flexibiliteit vooraf in de markt in te plannen. Zo kan bijvoorbeeld het gebruik van dure piekcentrales worden vermeden. Om dit mogelijk te maken moet deze flexibiliteit echter eerst bepaald en gekwantificeerd worden. In deze thesis wordt een methode ontwikkeld om de flexibiliteit van de residentiële vraagzijde te kwantificeren door middel van prijselasticiteiten m.b.v. een *bottom-up* aanpak. Deze methode wordt dan toegepast op een volledig geëlektrificeerde, CO_2-vrije maatschappij in 2050 voor België.

Deze thesis bestaat uit twee delen, namelijk 1) de modellering van de verschillende flexibele apparaten en de optimalisatie van hun elektriciteitsverbruik met het oog op kostenminimalisatie, en 2) het bepalen van de prijselasticiteiten met behulp van statistische methodes gebruik makende van de resultaten van voorgaande optimalisaties. Drie types van flexibele apparaten zijn geïmplementeerd: verwarming (d.m.v. warmtepompen en elektrische bijverwarming), elektrische voertuigen en witgoedtoestellen (wasmachines, droogkasten en vaatwassers). Deze apparaten worden samen gegroepeerd in huizen, rekening houdend met hun verwachte penetratiegraad. Elk huishouden krijgt een variërende elektriciteitsprijs doorgestuurd (bv. één dag op voorhand). Het elektriciteitsverbruik van hun flexibele apparaten wordt dan zo gepland zodat de elektriciteitskost minimaal is voor de verbruiker. Om een correcte weergave te krijgen van de bevolkingsstructuur en van de penetratiegraden van de verschillende apparaten worden huizen per 70 gegroepeerd in een wijk. Een wijk heeft voor elk prijssignaal een overeenkomstig elektriciteitsverbruik. In deze thesis wordt gezocht naar een lineair verband tussen een relatieve prijsverandering en een relatieve verandering in elektriciteitsverbruik voor een wijk, ten opzichte van een referentiescenario. Dit verband wordt gelegd m.b.v. lineaire regressies. De resultaten van deze regressies leiden dan tot de gezochte prijselasticiteiten voor een specfieke wijk. Deze prijselasticiteiten worden gegroepeerd in een 'elasticiteitenmatrix'. De dia-

gonaal van deze matrix bevat de eigen prijselasticiteiten per uur, de waarden buiten de diagonaal worden kruiselasticiteiten genoemd. De eigen prijselasticiteiten drukken het verband uit tussen de procentuele verandering van de prijs op een bepaald uur en de procentuele verandering in elektriciteitsverbruik op hetzelfde uur. Deze eigen elasticiteiten zijn doorgaans negatief. De kruiselasticiteiten drukken het verband uit tussen de procentuele verandering van de prijs op een bepaald uur en de procentuele verandering in elektriciteitsverbruik op ander uur. Deze zijn in het algemeen positief, met grote waarden nabij de diagonaal en kleinere waarden verder van de diagonaal. Verder wordt er een selectieve regressie toegepast om op een statistische manier het tijdsinterval te bepalen waarbinnen een verandering van de elektriciteitsprijs effect heeft op het elektriciteitsverbruik. Aangezien elke wijk is opgebouwd uit verschillende stochastische elementen (penetratiegraden van apparaten, bezetting van huizen, enz.), kunnen de karakteristieken van een 'gemiddelde' wijk bepaald worden via een Monte Carlo simulatie. De bekomen resultaten van een gemiddelde wijk kunnen dan worden opgeschaald naar het niveau van een regio of een land, in deze thesis toegepast op België. De Monte Carlo simulatie wordt uitgevoerd voor de vier verschillende seizoenen, zowel voor weekdagen als weekenddagen om de invloed op de flexibiliteit na te gaan.

Het gemiddeld jaarlijks elektriciteitsverbruik volgens het model in deze thesis verdubbelt t.o.v. de huidige residentiële elektriciteitsvraag. Dit is vooral te wijten aan de volledige elektrificatie. Verwarming en transport gebeuren nu immers vooral met fossiele brandstoffen, waar ze in ons model nieuwe elektrische lasten vormen met warmtepompen en elektrische voertuigen. Het piekvermogen neemt toe met een factor 5 tot 8, afhankelijk van het seizoen. Dit komt wederom door de nieuwe elektrische lasten en door de prijsstrategie die ervoor zorgt dat zoveel mogelijk lasten naar hetzelfde (goedkope) moment worden verschoven. De prijselasticiteiten tonen aan dat er in de winter het meeste flexibiliteit voorhanden is en in de zomer het minste. Dit is voornamelijk te wijten aan de belangrijke bijdrage van de elektrische verwarmingsapparaten tot de flexibiliteit. De grootste tijdspanne waarin een prijsverandering invloed heeft op de vraag volgens ons model is zeven uur. Dit wil zeggen dat (een deel van) de elektriciteitsvraag maximaal zeven uur verschoven wordt in de tijd t.o.v. zijn originele verbruikstijdstip bij de referentieprijs. De meeste flexibiliteit die beschikbaar is komt van de verwarmingsapparaten. Deze varieert zoals eerder gezegd naargelang het seizoen. Elektrische voertuigen zorgen ook voor een aanzienlijk deel van de totale flexibiliteit, voornamelijk tijdens de nacht. Witgoedtoestellen leveren een eerder beperkte bijdrage.

De bekomen elasticiteitsmatrices kunnen in een verdere stap gebruikt worden in een *unit commitment* model om de flexibele vraag mee te plannen in de elektriciteitsvoorziening.

List of Figures and Tables

List of Figures

List of Tables

List of Abbreviations and Symbols

Abbreviations

AUX	Auxiliary heater
COP	Coefficient of Performance
DER	Distributed Energy Resources
DHW	Domestic Hot Water
DLC	Direct Load Control
DR	Demand Response
DSM	Demand Side Managment
DW	dishwasher
EV	Electric Vehicle
HVAC	Heating, Ventilation and Air Conditioning
HP	Heat pump
IBP	Incentive Based Program
NH	Neighbourhood
PBP	Priced Based Program
PEM	Price Elasticity Matrix
PV	Photovoltaic
RTP	Real Time Pricing
RES	Renewable Energy Sources
SH	Space Heating
SLP	Synthetic Load Profile
SOC	State of Charge
TCL	Thermostatic Controlled Load
TOU	Time of Use
TD	Tumble dryer
V2G	Vehicle-to-grid
WA	Wet Appliances
WM	Washing Machine

Symbols

$\langle \cdot \rangle$	Population mean
$\bar{\cdot}$	Sample mean
α	Coefficient
Δ	Relative change
ϵ_{ij}	Price elasticity
$\boldsymbol{\epsilon_i}$	Price elasticity vector for electricity consumption at hour i
$\epsilon_{N\times N}$	Price elasticity matrix of size N
η^a	Efficiency of a
σ	Standard deviation
cap	Battery capacity
E_j^{req}	Energy required by the EV at time step j
err_i^k	Error of the linear model on time step i and the k$^{\text{th}}$ sample
$F(a,b)$	F-distribution with a and b degrees of freedom
H_0	null hypothesis
MS_{err}	Mean sum of squares of the error
MS_{reg}	Mean sum of squares of the regression model
n	Number of samples used
N	Time horizon
N_m	Number of Monte Carlo simulations
p	Price vector
p_j^k	Price of the k$^{\text{th}}$ sample at time step j
$P^{a,b}$	Electric power delivered by a to b
$\dot{Q}^{a,b}$	Thermal power delivered by a to b
q	Electricity consumption vector
q_j^k	Electricity demand of the k$^{\text{th}}$ sample at time step j
s^2	Sample variance
SS_{err}	Sum of squares of the error
SS_{reg}	Sum of squares of the regression model
T_j^{place}	Temperature of a certain place at time step j
x_j^b	Dummy variable

Chapter 1

Introduction

1.1 Context

In order to limit the global temperature rise to an average of 2°C, the leaders of the European Union and the G8 announced in July 2009 their objective to reduce greenhouse gas emissions at least 80% below 1990 levels by 2050 [1]. This is in accordance with the 450 ppm scenario of the 4th Assessment Report of the International Panel on Climate Change (IPCC). The European Commission translated this objective into two separate roadmaps: the Energy Roadmap 2050 [2] and the roadmap for moving to a low-carbon economy in 2050 [3], both implying near carbon neutrality for the power sector in 2050. Several major stakeholders in the energy sector have issued studies, either predating or following the Commissions roadmaps, with the goal of establishing scenarios for reaching this low-carbon energy system by 2050. Influential examples, besides the two aforementioned roadmaps, include the Power Choices study by Eurelectric [4], the Roadmap 2050 study by the European Climate Foundation [1] and the Energy [r]evolution study by Greenpeace [5]. In the outcome of these studies, as a result of the emissions constraint, a significant share of the electricity production in 2050 comes from Renewable Energy Sources (RES). To cope with these intermittent sources and to be able to balance electricity supply and demand, the electric power system will need to possess a high degree of operational flexibility. Fig. 1.1 summarizes the different tools of flexibility of which an operator disposes. Nowadays, flexibility is mostly provided by conventional (peak) power units and power exchange, although energy storage in the form of pumped hydro is also used extensively in some countries. Currently, demand side management (DSM) is mainly applied in the industry, and mostly in the form of ancillary services. In the future, especially with the advent of *smart grids*, this form of flexibility is expected to increase in importance, and is expected to also incorporate residential demand. In this thesis we will focus on the flexibility that can be obtained through DSM.

Our thesis is situated in the context of a project [7] at KU Leuven, which investigates whether it is possible to supply all end energy as demanded by the overall society without emitting any greenhouse gases by 2050. The vision in this study is a dominantly electric society at the end-consumer level, wherever possible.

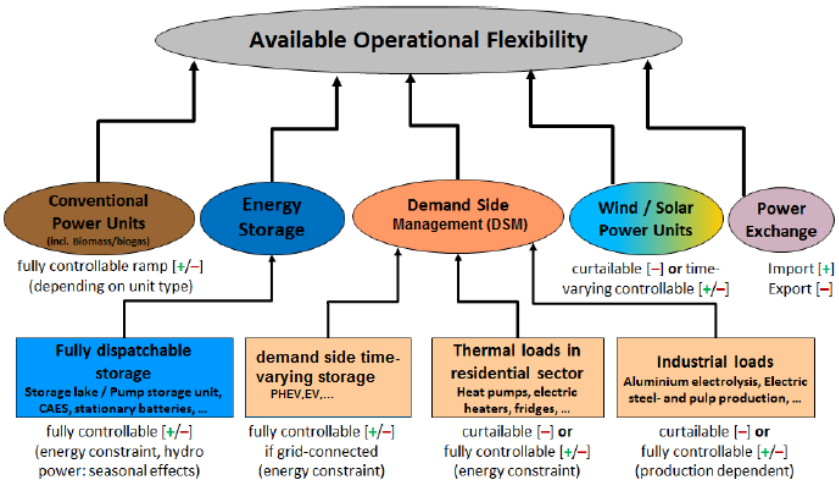

Fig. 1.1: Different forms of operational flexibility in power systems [6]

Consequently, in this thesis we assume that the energy system is 100 % carbon-neutral. This means e.g. that common energy consuming devices like gas boilers and passenger cars, which currently use fossil fuels to function, will be substituted by electric heat pumps and electric vehicles.

DSM is a corner stone of the aforementioned study and will be the field on which we will focus in this thesis. Through DSM, a certain amount of *flexibility* can be provided by the end-consumers. This flexibility should be quantified such that the system operator has an idea of the amount of available flexibility at a given time and of the corresponding costs. The aforementioned studies, as well as many others, have integrated this flexibility using a top-down approach (see section 2.4.1) in which a presumed percentage of the energy demand can be shifted. Since this is a very coarse approximation, it leaves some obvious room for improvement. In this thesis we will develop a method which allows to quantify the amount of flexibility available at each moment more accurately.

Since the purpose of this quantification is integration into other linear models that are part of the project [7], an important constraint is that the flexibility has to be quantified in a linear way.

1.2 Problem Statement

In this section we will narrow down the subject of this thesis in order to define more precisely the general problem. This problem was stated as: *quantifying the flexible electricity demand in 2050*. We refer to chapter 2 for a more in-depth discussion about relevant topics and an extensive justification on the choices we made.

In order to really empower the potential of demand side flexibility, a smart grid environment is needed. Within such a smart grid, several mechanisms, or demand response (DR) programs, exist to address the flexibility of the demand. Of

these DR programs, many economists believe that real time pricing (RTP) is the most effective [8]. Also, we believe that RTP will free up the most flexibility as this is the most advanced pricing mechanism. Therefore, we decided to implement this mechanism in our thesis.

In this thesis, we will only consider the flexibility of the *residential* electricity demand. Numerous devices are suitable to participate in a DR program. The ones that we considered to be suited for our purposes are:

- Heat pumps and electric auxiliary heaters
- Electric vehicles
- Washing machines, dishwashers and tumble dryers

Flexibility can be represented in different manners. Since we had to keep our model linear, and because of the direct link with an RTP program, we chose to quantify the flexibility by determining price elasticities. Besides, determining price elasticities in a smart grid context is still a research gap [9].

These price elasticities can be used to estimate the effect of price changes on the residential electricity demand. This could be employed in some kind of unit commitment model that schedules generation while taking into account this flexible demand. This should result in new prices that incorporate the effects of this flexible demand.

It is important to realize that some concepts often discussed in the context of demand response or smart grids are **not** incorporated in this thesis:

- We are investigating the full potential of residential electric flexibility. Therefore, we have considered the future distribution grid as if it would have been designed to facilitate this full potential. Grid constraints are thus not taken into account.
- This also means that e.g. load syncing is not punished in our model. At moments with a lot of renewable production, it might be desired to schedule as many loads as possible at a same moment. Peak shaving is not necessarily the purpose.
- We do not assume that electricity demand influences the price. The price signal received by the houses should already incorporate the effect of the flexible demand.

1.3 Goals of the Thesis

In this thesis, we aim to quantify the residential electric flexibility in 2050. Several DR programs exist to create this flexibility and flexibility can be modelled in different manners, as will be discussed in chapter 2. As the results of our research will be used as input in a linear model, an important constraint was the linearity of our model. Therefore, we decided to represent flexibility by price elasticity matrices (see section 2.4.3) and an RTP program. This flexibility will be quantified using a bottom-up

approach, which allows taking the technical characteristics of the different flexible devices into account.

In order for this thesis to succeed and to attain the stated target, some research questions will need to be answered. The main research question is:

> ***What is the potential for flexibility of residential electricity demand in 2050 when taking into account the technical characteristics of devices?***

This question cannot be answered immediately. Some sub questions can be raised to help answering the main research question:

1. Which devices are considered as 'flexible' and how to model them?
2. In which way do we represent the so called 'flexibility'?
3. What influences the amount of flexibility available?
4. What is the absolute minimum and maximum amount of this flexibility?
5. What is the time interval in which demand is shifted?
6. What is the influence of each separate device on the flexibility?
7. How sensitive are the results to an increase/decrease in devices' penetration rates?

These questions will be answered during the course of this thesis text and will help to draw some general conclusions.

1.4 Main Contributions

Flexibility can be represented by different modelling approaches. Most of the approaches found in the literature model either only one type of flexible device [10,11] or use an economic approach without considering the technical characteristics of the devices [12]. This thesis aims to combine the best of both worlds, using a bottom-up approach to quantify price elasticities of electricity demand. In more detail, our main contributions are:

- An object-oriented model programmed in MATLAB combining separate models of different flexible devices in one overall optimization problem. This was written in such a way that it could be easily adapted and extended. The model takes into account different stochastic parameters like e.g. penetration rates, occupancy, etc. It also allows to capture the interaction between the different devices. The model and some results of the optimization are presented in chapter 3.

- A way to calculate price elasticity matrices taking into account the technical characteristics of devices. The price elasticities in this thesis are determined by performing linear regressions on the data obtained by the optimizations. By performing a selective linear regression we are able to give a statistical interpretation of the time span in which a price change influences demand.
- In order to obtain results that are not specific to a certain configuration, we performed a Monte Carlo simulation. This allows to calculate averages of the results independent of a specific configuration. The results of these Monte Carlo simulations can then be scaled up to a Belgian level or another region.

1.5 Structure of the Text

In this section we give a brief overview of the structure of this thesis text.

Chapter 2 gives an extensive overview of the studied literature. In this chapter, we point out current gaps in research and synthesize the elements that we will use further on in this thesis. Also, we justify the choices we made to set up our model as used in later chapters.

Chapter 3 describes the modelling of flexible demand. First, we describe the separate models of all considered devices. Then, these devices are grouped together into houses according to their penetration rates. Each household is subject to the same RTP signal and its flexible energy consumption is optimized towards minimal electricity cost, subject to user constraints. The mathematical rigour of the mixed-integer problem is elaborated and demonstrated by examples.

In chapter 4 we build on this model and perform regressions in order to quantify the own- and cross-price elasticities. As our model contains several stochastic elements, we repeat this process using a Monte Carlo simulation to estimate the averages and the distribution of these elasticities. This allows scaling up the results to a whole region or country.

In chapter 5 we discuss the results of this bottom-up approach. The separate influences of the different devices are determined, and the seasonal impact is discussed. Furthermore, a sensitivity analysis on the penetration rate of EVs is performed.

Finally, in chapter 6, we draw some general conclusions and point out some possibilities for future work.

Chapter 2

Literature Review

2.1 Introduction

In this chapter, we summarize our literature study that gave us an insight in the research field and led to the models used for implementation in chapter 3 and 4. First, we give an overview of relevant aspects of smart grids and different demand response programs. Subsequently, we discuss potential flexible devices in section 2.3. Different modelling approaches to represent electric flexibility are presented in section 2.4. We made a comparison to assess which approach is best suited for our purposes. Along this chapter, gaps and shortcomings in existing research are pointed out. Finally, we conclude with an overview of the methodology and the different models that we considered best suited, which are further elaborated in chapter 3 and chapter 4.

2.2 Smart Grids & Demand Side Management

Historically, the electricity grid is built according to the idea that supply will always follow demand. In the traditional electricity grid, this resulted in a unidirectional energy flow from centralized production parks to the end consumers. Nowadays however, there is a need for changing the way the current electricity grid works. According to [13] there are three main drivers for this change. First, the government policies regarding climate change cause more decentralized renewable generation to be installed. Secondly, customer behaviour is changing. The growing number and increasing energy requirements of electrical devices is pushing up the peak demands in the networks. Thirdly, new technologies are available. These technologies include e.g. small scale solar generation and electric vehicles. They offer higher functionality and will have to be supported by the network. In the context of these changing needs, the concept of a *smart grid* is developed.

The European Technology Platform Smart Grid (ETPSG) [14] defines the smart grid as follows:

> *A Smart Grid is an electricity network that can intelligently integrate the actions of all users connected to it – generators, consumers and those*

that do both – in order to efficiently deliver sustainable, economic and secure electricity supplies.

The smart grid is supposed to support the wide-spread distributed energy resources (DER) and the increased penetration of EVs by managing bi-directional energy flows of power and real time information. One of the main benefits is that demand and supply will be able to be balanced to a certain extent within the distribution network. End consumers will receive more detailed information and will be able to optimize their energy use and participate actively in the market to meet demand response signals.

Demand side management is a very general term used in many applications and contexts. In its most broad sense DSM encompasses all utility activities designed to intervene in the end-use consumption pattern of electricity [15]. E.g. the utility paying of industrial customers to shut down their processes as a secondary reserve, raising awareness to reduce energy consumption, energy efficiency measures, etc. Demand Response is mostly used to indicate the more recent forms of DSM. The literature is not very consistent and both terms are often mixed up. In this thesis we will use the term DSM in its most broad sense as defined above, and DR as the DSM applications that become possible in a smart grid context.

Fig. 2.1 shows a structured overview of all possible DSM programs and the benefits of applying DSM as described by Albadi et al. [16]. A clear difference is made between incentive based programs (IBP) and price based programs (PBP). Incentive based programs can be further divided in classical programs and market based programs. In classical IBP, participating customers receive participation payments, e.g. in direct load control (DLC) where loads are switched off and on by a system operator. Although this program is very effective, it is difficult to implement on a wide scale because the operator needs a lot of information of each consumer. This is inherently in conflict with the privacy rights of consumers and has triggered public resistance in the past [17]. In market based IBP, participants are rewarded money on a more market based approach, depending on the amount of the load reduction realised. PBP are based on dynamic pricing rates in which electricity tariffs are fluctuating. These programs can be implemented in a decentralized manner and thus do not suffer from privacy concerns and a lack of scalability. The most advanced form of these PBP is Real Time Pricing (RTP). In this program, customers are charged hourly fluctuating prices reflecting the real cost of electricity in the wholesale market. RTP customers are typically informed about the prices on a day-ahead basis. In the other PBP, prices do not vary as much. Therefore RTP will free up the most flexibility of all the PBP programs and allows to estimate this flexibility on a more precise time scale. Also, many economists believe that RTP is the most direct and efficient demand response mechanism, and therefore should be the focus of policy makers [8]. These arguments, together with the fact that privacy rights are not violated, are the main reasons why we chose to implement the RTP program as the demand response program in our thesis.

Several benefits can be attributed to demand side management. These can be divided into four main categories: participant, market-wide, reliability and market

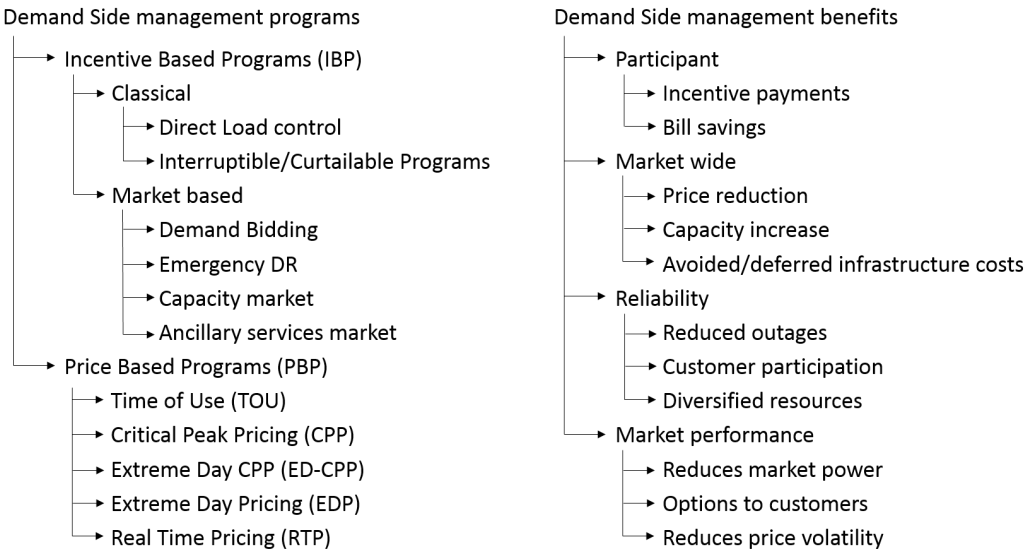

Fig. 2.1: Overview of different DSM programs and DSM benefits [16].

performance benefits (see Fig. 2.1). The participants, or customers can expect a lower electricity bill, as is also the case in our model (see section 3.5.6). An example of market-wide benefits is the overall reduction of the electricity price. This is due to a more efficient utilization of the available infrastructure. DSM is also expected to increase the reliability of the electricity system, as participants will have the opportunity to help reducing the risk of outages. Also, DSM improves the market performance, consumers will be able to better manage their consumption since they have the opportunity to affect the market.

This thesis is situated in the context of a greenhouse gas emission-free energy system [7]. Because of the carbon-neutrality, a large share of renewable energy sources (RES) is expected in the energy supply. By consequence the energy supply will fluctuate and prices will become more volatile. One of the benefits of applying DR is the ability of managing the demand-supply balance in systems with such intermittent renewables [18]. This will thus be the main purpose of demand response in our thesis. In the context of 100% carbon-neutrality this shifting of demand shall have to be scheduled in advance so it can be used to balance *forecast shortages* in the demand-supply equation. We will examine this application, rather than other applications where DR is used for immediate balancing of shortages due to *forecasting errors* with respect to real time generation on a shorter time scale. We can reformulate the objective of this thesis as:

> *Investigating the ability of using demand response on a transmission level to adjust demand to supply such that the TSO is able to plan this flexibility ex-ante in the market.*

In this context, DR could be seen as a new type of tertiary reserves that will eliminate the need for using expensive peak units.

2.3 Potential Flexible Loads

In this section we give an overview of the different loads that could be used in a demand response program. We can make a first distinction between industrial loads and residential loads. Residential loads can be classified into flexible and non-flexible loads. Loads are called *flexible* when they allow to (partially) shift their energy consumption to a different point in time. Not all loads are equally suited for this purpose. Some are subjected to a more stringent user behaviour as the user is not always willing to employ them at a different time, e.g. cooking a meal, watching TV,... These type of loads are called *non-flexible*. Flexible residential loads can be divided into loads that require changes in user behaviour[1] and loads that can be adjusted automatically, without affecting user behaviour. In this thesis we will focus solely on flexible loads that do not require change in user behaviour. Different flexible loads are considered in this thesis and will be studied in more detail in the sections below. Fig. 2.2 gives an overview of the different types of loads.

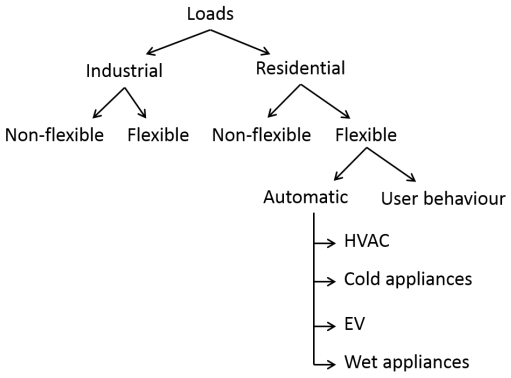

Fig. 2.2: Classification of different types of loads

2.3.1 Industrial Loads

Large industrial customers typically have a big potential for flexibility, due to the size of their loads and their ability to control a large part of it [19]. Industrial loads can be divided into controllable loads and non-controllable loads (e.g. uninterruptible processes). The controllable loads can be grouped into process independent loads, process-interlocked loads, storage constraint loads and sequential loads [20]. Each industrial process is very specific and it is difficult to assess the flexibility of these processes on a large scale. Most analyses of DSM in industrial processes are limited because they are case studies for a single industrial plant or sector and do not investigate interdependencies between DSM potentials and the total power market. Paulus [21] investigates the technical and economic potential of DSM in industries in Germany. He classifies the processes that can be used for DSM according to two

[1] Examples are turning down the heating because of high energy prices, doing the laundry in the weekend, knowing that the electricity price is cheaper then.

criteria: overall DSM potential and economic efficiency. He concludes that high energy intensity is the main lever for DSM to be attractive and withholds eight types of industrial processes. These processes could be able to provide approximately 50 % of German capacity reserves for the positive tertiary balancing market in 2020. This study proves that industrial loads have an enormous potential for participating in the power market.

There is a great variety of industrial processes and it is difficult to model them all separately. They are mainly used in DSM programs for ancillary services [22] and this is not the goal of our thesis. Although they have a large potential for flexibility, industrial loads fall out of the scope of this thesis.

2.3.2 HVAC

A first category of residential flexible devices are HVAC apparatus, consisting of *Heating, Ventilation and Air Conditioning*. As we are examining the Belgian case, only heating is considered. The amount of installed Ventilation and Air Conditioning systems in Belgian residences is a marginal part (currently $< 1\%$) of the total energy consumption in Belgian residences [23]. Because these devices would complicate our model considerably and they are of minor importance, we excluded them from our model. Of course when investigating more southern countries they might have to be taken into account.

As the background of our thesis is a carbon-neutral energy system, gas or other fossil fuels can no longer be used for heating purposes, as is the case now[2]. The heating of buildings will thus have to be provided by other sources. The most credible source of future heating is electrical heating. One alternative could be sun boilers but they can only be employed for water heating (no space heating) and they will always need a back up electric heater [23] so we would need electric heating anyway. We did not consider the usage of sun boilers further in this thesis. Hence, we assume that all Belgian residences will use electrical heating. This heating can be provided by two types of devices: heat pumps and ordinary electrical heaters. These heaters will represent a big part of future domestic electricity consumption and therefore the demand response of these devices will be of great importance.

Electrical heaters allow for flexibility by modifying their load pattern without affecting the thermal energy service they deliver. Different options are available to create this flexibility. A first option is to allow the temperature in the buildings to stay within certain limits. The heaters provide then some flexibility by using only the thermal inertia of the building. Since the temperature can vary between its limits, the heater can make the temperature increase higher than minimal required at a certain moment such that it does not have to work at another moment. A second option is to provide flexibility by a thermal storage tank [24]. One should only use this thermal flexibility if the benefits of a demand shift exceed the drawbacks that are associated with the energy losses of this thermal storage.

[2]Carbon capture and storage (CCS) has not been considered in this thesis, since micro-CHPs with some kind of residential CCS grid will then probably be needed, which falls our of the scope of this thesis.

DSM applied to electrical heaters has to be studied with detailed dynamic models. These models need to include a thermal model of the building, the HVAC system itself and the user behaviour. The last one is needed to know when the right temperature constraints have to be set. The first two items are required for capturing the interaction between the heating system and the building, the effects of ambient and inside temperatures, etc. [25]. Models of buildings can get pretty complex, depending on how many factors one is willing to integrate. An example of such a complex model is Energy+ of the US Department of Energy [26]. Although this model is very precise, it is difficult to integrate with DR algorithms and computationally expensive. A widely used model to capture the thermal behaviour of a building is a second-order equivalent electric circuit containing resistances and capacitances, whose parameters depend on the building geometry and the thermal properties of its materials. Because this is a linear model, this is much less computationally expensive and allows easier for integrating with DR algorithms [24, 27].

Since we did not include ventilation and air conditioning, our HVAC model only consists of ordinary electric heaters and heat pumps. The former are easily modelled: one only needs an efficiency (usually 100 %). The latter can be modelled based on its coefficient of performance (COP). In reality, this COP depends in a non-linear way on the ambient temperature. However, a linear approximation depending only on ambient temperature is permitted [25, 28].

2.3.3 Cold Appliances

Cold appliances refer to refrigerators and fridges. Just as with HVAC devices, load shifting of cold appliances is enabled by the thermal storage they incorporate. With respect to the average annual energy consumption at the residential level (in EU-27), the cold appliances correspond to a share of 15.2 %, i.e. ranked second place after heating systems/electric boilers [29]. Fridges have a penetration rate of 106 %, freezers are somewhat less represented with a penetration rate of 52 % in the EU [30]. Hence, although the power demand of an individual fridge or freezer is relatively small, the aggregate effect of large numbers of them can have a significant potential for flexibility.

Typical shifting periods of cold appliances are 15 to 30 minutes [31] as the stored food may not heat up too much. This is actually too short for our purposes (we are considering an hourly varying RTP, and so demand shifting with a time resolution of at least one hour). Also, consumers seem to be very reluctant to accept interference in their cold appliances because of health concerns [32]. Because of these last two reasons, we regard cold appliances as non-flexible.

2.3.4 Electric Vehicles

By 2050, plug-in electric vehicles and electric vehicles are expected to constitute around 60 % of the global car sales [33]. Because of this shift in technology, domestic electricity consumption will rise inevitably. For instance in Belgium, assuming an EV with a consumption of 200 Wh/km and an annually driven distance between

15 000 and 20 000 km, the energy required for the vehicle is of the same magnitude as the yearly household electric energy consumption as it is now [34]. EVs provide a flexibility, if one acknowledges that it does not matter when exactly they are charged, as long as they are charged sufficiently when they have to leave. DR applied to EVs offers thus a big opportunity for managing fluctuations in electricity generation and consumption [35]. Controlling charging of electric vehicles in a smart grid is therefore an important research topic. Apart from shifting their charging time, EVs could also offer ancillary services to the grid in the form of 'vehicle-to-grid' services (V2G). However, V2G operation falls out of the scope of this thesis.

In order to ensure that the EV users' driving requirements are met, it is necessary to study the driving patterns. Knowing these driving patterns, EV charge profiles can be constructed. The most important variables to construct these charge profiles are daily driving distance, home arrival times and home departure times assuming that EVs can only be charged at home. At this moment, EVs are not yet widespread but it is acceptable to assume that EV users will more or less have the same driving pattern as drivers of conventional cars. See [36], [37] and [38] for studies that construct EV charge profiles based on respectively Flemish, Dutch and Danish driving patterns.

An increasing share of EVs in the vehicle fleet will obviously have an increasing impact on the electricity system. A significant amount of research has already been performed on the charging of EVs. This charging can happen in a coordinated or an uncoordinated way (if charged immediately when arriving). Charging coordination strategies can reduce the impact on the power system by making more efficient use of the system's capacity [39]. Many different coordination strategies exist and different objectives can be taken into consideration. They can be subdivided in technical, economical and techno-economical objectives. Technical objectives include e.g. minimization of energy losses, minimal voltage deviations etc. Economical objectives are linked to the energy-market stakeholders (consumers, producers) and include financial benefits by shifting the charging process in response to price fluctuations. Techno-economical objectives are a combination of both. A comparative analysis of these strategies has been carried out by Leemput et al. [34].

2.3.5 Wet Appliances

Wet appliances include washing machines, dishwashers and tumble dryers. The electricity demand of these appliances is described extensively by Stamminger et al. [30]. This project assesses the possibilities for load shifting of wet appliances across Europe. It also features a detailed assessment of the acceptance of demand response applied to wet appliances by the end-user. The report includes starting probabilities of the different appliances, derived from a survey of 2500 customers from 10 countries in Europe.

According to Timpe [32], washing machines, dishwashers and tumble dryers are well suited for load shifting. The expected typical time shift of the cycle of a washing machine or a tumble dryer is 3 to 6 hours. For a dishwasher this amounts to 3 to 8 hours. Although the availability of these appliances is low, in practice this could be

compensated by large numbers of controllable appliances leading to an aggregated potential for flexibility that is not negligible.

Labeeuw [40] estimates the average potential for flexibility in Belgium to be 92 MW with peaks up to 353 MW. This is low when compared to the total installed capacity of 19 627 GW, but compared to the primary and secondary reserves this potential is not negligible.

2.4 Modelling Flexibility

In this section, we describe different modelling approaches to estimate electric flexibility enabled by smart grids. Three approaches are being considered. First, the top-down approach roughly estimates how much of the demand can be shifted in time. Secondly, aggregate models like the tank model and quantized population model are examined. Finally, we discuss flexibility from a more economical point of view, using price elasticities of demand. At the end we make a comparison between the different approaches to see which one is best suited for our purposes.

2.4.1 Top-Down Approach

Several studies model the flexibility obtained through DR explicitly using a top-down approach. Here, DR is represented as a given percentage of the energy demand which can be shifted in a time window of 24 hours as this is estimated to represent the expected aggregated capability of DR technologies [41, 42] . In Roadmap 2050 [1] for instance, DR has been capped at 20% of the daily energy demand. This modelling strategy does not consider the technical characteristics of flexible devices. Hence, there is some room left for improvement.

2.4.2 Aggregate Models

In order to represent the flexible demand at the wholesale level, we need a concrete, yet simple model that can capture the flexible demand offered by a large population of deferrable loads. This flexible demand consists of the sum of load contributions from each individual appliance whose load can be deferred. One could model the contribution of each appliance by looking at customer usage behaviour. However, this does not scale well. At the wholesale level, we cannot consider individual customer behavioural parameters because of computational complexity [43]. Aggregators are entities that interact with the wholesale market providing an interface to manage populations of flexible demand and can overcome this problem [44]. These aggregators are faced with three main challenges: dealing with a heterogeneous population, real time control of the appliances and the ex-ante modelling of flexibility in the market. The next paragraphs discuss some aggregate models. The concept of an aggregator directly influencing the loads of its population is in accordance with the direct load control program of Fig. 2.1.

Tank Model A first modelling approach for aggregating flexible demand on the wholesale level is to represent the deferrable load by a *tank* that has to be filled at the end of the day [45]. Fig. 2.3 shows a schematic representation of this model. The power system injects energy into a tank of finite capacity. Energy drains out of this tank to serve the deferrable load. In this model, some constraints of the load have to be specified. Since we're looking at an aggregated model, the average deferrable load has to be specified, which is the rate at which energy drains out of the tank. Furthermore, the storage capacity (i.e. the size of the tank) and the maximum and minimum rate at which power can be injected in the tank must be specified. Note that the tank model is just an analogy. The actual flexible load may have nothing to do with a tank (e.g. an electric vehicle).

This is a very coarse approximation, as all the valuable temporal information about the individual contributions is lost. These include appliance arrival patterns, the time evolution of their energy consumption and their time flexibility. However, it is a good model to just quantify the economic benefits [44].

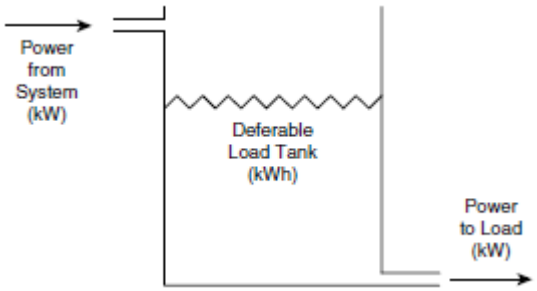

Fig. 2.3: Deferrable load tank analogy [45]

Quantized Population Model A third aggregate model is named *quantized population model*. It is named as such because several appliances of a population are grouped together according to a certain property. A first example of this is a state space model for Thermostatically Controllable Loads (TCL) [10, 27, 46]. Here, local device states are described in discrete temperature-related *state bins*. The aggregated probability mass is allowed to move through these bins. Each TCL in the population is in a certain temperature interval and can be either ON or OFF. The TCL population can now be represented by a discrete linear time invariant system in state space form: $\boldsymbol{x}(t) = \boldsymbol{A}\boldsymbol{x}(t-1) + \boldsymbol{B}\boldsymbol{u}(t)$. The state vector $\boldsymbol{x}$ contains the number of TCLs in each state bin. The $\boldsymbol{A}$ matrix can be thought of as a Markov transition matrix describing the probability of TCLs moving from one state to the next. The vector $\boldsymbol{u}$(t) controls what to turn off. A schematic of this state bin transition model is shown in Fig. 2.4.

Another example of such an aggregate model is the queuing of a fleet of EVs to be charged. In [11] a direct load control mechanism is provided in which individual requests for energy are unbundled. Rather than storing energy or interrupting the charging, requests for energy are hold in queues and the service time of individual

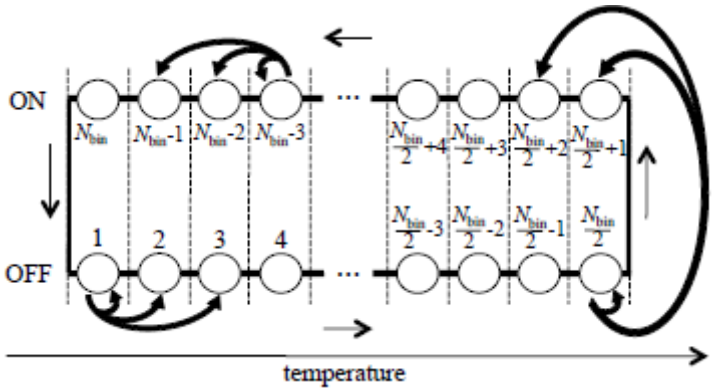

Fig. 2.4: State bin transition model [10]

appliances is optimized. A neighbourhood scheduler (aggregator) has to optimize the time at which the EVs start to function. This model can also be extended to other deferrable loads such as washing machines, dishwashers, etc.

Multi-Agent Bidding In this approach, every participant, operating in a virtual power market, is represented by an agent who places priority bids. Agents represent the interests of the participants and ensure that local constraints are met. Bid functions of multiple agents are aggregated by an aggregator agent. In this hierarchical structure all bid functions are aggregated at the top and a clearing priority is determined based upon a balance between production and consumption. This approach is mostly applied for coordinated charging of EVs. Examples are Intelligator [39] and [47].

2.4.3 Price Elasticities

Another way to represent flexibility is through price elasticities. In economics, price elasticity of demand is a measure to indicate the change in the quantity demanded of a good in response to a price change [48]. These quantities are expressed relative w.r.t. the current market equilibrium. The larger the relative change in demand after a price change, the more elastic is the demand. Presently, residential demand is almost completely unresponsive to price in power markets because wholesale price fluctuations are not usually passed on to retail customers. As mentioned earlier, the introduction of smart grids will enable the consumer to participate in the market. When introducing smart pricing strategies (e.g. RTP, TOU, ...), the customers will become responsive to price changes. The demand curves of both a responsive and unresponsive user are shown in Fig. 2.5.

Classically, two types of elasticities can be defined: long-term and short-term price elasticity. Long-term price elasticity indicates the willingness of consumers to adjust their general behaviour in response to electricity price changes. Short-term price elasticities represent the responsiveness to short-term price signals (e.g. price signals varying each hour). Currently, these are typically lower than long-term price

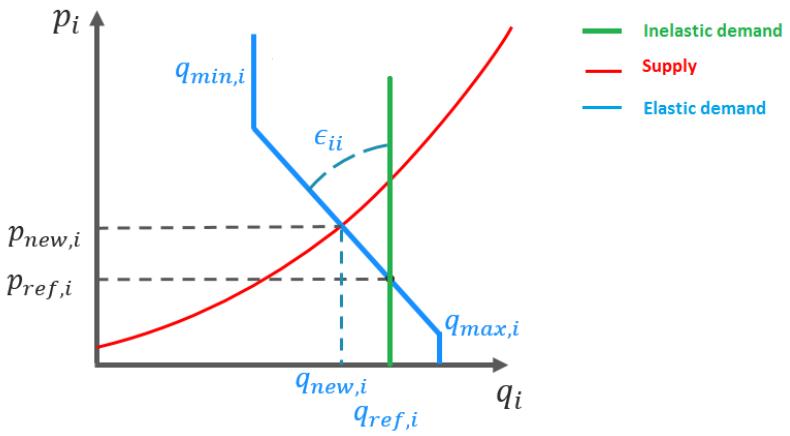

Fig. 2.5: Supply and demand curve when users are not responding to price changes (vertical line) and when users are price responsive with elasticity ϵ_{ii}. The reference price $p_{ref,i}$ is taken as the market equilibrium when demand is inelastic. When demand becomes flexible, a new equilibrium price $p_{new,i}$ is established. Also, note that there is a minimum (non flexible) demand $q_{min,i}$ and a maximum demand $q_{max,i}$ beyond which demand becomes inelastic.

elasticities. They result from changes in the operation of electric equipment [12] triggered by e.g. demand response programs. Short-term price elasticities will therefore be interesting in the context of this thesis.

When considering short-time price elasticities, one has to make a difference between own-price elasticities and cross-price elasticities [12]. Given e.g. hourly time steps, the own-price elasticity ϵ_{ii} indicates the relative change in the demand q at the hour i in response to a change in the price p in the same hour i. It is defined as:

$$\epsilon_{ii} = \frac{\partial q_i(p_{ref,i})}{\partial p_i} \cdot \frac{p_{ref,i}}{q_{ref,i}} \tag{2.1}$$

where $p_{ref,i}$ and $q_{ref,i}$ are respectively the reference price and the reference demand in hour i. This elasticity is typically negative as an increase in electricity price yields a decrease in consumption.

Cross-price elasticities ϵ_{ij} express the change in demand in hour i in response to a price change in another hour j and is defined as:

$$\epsilon_{ij} = \frac{\partial q_i(p_{ref,j})}{\partial p_j} \cdot \frac{p_{ref,j}}{q_{ref,i}} \tag{2.2}$$

Positive cross elasticities mean that an increase in the price of an hour j stimulates an increase in the demand at hour i. In the electricity sector these cross elasticities between electricity consumption in different periods are typically positive [49].The electricity demand at two different hours i and j can thus be thought of as substitutes [48]. However, negative cross-price elasticities have been found too [50]. The cross-price elasticities can be seen as a measure for the willingness of load shifting.

During a time horizon N, all the time-periods' price influence on electricity demand can be summarized in a price elasticity matrix (PEM) as [9]:

$$\epsilon_{N\times N} = \begin{pmatrix} \epsilon_{11} & \cdots & \epsilon_{1N} \\ \vdots & \ddots & \vdots \\ \epsilon_{N1} & \cdots & \epsilon_{NN} \end{pmatrix} \tag{2.3}$$

The change in demand Δq in response to a change in price Δp can then be calculated as $\epsilon_{N\times N} \cdot \Delta p = \Delta q$. End-user response depends on the end-user load type. Three different load types can be distinguished and they are all described by a unique PEM topology. First, fixed loads are inelastic to price and all entries for this load type will be zero in the PEM. Second, curtailable loads can be shed and they are represented by a PEM with negative values along the diagonal and zeros for all off-diagonal entries. Third, shiftable loads can be moved to other periods during the day. They are expected to be represented by a PEM with negative on-diagonal entries and positive off-diagonal entries. These shiftable loads will be the main focus of this thesis. Real world consumers have a higher preference to schedule their load close to the originally scheduled time period. By consequence, their PEM is expected to be a band matrix with nonzero entries only within a range around the diagonal where the consumer is willing to shift to [51].

One major research gap is the determination of the price elasticity values for a PEM for given smart grid technologies. According to Wang et al. [9] they can potentially be determined by the user-end load control algorithms or be estimated through loads' consumption data collected by smart meters. Interesting research can be done in this area by taking into account the technical characteristics of flexible loads. The determination of PEM in a smart grid context will be the main research goal for this thesis.

2.4.4 Comparison

Three main methods to model electric flexibility have been described in the previous sections. The top-down approach presumes a certain amount of flexibility. As it is the purpose of this thesis to quantify this flexibility, this method is of little use for us. We are left with the choice between an aggregate model and price elasticities. Aggregate models are scalable methods, computationally not intensive and can represent flexibility in an accurate manner. However, these models also suffer from some drawbacks. First, they are all mainly suited to only represent one type of appliance which causes the interaction between different devices to get lost (e.g. at a household level). Secondly, these models suggest DLC programs which might lead to privacy issues, as explained in section 2.4.2. Price elasticities are a linear approximation of flexibility. They link the electricity consumption with the price of electricity and thus suggest using an RTP program, which we pointed out earlier as the most efficient DR mechanism (see section 2.2). Also, we believe that RTP will free up the most flexibility of all PBP. Because of this link, it is possible to obtain an economical value of this flexibility. It would be possible to get the real cost of

shifting demand, which makes comparison with other types of electrical flexibility (Fig. 1.1) possible. This is a flaw of the other methods. Besides, since we have to keep our model linear (see 1.3) price elasticities are a logical choice. Furthermore Wang [9] pointed out that the determination of the PEM in a smart grid is still a gap in current research. Because of these reasons stated above, we chose to quantify the residential electric flexibility using price elasticity matrices.

2.5 Summary

In this section, we briefly summarize the literature review and the elements that we retain to build our model upon. First, we chose RTP from the different applicable DR programs, as this is believed to be the most direct and efficient, and the most realistic with regard to privacy concerns. Looking back to Fig. 2.2, we can now identify the load types that we chose to take further into account. We decided to focus only on quantifying residential flexibility and thus excluded industrial loads from possible flexible loads. The flexible residential loads that are considered further in this thesis are:

- Heat pumps and electric heaters (part of HVAC): buildings will be modelled by second-order RC models, heat pumps by their COP and electric heaters by their efficiency.
- Wet appliances (washing machines, dishwashers, tumble dryers) will be represented by particular load cycles.
- Electric vehicles: charging of EVs will be modelled based on driving patterns of users. V2G will not be possible in our model.

Cold appliances are considered non-flexible because of health concerns. Ventilation and air conditioning are excluded too because they are of minor importance in Belgium. The modelling and scheduling of these flexible devices will be explained further in chapter 3.

Chapter 3

Modelling Residential Demand

3.1 Introduction

This chapter discusses the models of the different household devices taken into account for the evaluation of demand response. A distinction can be made between flexible and non-flexible demand. Non-flexible demand is subjected to user behaviour and cannot be shifted in time. Flexible devices are all the devices whose consumption can be shifted in time, subject to the comfort constraints imposed by the users. This group of appliances can be further divided in continuous and discrete devices. *Continuous devices* can be interrupted and their power consumption may vary, e.g. a heat pump. With *discrete devices* we mean those devices that draw a predefined load cycle once switched on, e.g. a washing machine. We modelled and programmed all household devices in MATLAB, following an object-oriented approach. A house is equipped with these devices in function of assumed appliance penetration rates. Subsequently, the household receives a RTP signal which allows for scheduling the flexible devices towards minimal electricity cost for the user. This results in a mixed integer problem. In section 3.5.6, we perform a case study of a house subject to RTP and compare the scheduling and energy consumption when subject to a flat price and when subject to a varying price. Finally, households are grouped together into *neighbourhoods*, taking into account the population structure of Belgium. This is explained in section 3.6 followed by an example of the mixed integer problem on a neighbourhood level.

3.2 Non-flexible Demand

The non-flexible consumption is the part of a household's electricity consumption that cannot be influenced by demand response. These appliances typically are subjected to user behaviour. It would require a change in consumer behaviour to shift their consumption but we did not consider this in our research. Examples include switching the lights, watching TV, cooking a meal, etc. Usage of those appliances typically depends on the occupancy of the house, which in turn depends on the number of residents. We assume that a household counts between one and

five persons. The model for non-flexible electricity use is based upon Richardson et al. [52] and consists of two different parts. On the one side the occupancy profile during a day is generated based on [53]. The model generates realistic statistical occupancy time-series data and takes account for a difference between weekdays and weekends. Given the occupancy profile, the non-flexible electricity consumption for a house is generated. This non-flexible consumption is generated by two different models. The first model generates the use of lighting, the second one generates the usage of all other non-flexible appliances. The use of lighting in the residential sector mainly depends on the level of natural light incoming from outdoors and the activity of the residents. Hence, the model for lighting usage couples the occupancy profile and the weather data and is based on [54]. The usage of other electrical appliances only depends on the activity and this model is based on [55].

The model is calibrated in order to have a certain average annual electricity consumption per household. This should correspond to an estimate of the residential electricity use in 2050 and it is calculated as follows. According to the IEA [56], the total residential electricity consumption in Belgium amounted to 20 210 GWh in 2012. Following the predictions of [42] (see table 3.1), this will rise to 21 544 GWh in2050. In 2009, there were 4 606 544 private households in Belgium [57] . Assuming that this number remains constant, we obtain a total average annual consumption of 4 677 kWh per household. Subtracting the energy consumption of appliances that we consider flexible (see section 3.3), this leads to an average non flexible electricity consumption of 3 091 kWh. All aforementioned models were available in Excel. To ease the integration with our own model we translated them to MATLAB code.

Period	2010-2020	2020-2030	2030-2040	2040-2050
Growth rate [%]	0.3	0.0	0.2	0.2

Table 3.1: Average annual growth rate prediction per decade of residential electricity demand in Belgium [42]

3.3 Flexible Devices

Flexible devices are those devices whose consumption can be influenced by demand response. Two groups of flexible appliances can be identified. The first group consists of those appliances that have to run a complete predefined cycle once started and that cannot be interrupted. We call them *discrete devices*. Secondly, there are appliances that can run continuously and that can draw a variable power. We call them *continuous devices*. Two characteristics are common to all flexible devices:

- **Penetration rate:** In order to estimate the amount of flexibility for each flexible device, we have to know how many of them are installed. To this end, the penetration rate of each appliance is an important input parameter and it is defined as the percentage of households that own a certain appliance.

- **Willingness:** Not everyone may be willing to shift their electricity consumption. Because we want to explore the limits of electric flexibility, we assume that by 2050 demand response will be accepted by the public and that there is a willingness of 100 %, meaning that every household participates in the demand response program.

3.3.1 Discrete Devices

Discrete devices must run their entire load cycle at a time. In this thesis, three different discrete devices are considered: a washing machine, a dishwasher and a tumble dryer. Further in this text these are also referred to as *wet appliances*. Before continuing, several properties have to be known in order to model the wet appliances correctly:

- **Load cycle:** Every discrete device has its own load cycle which has to be run entirely when started. The power sequence drawn is not the same in every time step. For instance, a washing machine draws more power at the beginning of its cycle while heating up the water than at the end when it's rinsing.

- **Start - Stop time:** Depending on the preferences of the user, an appliance has a certain start- and stop time. The start time is the moment that the user would start the appliance when no incentive is given to shift to a later time. The stop time is the time when the appliance has to be finished at the latest. The load cycle can then be shifted within these two boundaries.

- **# Cycles per week:** Not all appliances run every day. Knowing the number of cycles per week, the usage of an appliance in a certain day can be determined.

All data is taken from the Smart-A project [30]. This data contains a set of 5000 appliances of each type, which all differ in their load cycle, start and stop times. According to the penetration degree, a household is or is not in possession of a certain appliance. When an appliance is owned by the household, it is first determined whether it runs that day or not on the basis of the number of cycles per week. If this is the case, one of the 5000 cycles is drawn at random.

Washing Machine For washing machines in the EU-15[1], the following data are available. The penetration level of a washing machine is assumed to be 95 % with an average of 4.9 cycles in a week. Washing machines differ in start and stop times and in their programme. An example of a load cycle of a washing machine is shown in Fig. 3.1.

[1] No recent specific data for the penetration rates of wet appliances in Belgium were available. The penetration rates assumed here date back to 2003, but no big changes in these penetration rates are expected.

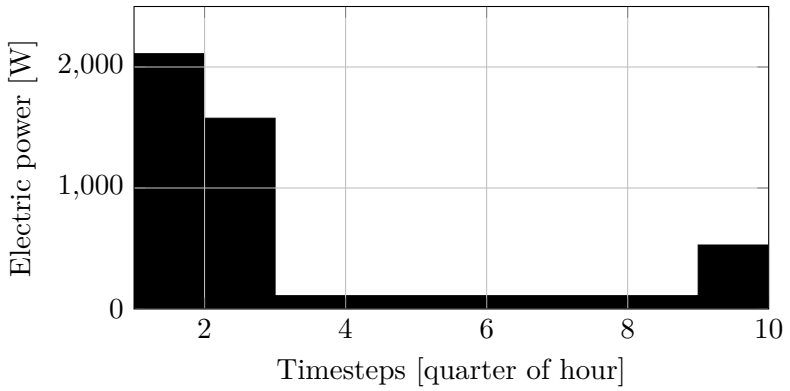

Fig. 3.1: Typical load cycle of a washing machine

Dishwasher For dishwashers, the same approach is used. According to Stamminger et al. [30] a penetration level of 42 % is assumed with on average 4.06 cycles in a week.

Tumble Dryer Similarly, for tumble dryers a penetration level of 34.4 % is assumed with an average of 1.96 cycles a week.

3.3.2 Continuous Devices

Continuous devices do not run a predefined load cycle but will react to the comfort constraints that are imposed by the user. These devices can be interrupted as much as desired and can draw a varying power. Continuous devices taken into account in this thesis are a heat pump, electric auxiliary heaters and electric vehicles.

Heat pump and Auxiliary Heaters

Each residence is equipped with an air coupled heat pump (HP) that can deliver both space heating $\dot{Q}^{HP,SH}$and domestic hot water $\dot{Q}^{HP,DHW}$. To ensure that the temperature constraints set by the inhabitants can always be met, the heat pump is backed up with two auxiliary electric heaters AUX1 and AUX2. The first electric heater can be used for space heating ($\dot{Q}^{AUX1,SH}$) and for domestic hot water production ($\dot{Q}^{AUX1,DHW}$). The second electric heater is placed directly in the room and is only able to deliver space heating ($\dot{Q}^{AUX2}$) The system is schematically represented in Fig. 3.2. The building model and the DHW model are both based on [58].

Building Model The building model consists of one zone, heated by a floor heating system and is represented by an RC model [59] as described by Fig. 3.3. The resistances represent the thermal conductivity in the house, the capacitances represent the thermal mass of the different parts. Since we use a linear approach, the evolution of each temperature indicated in Fig. 3.3 can be described by a first-order

differential equation. This can be discretized in order to obtain the thermal behaviour of the building in a linear state space model with time step j:

$$\forall j : T_{j+1} = A \cdot T_j + B \cdot U_j + E \cdot D_j \tag{3.1}$$

This model allows to relate the states T_j, the inputs U_j and the known disturbances D_j through the state space matrices A,B and E, which are based on the model found in Van Oevelen [59]. Three different house types (i.e. different values in A,B and E) are considered in this thesis. The first dwelling is a typical newly built residential building in Belgium. Model parameters taken from [59]. The second one is a typical Belgian single family house (SFH III from [60]). The third house type is a multi family house (MFH III from [60]). Based on the current building stock in Belgium, 25 % of the houses is assumed to be a multi family house and 75 % of the houses are assumed to be single family houses. Of these single family houses, half of them is assumed to be of the first type, the other half of the second type. The model is built up in such a way that it could be easily expanded if a larger building stock would be available. The state space vector T_j contains all modelled temperatures in the house:

$$T_j = \{T_j^{w2}, T_j^{w1}, T_j^{r2}, T_j^{r1}, T_j^{z}, T_j^{f2}, T_j^{f1}, T_j^{ret}, T_j^{sup}\}. \tag{3.2}$$

In this vector T_j^{w2}, T_j^{w1}, T_j^{r2} and T_j^{r1} are temperatures of specific layers in the walls and the roof. T_j^{z} is the zone temperature, which is bounded by certain limits (see section 3.5). T_j^{f2} and T_j^{f1} are floor temperatures and the hydronic floor heating system is described by T_j^{ret}(i.e. temperature of the water returning) and T_j^{sup}(temperature of the water supplied to floor heating system). The input vector U_j holds all thermal powers supplied by the heating system:

$$U_j = \{\dot{Q}_j^{HP}, \dot{Q}_j^{AUX1}, \dot{Q}_j^{AUX2}\}. \tag{3.3}$$

with $\dot{Q}_j^{HP}$ the thermal power supplied by the heat pump and $\dot{Q}_j^{AUX1,2}$ the thermal power coming from the auxiliary units during time j. Finally, the disturbances vector D_j contains the surrounding temperatures and other heat gains:

$$D_j = \{T_j^{amb}, \dot{Q}_j^{gains}, T_j^{ground}\}. \tag{3.4}$$

T_j^{amb} is the ambient temperature. $\dot{Q}_j^{gains} = \dot{Q}_j^{sol} + \dot{Q}_j^{int}$ are the thermal heat gains due to solar radiation $\dot{Q}_j^{sol}$ and internal heat gains due to occupants and appliances $\dot{Q}_j^{int}$. Weather data needed to model T^{amb} and $\dot{Q}^{sol}$ are obtained from Meteonorm [61]. The internal heat gains depend on the presence of occupants in the house. When the house is occupied, each resident represents a heat gain of 50 W and appliances produce unit[250]W. When all residents are absent or sleeping, internal heat gains are set to zero. T_j^{ground} is the ground temperature at time j and is taken to be constant at 10℃. All the aforementioned heat gains are schematically presented in Fig. 3.2. Hereby the thermal behaviour of the building is entirely modelled. We have thus a linear system of the form:

$$T_{j+1} = f_d(T_j, U_j, D_j). \tag{3.5}$$

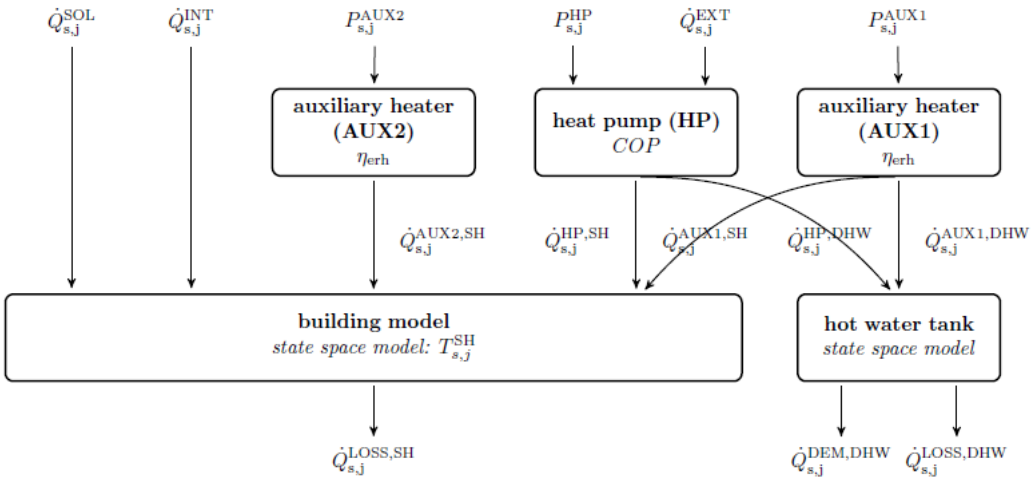

Fig. 3.2: Heating system of a residence [58]

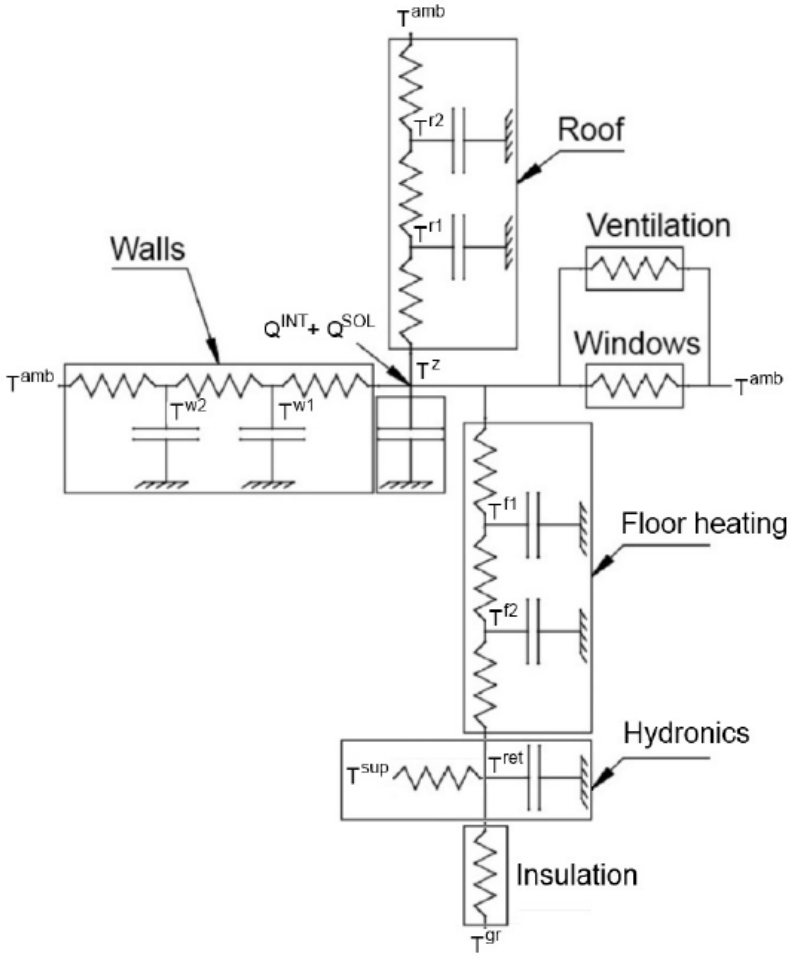

Fig. 3.3: The thermal behaviour of the building is represented by an RC model [59]

Domestic Hot Water Model The domestic hot water is supplied by and stored in a hot water storage tank. This tank is assumed to be perfectly stirred. The water in this tank can be heated up by the heat pump ($\dot{Q}^{HP,DHW}$) and by first the auxiliary electric heater ($\dot{Q}^{AUX1,DHW}$). Applying the law of energy conservation for the water tank leads to:

$$\rho \cdot V_{tank} \cdot c_p \cdot \frac{dT^{tank}}{dt} = \dot{Q}^{HP,DHW} + \dot{Q}^{AUX1,DHW} - \dot{Q}^{dem,DHW} - G \cdot (T^{tank} - T_{sur}) \quad (3.6)$$

with ρ and c_p the density and heat capacity of the water. The volume of the water in the tank, $V_{tank}\text{m}^3$, is assumed to be constant. When hot water is taken from the tank, it is immediately replaced by an equal amount of cold water. The last term $G \cdot (T^{tank} - T^{sur})$ represents the heat loss $\dot{Q}^{loss,DHW}$ of the tank to the surroundings at T^{sur}. The temperature of the cold water T^{cold} and the water demanded by the occupants at T^{dem} are both assumed to be constant. A three way valve is used to mix the water of the tank at T^{tank} with cold water to get water at temperature T^{dem}. The thermal power $\dot{Q}_j^{dem}$ that needs to be supplied to the hot water tank at each time step j can be calculated from the energy equation as:

$$\dot{Q}_j^{dem} = \rho \cdot c_p \cdot (T^{tank} - T^{cold}) \cdot \dot{V}_j^{tank} \quad (3.7)$$

with $\dot{V}_j^{tank}$ the volume of water extracted from the tank in time step j. It is assumed that the first two inhabitants use 50 liter per person per day. Each next inhabitant consumes an extra 30 liter per day. Per person 2 to 3 tapping moments per day are assumed and the probability of hot water consumption over a day is based on Peuser et al. [62] (see Fig. 3.4).

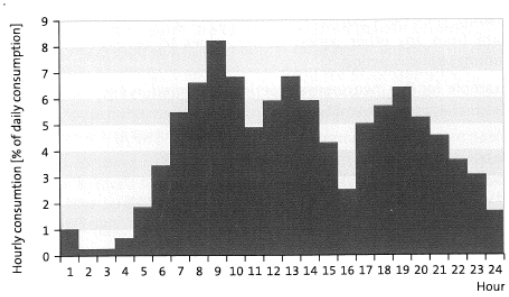

Fig. 3.4: Typical daily regime of domestic hot water consumption [62].

In the same way as with the building model, (3.6) can be discretized and written in the same form as (3.1):

$$T_{j+1}^{tank} = A \cdot T_j^{tank} + B \cdot U_j + E \cdot D_j \quad (3.8)$$

with the inputs U_j the same as in (3.1) and disturbance vector $D_j = \{\dot{Q}^{dem,DHW}, T_j^{sur}\}$.

Electric Vehicles

Because we investigate the electric flexibility in 2050, we assume that electric vehicles will be a substantial part of residential electricity demand. According to the IEA [33], electric vehicles will have a market share of 60% in 2050 and we assume an average number of 1.19 cars per household [63]. Combining these two numbers gives a probability of 71.4% of having an EV per household. It is assumed that a household does not possess more than one EV. A lot of research has already been done in the field of electric vehicles (see chapter 2). In order to take into account its energy consumption, yet not to overload our model, we implemented a simplified model.

The moments when EVs can charge depend on the driving behaviour. Data of the driving behaviour is based on [36] and include 100 different driving patterns for each day of the year. These data include the moments when an EV is at home (and thus can be charged), when it's driving and how much energy is needed to drive the desired distance. However, as these driving patterns are based on an other model than the occupancy of the house, we did not link those two in our model. If a household owns an EV, one of the hundred possible driving patterns is drawn at random. All EVs have an equal battery capacity of 60 kWh and a maximum charge rate of $P^{charge,max} = 3.3\,\text{kW}$, assuming that an EV can only be charged at home on a regular household connection. Some of the electric input power is lost and converted to heat due to battery charging losses and losses in the rectifier. Both the charging efficiency and the rectifier efficiency are assumed to be 95%. This results in a total charging efficiency of $\eta^{charge} = 90.25\%$. Knowing the departure and arrival times during the day, the EV will be charged at minimum cost and such that it will always be able to drive the desired trips (see Section 3.5). The state of charge (SOC) of an EV at each time step j is governed by the following equation:

$$SOC_{j+1} = SOC_j + \eta^{charge} \cdot \frac{P_j^{charge} \cdot \Delta t}{cap \cdot 60} - \frac{E_j^{req}}{cap} \tag{3.9}$$

with SOC between 0 and 1, P_j^{charge} in Watt and Δt the time resolution of each time step in minutes. E_j^{req} is the required energy in kWh at time step j and *cap* is the battery capacity. One of the two last terms in the equation above is always zero. When the EV is getting charged, it stands still and no energy is required to drive some distance. Consequently, the last term is zero. When driving, it cannot be charged and the second term will be zero.

3.4 Solar Panels

Our thesis is situated in a carbon-neutral energy system [7] and by consequence, strict limits will be imposed on greenhouse gas emissions for 2050. Renewable energy sources (RES) will be a significant part of the energy supply. In this thesis we assume that solar panels will represent the only important RES in the distribution grid. According to the projections of the IEA [64], the efficiency of solar panels in the residential sector η^{PV} will be around 25 % in 2050 and it is assumed that 70 % of

the households will have solar panels on their roof. The nominal power of these PV installations has a distribution according to the probabilities in table 3.2. Because special measures are needed to connect PV installations with a nominal power higher than 10 kVA [65], it is assumed that they are connected at the medium voltage grid, hence they are not taken into account in this thesis.

Nominal Power (kW)	Probability(%)
0-1	0.2
1-3	90.7
3-6	6.7
6-9	2.4

Table 3.2: Nominal power distribution of solar panels [66]

We assume that each of the solar panels is oriented and inclined optimally. The nominal power is measured at a light intensity of 1 000 $\mathrm{W/m^2}$, so the area of the photovoltaic panels on a house is determined as:

$$A^{PV} = \frac{P^{nom,PV}}{1000 \cdot \eta^{PV}} \mathrm{m}^2. \tag{3.10}$$

The actual electric power produced depends on the weather conditions. Data for incoming solar irradiation $\dot{Q}^{sol}$ are taken from Meteonorm [61]. The electric power produced from photovoltaic panels at each time step j is then calculated as:

$$P_j^{el,PV} = A^{PV} \cdot \dot{Q}_j^{sol} \cdot \eta^{PV}. \tag{3.11}$$

In this thesis we will assume that residential electricity production from PV can be sold at the same price as electricity can be bought. This means prices passed on to the houses should already incorporate the effect of the PV production. The houses will thus have no incentives to use their own PV production instead of buying from the grid.

3.5 Scheduling Household Devices

All devices are grouped into a house according to their penetration rate. This house receives an RTP signal and a central optimizer schedules the flexible devices with the aim of minimizing the electricity cost. Daily price profiles are taken from Belpex [67]. A typical price profile for one day is shown in Fig. 3.5. The devices are scheduled with a time resolution of 15 minutes.

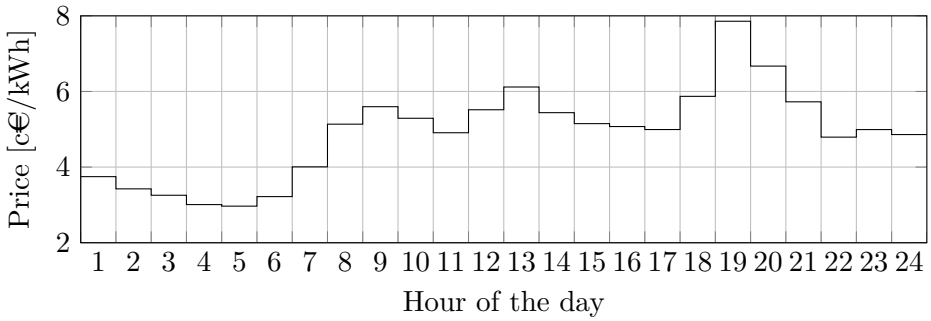

Fig. 3.5: Typical price profile from Belpex [67]

The objective of the optimization is to minimize the electricity cost with regard to the comfort constraints imposed by the user. This yields solving a mixed integer linear program (MILP), which can be written in the following general form:

$$\begin{aligned} \min_{x} \quad & \mathbf{c}^T \cdot \mathbf{x} \\ \text{subject to} \quad & \mathbf{A} \cdot \mathbf{x} = \mathbf{b}_{eq} \\ & \mathbf{H} \cdot \mathbf{x} \leq \mathbf{b}_{ineq} \\ & \mathbf{x}_l \leq \mathbf{x} \leq \mathbf{x}_u. \end{aligned} \tag{3.12}$$

where $\mathbf{c}$ is the coefficient vector and $\mathbf{x}$ the vector containing all variables. This is a mixed integer problem because of the discrete devices that are either on (1) or off (0). The detailed composition of these vectors and matrices is explained in appendix A. The constraints for the optimization will be explained in the sections below.

3.5.1 Wet Appliances

Each wet appliance owned by the household, either a washing machine, dishwasher or tumble dryer, has a certain start time t^{start} and a stop time t^{stop}, when the user wants the cycle to be completed at the latest (see Section 3.3.1). Between these two moments the cycle can be shifted so that it is as cheap as possible for the user. This is the only constraint on wet appliances and it can be written as:

$$t^{start} \leq cycle \leq t^{stop}. \tag{3.13}$$

3.5.2 Space Heating and Hot Water Production

The heat pump and auxiliary heaters are used for both space heating and domestic hot water production. First we describe the space heating, then the domestic hot water and finally the devices' power constraints.

Space heating The temperature evolution in the house is governed by (3.1) and the temperature evolution of the water in the tank by (3.8). As thermal comfort must be achieved, the temperatures in the room must always be within bounds that are perceived as comfortable. The zone temperature T_j^z in (3.2) must each time step

lie between 16℃ and 22℃ when occupants are absent or sleeping and between 20℃ and 23℃ when the house is occupied. On a warm summer day the temperature in the room can exceed these bounds because the solar gains $\dot{Q}^{sol}$ and the ambient temperature T^{amb} can be high, making the zone temperature T_j^z exceed 23℃ without any heating appliance turned on. Since we did not consider cooling devices (see section 2.3.2), the zone temperature has to be able to exceed the upper bound of 23℃ on such a warm summer day. To enable this, a binary dummy variable x_j^{SH} is introduced. When a space heating appliance is turned on (either the HP, AUX1 or AUX2) at a time step j, x_j^{SH} equals 1. When the room is not heated by any appliance, x_j^{SH} equals zero. The comfort constraint on the zone temperature T^z for each time step j can then be written as:

$$\forall j : T_j^{z,min} \leq T_j^z \leq x_j^{SH} \cdot T_j^{z,max} + (1 - x_j^{SH}) \cdot T^{z,nhmax}, \tag{3.14}$$

with $T^{z,min}$ and $T^{z,max}$ the minimum and maximum zone temperatures depending on the occupancy as explained earlier. $T^{z,nhmax}$ is the maximum temperature when no space heating is applied and it is set high enough such that the optimization will always be feasible. The thermal power delivered by each of the electric heating systems is limited by their rated electric power:

$$\forall j : \frac{\dot{Q}_j^{HP,SH}}{COP_j^{HP,SH}} \leq x_j^{SH} \cdot P^{HP,max}, \tag{3.15a}$$

$$\frac{\dot{Q}_j^{AUX1,SH}}{\eta^{AUX1}} \leq x_j^{SH} \cdot P^{AUX1,max}, \tag{3.15b}$$

$$\frac{\dot{Q}_j^{AUX2}}{\eta^{AUX2}} \leq x_j^{SH} \cdot P^{AUX2,max}. \tag{3.15c}$$

Because of the thermal mass of the building, it can happen that a heater is turned on at time step j, and the temperature increases at a next time step $j+1$ above the limit of 23℃. This is of course not desired, and to eliminate this effect, equation (3.14) is complemented with:

$$\forall j : T_{j+1}^{z,min} \leq T_{j+1}^z \leq x_j^{SH} \cdot T_{j+1}^{z,max} + (1 - x_j^{SH}) \cdot T^{z,nhmax}, \tag{3.16a}$$

$$\forall j : T_{j+2}^{z,min} \leq T_{j+2}^z \leq x_j^{SH} \cdot T_{j+2}^{z,max} + (1 - x_j^{SH}) \cdot T^{z,nhmax}, \tag{3.16b}$$

$$\forall j : T_{j+3}^{z,min} \leq T_{j+3}^z \leq x_j^{SH} \cdot T_{j+3}^{z,max} + (1 - x_j^{SH}) \cdot T^{z,nhmax}. \tag{3.16c}$$

In practice, the zone temperature never exceeds 25.5℃, even on the hottest summer day.

Domestic hot water The temperature of the water in the tank depends on the residents' water usage. When hot water is requested, the temperature in the tank must be at least T^{dem}, which is assumed to be 60℃. If no hot water is needed, the temperature in the tank may be as low as the cold water temperature $T^{cold} = 10$℃. The heat pump can only deliver water up to a temperature of $T^{HP,max}$, which is

taken to be 65 ℃. This is lower than the maximum allowed temperature of the water in the tank $T^{tank,max} = 90$℃. To raise the tank temperature higher than 65 ℃, the first auxiliary heater AUX1 must be turned on. Mathematically this is included in the constraints by adding an binary dummy variable x^{DHW}:

$$T_j^{tank} + \frac{\Delta t}{\rho \cdot V_{tank} \cdot c_p} \cdot \dot{Q}^{HP,DHW} \leq (1 - x_j^{DHW}) \cdot T^{HP,max} + x_j^{DHW} \cdot T^{tank,max}, \tag{3.17}$$

$$\frac{\dot{Q}^{HP,DHW}}{COP^{HP,DHW}} \leq (1 - x_j^{DHW}) \cdot P^{HP,max}.1 \tag{3.18}$$

If x_j^{DHW} is zero, T_j^{tank} is lower than $T^{HP,max}$ and the heat pump is limited by its rated electric power. If x_j^{DHW} is one, the water temperature in the tank exceeds $T^{HP,max}$ and the heat pump's output for domestic hot water is set to zero.

Power constraint The thermal power the heat pump and auxiliary heaters can produce is limited by their maximum rated electric power. The heating system is sized based on the maximal heat demand at the design operation temperature. Following the same approach as in [58], this is taken at an ambient temperature of -10℃ and a room temperature of 20℃. This leads to $P^{HP,max} = 3.8\,\mathrm{kW_e}$, $P^{AUX1,max} = 6.6\,\mathrm{kW_e}$ and $P^{AUX2,max} = 2\,\mathrm{kW_e}$. The maximum constraints on the heating appliances can now be written as:

$$\forall j : \frac{\dot{Q}_j^{HP,SH}}{COP_j^{HP,SH}} + \frac{\dot{Q}_j^{HP,DHW}}{COP_j^{HP,DHW}} \leq P^{HP,max}, \tag{3.19a}$$

$$\frac{\dot{Q}_j^{AUX1,SH}}{\eta^{AUX1}} + \frac{\dot{Q}_j^{AUX1,DHW}}{\eta^{AUX1}} \leq P^{AUX1,max}, \tag{3.19b}$$

$$\frac{\dot{Q}_j^{AUX2,SH}}{\eta^{AUX2}} \leq P^{AUX2,max}, \tag{3.19c}$$

with $\eta^{AUX1,2} = 1$ as all electric energy is converted into heat. The COP at each time step j can be obtained following the approach of Verhelst et al. [68], which states that the COP depends in a linear way on the ambient temperature T^{amb} and on the expected supply temperature $T_{sup,exp}$:

$$COP_j = c_0 + c_1 \cdot T_j^{amb} + c_2 \cdot T_{sup,exp}. \tag{3.20}$$

The coefficients c_i in (3.20) are constants fitted to catalogue data [58]. The expected supply temperature for space heating is 35℃ and for domestic hot water 60℃. The heat pump and auxiliary heaters can only consume energy, so:

$$\dot{Q}_j^{HP,SH}, \dot{Q}_j^{HP,DHW}, \dot{Q}_j^{AUX1,SH} \dot{Q}_j^{AUX1,DHW}, \dot{Q}_j^{AUX2} \geq 0. \tag{3.21}$$

3.5.3 Electric Vehicles

The evolution of the state of charge of the EV's battery is governed by (3.9). For the sake of a longer battery life, the battery may not be depleted entirely and the SOC has to be at least 20%:

$$0.2 \leq SOC_j \leq 1. \tag{3.22}$$

It is assumed that an EV can only be charged when it is at home. So $P_j^{charge} = 0$ if the vehicle is driving or at another location. We did not include the possibility of vehicle to grid operation, hence P^{charge} cannot be negative. When the vehicle is at home, the following constraint is active for each time step j:

$$0 \leq P_j^{charge} \leq P^{charge,max} \tag{3.23}$$

3.5.4 Overall Power Constraint

Every dwelling can only draw a certain amount of power. According to the Flemish regulator of electricity and gas (VREG) [69], a single phase connection of $P^{tot,max} = 9.2\,\text{kVA}$ at the low voltage level is the standard for an average household. Of course, self-consumed PV power has to be added to this maximum. Hence, we can impose one last overall constraint for the entire house for each time step j:

$$P_j^{WetApps} + P_j^{HP} + P_j^{AUX1} + P_j^{AUX2} + P_j^{charge} + P_j^{nonflex} \leq P^{tot,max} + P_j^{PV}. \tag{3.24}$$

3.5.5 Cyclical Constraints

Equation 3.12 represents the optimization problem for a single house within a finite horizon N. This means that start and end conditions have to be imposed. This should be done carefully: e.g. a washing machine that wants to start in the last time step N of the scheduling horizon should be able to do so and take into account that electricity has also a cost in the next time step $N+1$, although no prices are (yet) available. Therefore we impose extra *cyclical* constraints to all variables. This is justified by the fact that the electricity consumption at a certain time j is only influenced by the electricity prices on time steps that are close to time step j, as will be demonstrated in section 4.2.2. The electricity consumption of the last time step N of the scheduling horizon will therefore never be influenced by the electricity price of the first time step, but rather by the first following time step $N+1$, which is not considered in the scheduling horizon. By imposing cyclical constraints, the influence of this first following time step $N+1$ is taken care of by the first time step, which is an actual part of the optimization problem (3.12).

The cyclical constraint for a scheduling horizon of N time steps is implemented as follows. The wet appliances that are scheduled to have at least a part of their cycle at time steps $t > N$, will be scheduled further during the first time steps of the scheduling horizon. The temperatures of the building model (3.2) and T_j^{tank} of the DHW model (3.6) are imposed an extra constraint:

$$T_1 = T_{N+1}. \tag{3.25}$$

This is analogous for the SOC of an EV (3.9).

3.5.6 Case Study: an Average Winter Day

In this section, we perform a short case study of a single family house with three occupants. The flexible electricity consumption is optimized for an average winter weekday. Apart from the heating devices owned by every house, this household owns a washing machine and a tumble dryer that run both during the optimized day. Furthermore, this family is in possession of an electric vehicle and a PV installation. In order to gain a good understanding of the influence of a varying price, one can compare it with a flat price with the same average value. The varying price signal that is given to the house is the same as the one displayed on Fig. 3.5, the flat price signal is taken as the average value of the RTP.

When no varying price signal is given to the users, the washing machine would start at 8h45 (t^{start}). The load cycle of this machine has a duration of one hour and it has to be finished by 13h15 at the latest (t^{stop}). The tumble dryer's earliest start time in this case is 16h45. Its cycle has a duration of one hour and a half and it has to be finished by 20h30 ultimately. The EV leaves the house at 13h30 and arrives back at home at 23h45 in the evening. In between these two moments, it cannot be charged.

When occupants are sleeping or not at home, the temperature may fall to 16°C and when they are at home the temperature must always be higher than 20°C. From Fig. 3.6, one can see clearly that the temperature constraints are not violated, nor with a flat price, nor with a real time price. Notice the difference between the temperature at the real time price and the flat price. The temperature with real time pricing is almost always higher and reaches higher peaks than the temperature with a flat price. The areas between these two temperatures can be seen as a measure for the 'superfluous' heat energy consumed when subject to RTP as will be explained later.

Take for example the temperature rise to 22°C around 7h00. Although no occupants are awake, the heat pump heats up the room until the maximum allowed temperature. This is because at later hours, when occupants wake up, it is more expensive to heat up the room (see Fig. 3.6a). In fact, it is unnecessary to heat up the room to such a high temperature. Hence, this heating behaviour is accompanied by a higher energy consumption but the cheaper price compensates for the final price the customer has to pay.

The total electricity consumption during the day of each appliance is shown in Fig. 3.7a and Fig. 3.7b for the average flat price and the real time price respectively. For both price profiles, the PV production and the non flexible consumption remain the same. Notice the big peak at 4h45 in Fig. 3.7b, which can be explained by the very cheap electricity price at that moment. When receiving the RTP, the heat pump's energy consumption is shifted to earlier hours w.r.t. the consumption when subject to the flat price. Also, the room is heated for a longer time as explained above. For a flat price profile, energy is consumed only when it is really needed. As mentioned earlier the total energy consumption will be higher when the user receives a real time price signal. In this case, the usage of the heat pump in the morning is of particular importance. The house heats up more than necessary, hence there

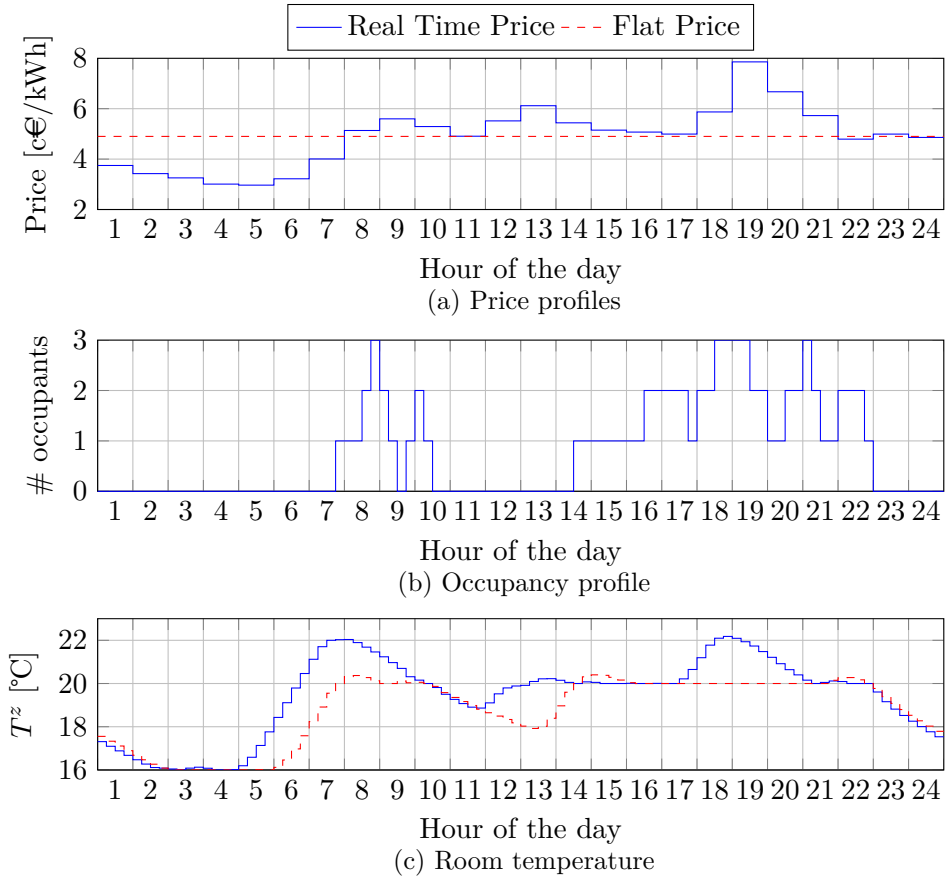

Fig. 3.6: Price profile (a), occupancy (b) and room temperature (c) for the real time price profile and the flat price profile

	Flat price	RTP
Total Price [€]	2.12	1.70
Total Energy [kWh]	43.16	44.43

Table 3.3: Total energy consumption and total price paid by the user for a real time price and an average price

are more energy losses. Nevertheless, the residents will have to pay less because electricity is consumed at cheap moments (see table 3.3).

As it is a winter day, the heat pump is working quite often. The heat pump is preferred over the auxiliary heaters because the COP is much higher than the efficiency η^{AUX} of the auxiliary heaters. The peak of AUX1 that can be noticed around the 4h45 is due to heating up water in the hot water tank. As it is very cheap to heat up the tank then, and the heat pump is being used at its full power for space heating, the water tank is heated up by the auxiliary heater. The washing machine's

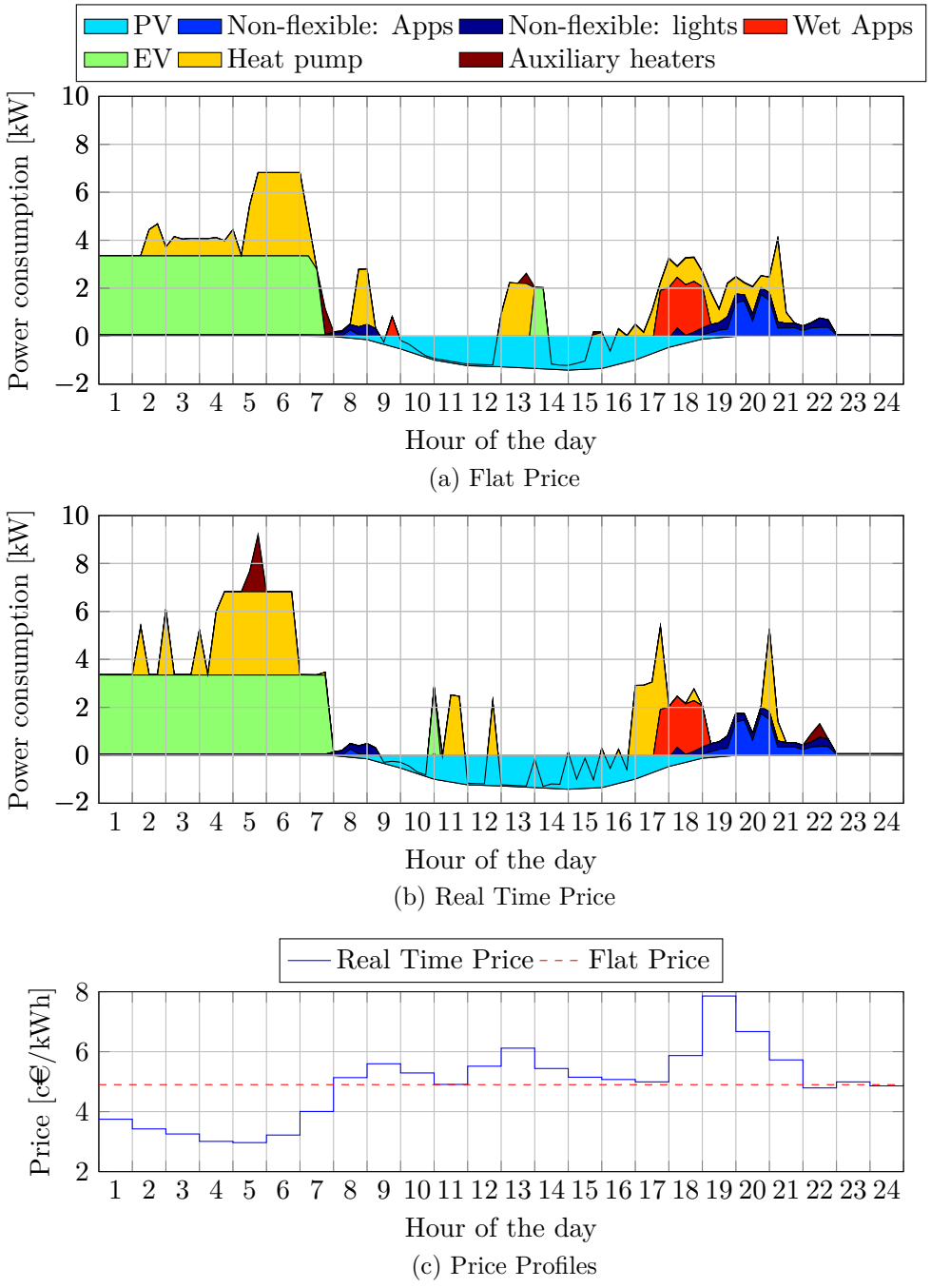

(a) Flat Price

(b) Real Time Price

(c) Price Profiles

Fig. 3.7: Total electricity consumption on a average winter day for (a) the average flat price and (b) a real time price. The price signal and its mean average price are repeated in (c)

consumption is shifted by 1h15 to 10h00 (not visible on the figure). This makes sense as this is the cheapest moment before 13h00 (stop time of the washingmachine). The tumble dryer starts at its normal start time. The EV's consumption in not shifted much and it is charged at full power overnight. At 7h00 the price is more expensive and the EV stops charging. At 10h00 it resumes to charge its last needed energy. When receiving a flat price, it doesn't matter when wet appliances are used and EVs are charged. Also notice that the overall power constraint of the house is never violated. Only during the morning peak the maximum amount of power is drawn.

3.6 Neighbourhood

In the previous sections, the model of a house and all the devices it may contain were described. In this model, several parameters are stochastically defined. Among these parameters are penetration rates of the appliances and different types of houses (the matrices A and B in (3.1)). An additional parameter that needs to be defined is the number of occupants per household. This number is also defined as a stochastic parameter in each house and is inspired on the population structure of Belgium, which is shown in table 3.4. Because of these stochastic parameters, multiple houses have to be created to represent the reality more or less correctly. These houses can be grouped together into a *neighbourhood*.

# occupants per household	1	2	3	4	≥ 5
% of total households	33.6	31.8	15.2	12.7	6.7

Table 3.4: The percentage of private households per household size inspired by the population structure in Belgium [57]

Also, the profiles of individual consumers are unique, but for a large number of customers, individual peak demands are levelled out. According to Veldman [70] individual peaks are flattened out from 70 households and more. In order to obtain more aggregated profiles, we create neighbourhoods. A neighbourhood consists of several stochastic generated, thus different houses. The neighbourhood can be seen as a group of customers that are all connected to the low voltage transformer. Following Veldman [70], all neighbourhoods will consist of 70 individual households. A neighbourhood's energy consumption can be optimized in the same way as an individual household. An RTP is sent to the neighbourhood, which in turn sends this to all households which then optimize individually their electricity consumption as described in section 3.5. Hence, this results in 70 small optimizations instead of one big optimization. This was done in this way because of computational reasons.

Also, by writing the optimization in this way, it could be extended in future work, e.g. taking into account the limit of a distribution transformer of a neighbourhood and taking into account more characteristics of the distribution network. Introducing nodal pricing [71] or distributed algorithms for smart grids like those in [72] would

also be improvements that could be made to our model in the future as they will lead to a more economical use of the grid.

3.6.1 Minimum and Maximum Power Consumption

In chapter 4 the amount of flexibility in residential electricity demand for each hour will be determined. However, every hour there is a minimum amount of power P_{min}^{NH} (e.g. non flexible appliances) that must be consumed and a maximum amount of power P_{max}^{NH} (e.g. the overall constraint on a dwelling) that can be consumed. In order to get these limits for a neighbourhood for each time step, we impose price signals like those in Fig. 3.8. To determine the maximum power limit in hour j, the price is set to zero at this hour and to one at all other hours. The inverse is done for determining the minimum power limit at hour j.

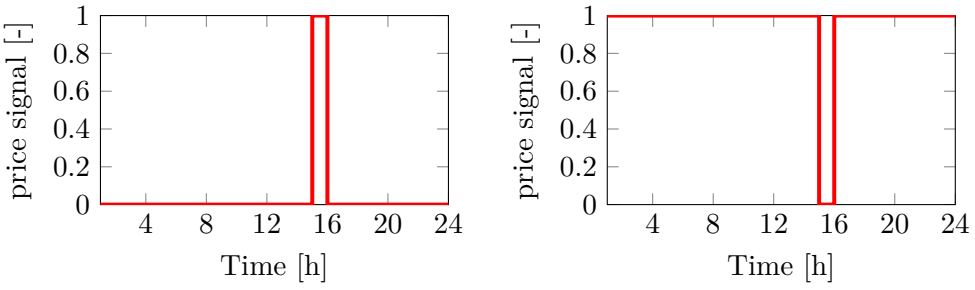

(a) Minimum (b) Maximum

Fig. 3.8: Price signals for (a) determining the minimum possible electricity consumption and (b) the maximum possible electricity consumption at the 15^{th} hour

3.6.2 Example: Optimization of a Neighbourhood

Here, we give an example of the optimization of a neighbourhood of 70 households. We do this for three subsequent typical winter weekdays to show the daily patterns. The electricity consumption for the average flat price and for an RTP signal are plotted in Fig. 3.9. Note the difference in peak consumption between these two figures. The biggest peak in the RTP case is twice as big as the one when the neighbourhood is subject to a flat price. This can be explained by the *load syncing* of the heat pumps and EVs at the moments when the price is cheap, which is allowed since we did not implement any hard grid constraints. As explained earlier, we assume that our load shifting does not influence the price. For such a massive shift in demand this assumption will obviously not hold. Production will be rescheduled and the price profile will smooth out. This will reduce the load syncing behaviour.

For every household, one could draw the same conclusions as made in section 3.5.6. In every house of this neighbourhood, all comfort constraints will be satisfied. Since we are looking at the aggregate neighbourhood level, these individual constraints are of less interest. However, we can draw some overall qualitative conclusions:

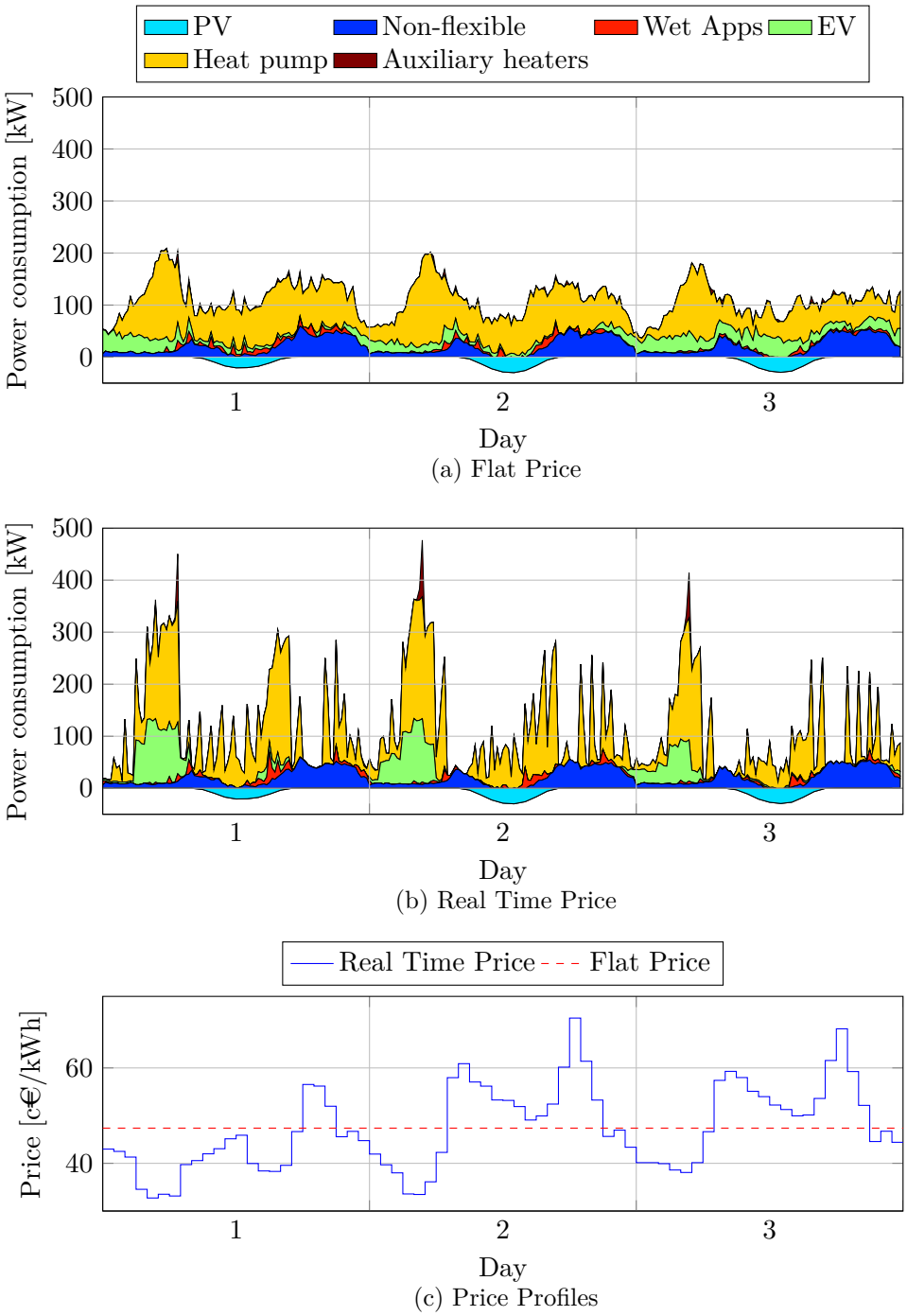

(a) Flat Price

(b) Real Time Price

(c) Price Profiles

Fig. 3.9: Total electricity consumption for a neighbourhood of 70 households for three subsequent winter weekdays for (a) the average flat price and (b) RTP. The RTP and its average flat price are shown in (c)

- When the households are subject to a flat price (no incentive to shift consumption) the electricity consumption of heat pumps and EVs is spread out more or less equally over all time slots. Imposing an RTP induces load syncing of these devices when prices are cheapest. Although difficult to see, wet appliances are shifted as much as possible to these moments too.
- One can notice a peak in the consumption of auxiliary heaters each day when the price is cheapest. This is due to extra space heating and heating the water in the tank in order to heat less later. As explained in section 3.5.6 this will cause more energy losses than in the flat price case.
- We did not include a distribution transformer limit or other grid constraints. Hence, the maximum allowed amount of power would be the overall power constraint for each house, namely 644 kW ($70 \cdot 9.2$ kW). As can be noticed in Fig. 3.9b this limit is not, and will almost never be reached.

3.7 Conclusion

In this chapter, we described the models for the different devices taken into account. The part of electricity demand that we consider to be non-flexible and the occupancy of the different houses is based on a stochastic model. Flexible demand consists of part discrete devices and part continuous devices whose electricity consumption can be shifted in time. Discrete devices include washing machines, tumble dryers and dishwashers. Continuous devices include EVs and heating. These devices are grouped together into a house based on their penetration rates. A house can be one of the three types we consider as explained in section 3.3.2. Then, a house's flexible demand is optimized to least cost considering a RTP signal (e.g. this is known on a day-ahead basis). This results in a mixed-integer problem where flexible appliances can be shifted within the comfort constraints imposed by the users. These comfort constraints are mathematically elaborated in section 3.5. We can perform this optimization for any day of the year. For each day the ambient temperature and incoming solar radiation are different and hence the energy needs differ. An example of the optimization of a single house is presented in section 3.5.6. In order to represent a correct population structure, level out individual peaks and to have a correct penetration rate of devices, a neighbourhood consisting of multiple houses is created. The flexible demand of such a neighbourhood can again be optimized in the same way as a single house as was explained in section 3.6.2. In the next chapter the optimization of such neighbourhoods will be used further to quantify the electric flexibility in the form of price elasticities.

Chapter 4

Linear Regression and Monte Carlo Simulation

4.1 Introduction

In chapter 3 we have explained how we have designed a bottom-up model of a neighbourhood with three types of flexible devices allocated in different houses: electric heating equipment, EVs and wet appliances. The neighbourhood is able to react to a RTP signal: the energy consumption of the flexible devices of each household is scheduled in such a way as to minimize cost. This results in a certain electricity consumption that is related to the price signal given.

In a first part, this chapter discusses how the relationship between the given price signal and the electricity output for a particular neighbourhood can be approximated in a linear way. First, we explain the processes needed to prepare the data for the regression. Subsequently, we perform a linear regression on this data to get an estimate of the price elasticity matrix. This PEM determines the relationship between a relative increase in price and a relative increase in electricity consumption w.r.t. a reference scenario (a reference price signal and corresponding electricity consumption). Then, we perform a selective regression in order to retain only the significant values in the final model. This allows to determine the time span in which prices have an influence on the electricity consumption of a certain hour. Subsequently, we explain how we can determine the influence of the three different types of appliances, by calculating their separate elasticities. Finally, we discuss a logistic regression as a higher order approximation. This gives insight in the limitations of the linear regression. Throughout this section the same neighbourhood — a neighbourhood on an average winter weekday of 70 households — is used to give some illustrative examples.

In a second part, we explain the Monte Carlo simulation. This is used to obtain an estimation of average values over all possible neighbourhoods, since every neighbourhood is different. The goal is to obtain an estimate of the mean and the statistical variance of the values of the elasticity matrix, the minimal and maximal electricity use and the reference electricity use at a certain reference price.

4.2 Linear Regression

Elasticities The goal of the linear regression is to obtain the elasticity matrix $\epsilon_{N\times N}$ as described in 2.4.3. This matrix assumes a linear relationship between a relative change in price and a relative change in electricity demand, at a certain point (p_{ref}, q_{ref}) on the demand curve:

$$\epsilon_{N\times N} \cdot \Delta p = \Delta q \tag{4.1}$$

with

$$\epsilon_{N\times N} = \begin{pmatrix} \epsilon_{11} & \cdots & \epsilon_{1N} \\ \vdots & \ddots & \vdots \\ \epsilon_{N1} & \cdots & \epsilon_{NN} \end{pmatrix} \tag{4.2}$$

and:

$$\Delta q = \frac{q - q_{ref}}{q_{ref}} \tag{4.3a}$$

$$\Delta p = \frac{p - p_{ref}}{p_{ref}} \tag{4.3b}$$

the relative differences in electricity consumption and price respectively. In this equation, $q = (q_1, \ldots, q_N)$ is the hourly electricity consumption vector in Watt corresponding to the electricity price vector per hour $p = (p_1, \ldots, p_N)$ and q_{ref} the known reference electricity consumption vector with p_{ref} as a reference electricity price vector.

Price elasticities are formally defined in a point (p_{ref}, q_{ref}) as:

$$\epsilon_{ij} = \frac{\partial q_i(p_{ref})}{\partial p_j} \cdot \frac{p_{ref,j}}{q_{ref,i}}. \tag{4.4}$$

If we assume a linear demand curve ($q_i = \sum_{j=1}^{N} \alpha_j p_j$), the partial derivative in (4.4) is just the coefficient α_j, and the same as a finite difference. The elasticity ϵ_{ij} can then be calculated as $\epsilon_{ij} = \Delta q_i / \Delta p_j$. This justifies the use of equation (4.1) and the linear regression as a linear approximation of the real price elasticity. Of course this omits higher order effects, but since the goal of this thesis is a linear model, this will always be the case. Further on in this chapter (section 4.2.4) we will discuss a non-linear, logistic model that offers more insight in the limitations of assuming a linear demand curve.

Cyclical Constraints The cyclical constraints (see section 3.5.5) need some extra attention. For the electricity use at hour 1 (q_1) for example, the price at hour N will have a negligible effect on q_1. However, because of the cyclical constraint this price has actually also the function of an hypothetical price at hour 0, of which the influence will be much stronger, since it is an adjacent hour. This means that the prices at the upper right triangle of the elasticity matrix have actually the function of being left of the matrix. This is analogous for the lower left triangle, as is displayed

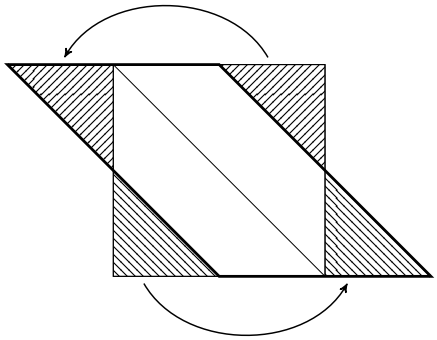

Fig. 4.1: Effect of the cyclical constraints on the elasticity matrix (4.2).

in Fig. 4.1. So, given a time horizon N, we are actually investigating the effect of the prices $j = i \dots i \pm (N-1)/2$ around the hour i. We can thus speak of the diagonal values ϵ_{ii} as the *middle* ones, since the other elements are really placed symmetrically around them. With this in mind, different days can be put after each other, in order to get a long shifted *band* of values that spans more than the original time horizon N.

The time horizon N of prices that have an influence on the electricity use needs to be determined, since this sets the size of the elasticity matrix. An intuitive answer would be $N = 24$ since the typical cycle of residential electricity use repeats itself every 24 hours. Also the wholesale market works with day ahead scheduling. However, it might be possible that electricity use can be shifted more than 24 hours if sufficient big storage would be available in some form. Later on in this chapter (section 4.2.2) we will prove however that these influences are not significant in our approach and a horizon of $N = 24$ is sufficient.

4.2.1 Data Gathering and Processing

First thing needed for performing a regression is data: in our case a sufficient big number of price vectors p and their corresponding electricity consumption vectors q, for a specific neighbourhood. We will refer to such a couple as a specific (p, q) point. The price vectors p used here are obtained from Belpex prices [67]. In order to have a sufficient amount of price vectors we use the spot prices of the wholesale market of 2012 and 2013. We will use the superscript k to denote a specific price p^k with corresponding electricity use q^k, further also referred to as *samples*. The total *sample size* used is then $n = 728$, which is the total number of prices available for 2012 and 2013.

Relative Prices The cost of a house's or a neighbourhood's energy consumption is minimized within a given time horizon N (e.g. one day). The relative price values, rather than the absolute ones, determine the final electricity use. We observe indeed that price vectors with the same course but different average values return the same

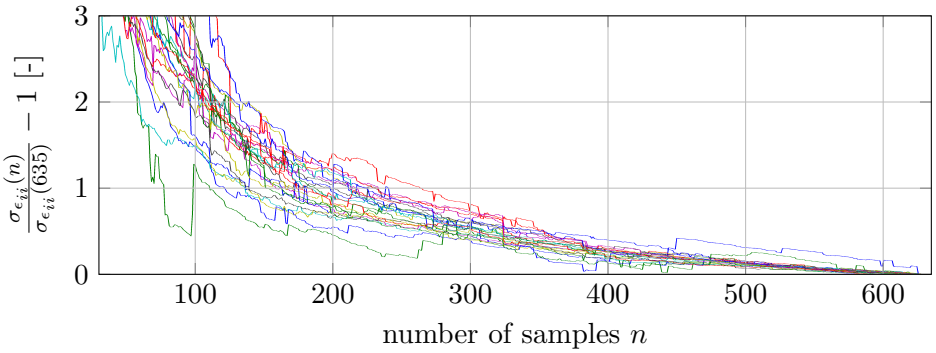

Fig. 4.2: Convergence of the standard deviance $\sigma_{\epsilon_{ii}}$ of the own price elasticity ϵ_{ii}, in function of the number of samples n used. Each line represents one own elasticity.

electricity use as output. This is logical since we are not considering a decrease in electricity consumption caused by an increased average price over the time horizon N (i.e. the long-term elasticities), but rather the shifting of electricity consumption within this time horizon (the short-term elasticities). To eliminate this effect of prices with a different mean value, each price vector p^k is rescaled so it has a mean value of one:

$$p^k_{rel} = \frac{p^k}{\bar{p}^k} = \frac{p^k}{\sum_{i=1}^{N} p^k_i / N}, \quad k = 1, ..., n \tag{4.5}$$

with $\bar{p}^k$ the average value of the price vector p^k.

To not let them influence the regression, extreme situations or outliers — price vectors with a price more than 3 times the standard deviation of the mean value for that hour[1] — are removed. For a time period of 1 day ($N = 24$), 635 price vectors are remaining after this step.

Sample Size The price signals p^k_{rel} are passed on to the neighbourhood which optimizes consumption every time, as described in section 3.6. The corresponding electricity use of the neighbourhood is retained as the corresponding q^k vector. This is the most time-consuming step of the simulation so a compromise had to be made between the number of (p^k, q^k) samples n needed and the computational time. A higher number of samples will result in a better regression, but the computational time increases linearly with n. To get an idea of the number of samples needed, we performed 635 optimizations on a particular neighbourhood and calculated every time an elasticity matrix $\epsilon^n_{N\times N}$. The coefficients ϵ_{ij} and their statistical error $\sigma_{\epsilon_{ij}}$ (as explained further, equation (4.17)) should converge with a larger number of samples. Since the own-price elasticities ϵ_{ii} are the most important ones, we look at the convergence of their standard deviation $\sigma_{\epsilon_{ii}}$. These are plotted in Fig. 4.2, with

[1] Three times the standard deviation includes 99.7 % of the values in a normal distribution.

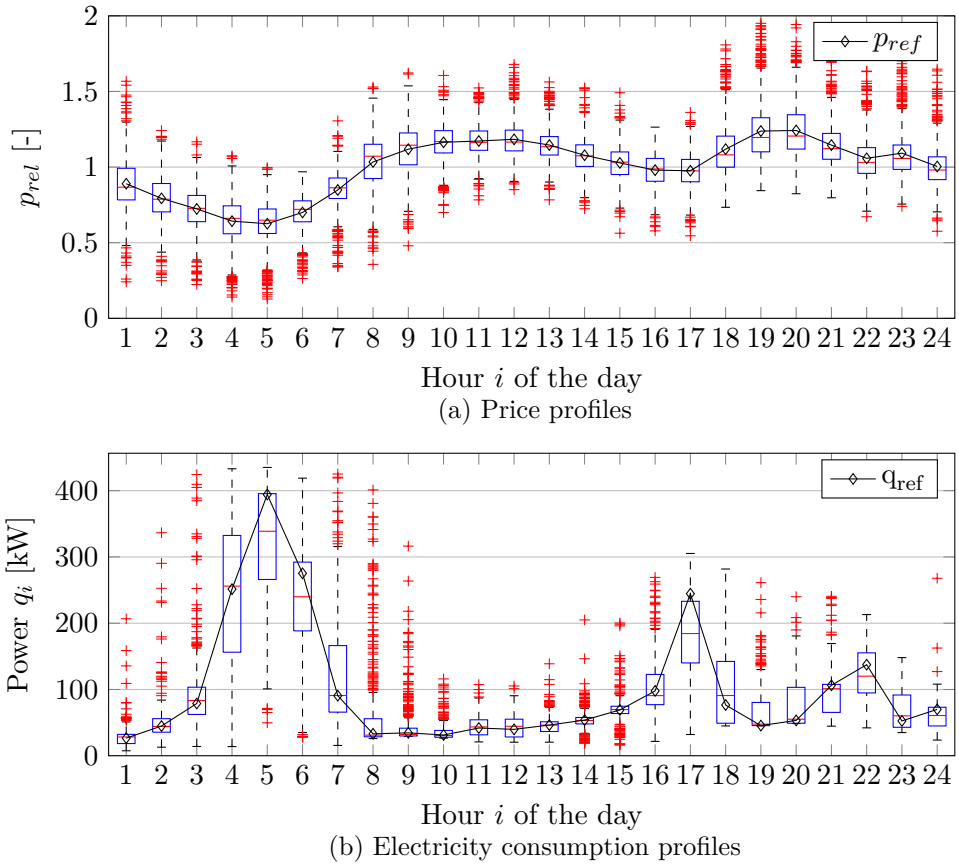

Fig. 4.3: Box plot of all price vectors p^k_{rel} with mean reference price p_{ref} (a) and electricity use q^k with corresponding reference electricity use q_{ref} (b). Neighbourhood of 70 houses on a winter weekday.

respect to the $\sigma_{\epsilon_{ii}}$ obtained after all 635 samples used. One can clearly see a trend of convergence, and we chose $n = 350$ as a good number of samples, which is further used for the regressions.

Resulting Data Fig. 4.3b shows a box plot[2] of all the q^k vectors obtained from the neighbourhood, corresponding to all the price profiles of Fig. 4.3a. Notice that there is a lot of variation in electricity consumption during the night, notably less during the day and again more during the evening. This might be interpreted as more flexibility being available during the night and less during the day, which can mainly be explained by the fact that more EVs are available then, and the heat pumps that are active since they need to warm up the houses for the morning, when people wake up.

[2]In the box plots, the box itself is defined by the 25$^{\text{th}}$ percentile q_1 as lower border and the 75$^{\text{th}}$ percentile q_3 as upper border. Outliers, the crosses, are then defined as points $> q_3 + 1.5(q_3 - q_1)$ or $< q_1 - 1.5(q_3 - q_1)$.

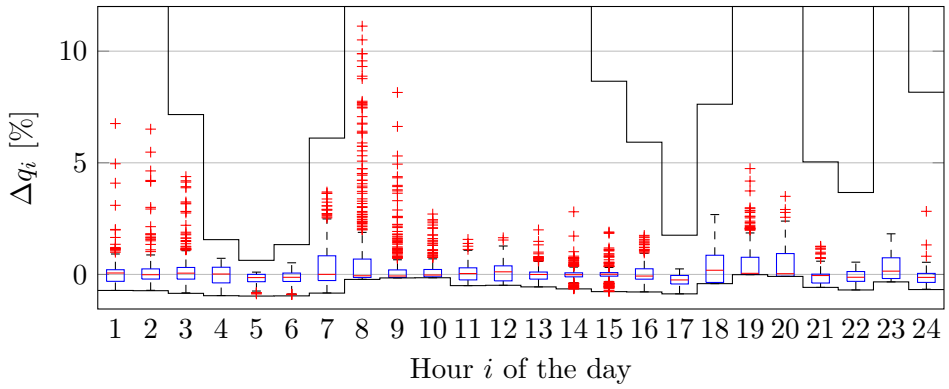

Fig. 4.4: Box plot of Δq for a neighbourhood of 70 houses on a winter weekday, for 350 prices. The upper black line is Δq_{max} and the lower black line Δq_{min}, the maximal and minimal relative shift in electricity consumption possible.

The (p^k, q^k) pairs obtained from the optimizations described above have to be made relative w.r.t. a reference price p_{ref} and related electricity consumption q_{ref} respectively, in order to meet equation 4.1. This can be done with regard to any reference price p_{ref} possible. The reference price we use is the mean value of all 635 price vectors, as shown in Fig. 4.3a. The differences between the prices and this reference price are then minimal and a more linear behaviour can be expected, but of course other reference prices are possible.

The reference electricity consumption q_{ref} is the electricity use of the neighbourhood when subject to the reference price p_{ref}. The electricity use without PV is taken as q_{ref}, as plotted in Fig. 4.3b. This because the PV production makes the electricity demand drop below zero around noon. If we then would apply (4.3a), the sign of Δq_i would reverse and so would the sign of ϵ_{ij}. Furthermore, at the zero crossing of $q_{ref,withPV}$, (4.3a) would become very big because of the division through a small value $q_{ref,i}$. Both cases are unwanted, and with choosing q_{ref} without the effect of PV production, these issues do not occur. The q_{ref} for the neighbourhood is plotted in Fig. 4.3b and peaks can clearly be observed during the cheap hours.

Once a reference price and related electricity use are determined, (4.3) can be applied to all (p^k, q^k) pairs in order to get $(\Delta p^k, \Delta q^k)$ pairs, which can be used for the linear regression.

As a last step, outliers, samples Δq_i^k that differ more than 3 times the standard deviations from the mean value of Δq_i, are also removed from the sample set[3]. An example of all resulting Δq^k after performing these steps is given in Fig. 4.4 for the same neighbourhood as in Fig. 4.3b. The small values during noon are as expected, since in absolute values (Fig. 4.3b) deviations are small too. The small variations at hours 4–6 can be explained by the high q_{ref} at those moments. Hour 8 has many higher values because q_{ref} is small there, and in many situations a lot of demand can be shifted to this hour.

[3]Three times the standard deviation includes 99.7 % of the values in a normal distribution.

The minimum and maximum relative shift in electric consumption possible for a neighbourhood, $\Delta q_{min,i}$ and $\Delta q_{max,i}$ respectively, need to be determined, since these values limit the linear range of the price-demand curves. These are calculated by performing (4.3a) on $P^{NH}_{max,i}$ and $P^{NH}_{min,i}$ from section 3.6. Fig. 4.4 also plots these values. One can see that the electricity shift Δq_i is indeed never below the minimum value Δq_{min}, but does equal it sometimes. This is in contrast to the maximum shift Δq_{max} which is never reached.

For each time step i, Δq_i, can thus only take on values in between $\Delta q_{min,i}$ and $\Delta q_{max,i}$. Since we are only interested in determining the slope of the linear part of Δq_i, samples Δq_i^k that are equal to $\Delta q_{min,i}$ or $\Delta q_{max,i}$ are removed from the sample set as they are not part of the linear slope and would bias the regression.

Different Price Profile The price profiles imposed on the neighbourhood (Fig. 4.3a) have an influence on the results obtained from the optimizations and consequently affect the points that are taken into account in the regression. The regression determines the values of the price elasticities and thus the final values of these elasticities depend on the price profiles used. In this thesis, we have used wholesale price profiles from Belpex [67] of 2012 and 2013 as this was the only data available. In 2050, however, one can imagine that the course of the price profiles will be different from the one we experience today due to the integration of a large share of intermittent RES. A question that can be raised now is whether our regression will still be valid if a price profile with a completely different course would be imposed.

Take for example a price profile that is cheap during noon (e.g. when the sun is shining and a large amount of cheap PV power is produced) and more expensive in the morning and the evening. This course is more or less the opposite of the reference price signal we used throughout this thesis (see Fig. 4.3a). Such an (artificial) price profile and the corresponding electricity demand for a neighbourhood of 70 households are shown in Fig. 4.5. The box plots represent the 350 different points used in the regression and are the same as in Fig. 4.3b.

As can be seen from Fig. 4.5b, the resulting demand profile from this new price signal still lies comfortably within the range of points we included in our regression. This is of particular interest from hour 10 to 13 as in these hours the consumption only varies slightly. It is clear now that this is not the consequence of the price profiles we imposed, but rather of less electricity that can be consumed during these hours. Only in the 14^{th} hour (when the price is cheapest), the demand attains a value that exceeds slightly the biggest outlier taken into account in our regression. Overall, we can say that the regression will also take into account values that occur with completely different price profiles.

4.2.2 Regression

To obtain the linear price elasticities, we perform a linear regression that relates a vector Δp of size N (24 in case of one day) to a vector Δq, also of size N. These are actually N independent regressions for each $\Delta q_i, i = 1, \ldots, N$ if we assume that each element Δq_i is only dependent on Δp. Hence, we have to perform N multiple

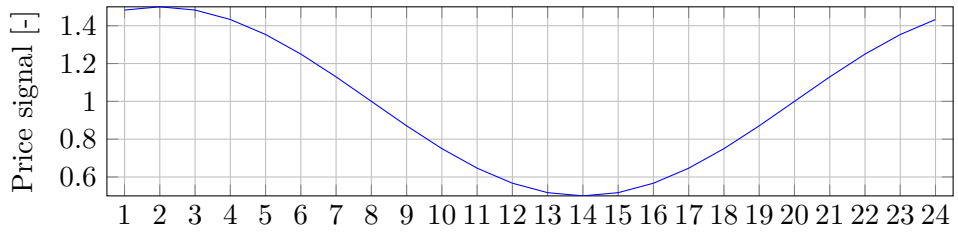

(a) Price profile

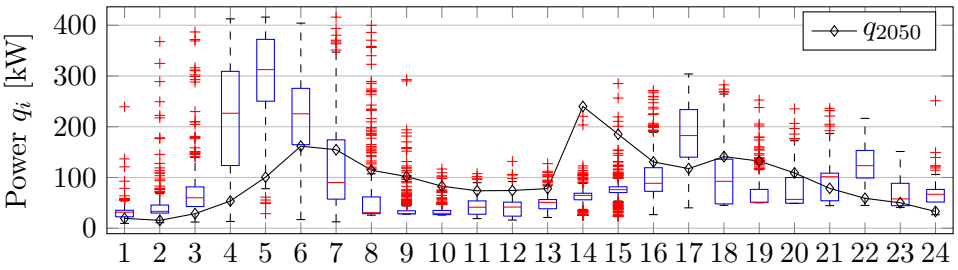

(b) Electricity consumption

Fig. 4.5: Example price profile in 2050 (a) and box plot of electricity use q^k as displayed in Fig. 4.3b with the electricity use q_{2050} subject to the example price profile denoted by the black diamond line.

linear regressions. This means finding a vector $\boldsymbol{\epsilon_i} = (\epsilon_{i1}, \epsilon_{i2}, \ldots, \epsilon_{iN})$ such that:

$$\Delta q_i^k = \boldsymbol{\epsilon_i} \Delta p^k + err_i^k \tag{4.6}$$

with err_i^k the error on the linear model for time step i and sample k.

If we define:

$$\boldsymbol{err_i} = (err_i^1, \ldots, err_i^n) \tag{4.7}$$

$$\boldsymbol{\Delta q_i} = (\Delta q_i^1, \Delta q_i^2, \ldots, \Delta q_i^n), \quad \forall i = 1, \ldots, N \tag{4.8}$$

and:

$$\boldsymbol{\Delta p} = \begin{pmatrix} \Delta p_1^1 & \cdots & \Delta p_1^n \\ \vdots & & \vdots \\ \Delta p_N^1 & \cdots & \Delta p_N^n \end{pmatrix} = (\Delta p^1, \ldots, \Delta p^n) \tag{4.9}$$

we have a linear multiple regression from $\boldsymbol{\Delta p}$ to $\boldsymbol{\Delta q_i}$, which can be completely summarized as:

$$\boldsymbol{\Delta q_i} = \boldsymbol{\epsilon_i} \boldsymbol{\Delta p} + \boldsymbol{err_i}, \quad \forall i = 1, \ldots, N \tag{4.10}$$

Least Squares

An unbiased estimator for $\boldsymbol{\epsilon_i}$ is the least square estimator $\hat{\boldsymbol{\epsilon}}_{\boldsymbol{i}}$:

$$\hat{\boldsymbol{\epsilon}}_{\boldsymbol{i}} = (\boldsymbol{\Delta p}^T \boldsymbol{\Delta p})^{-1} \boldsymbol{\Delta p}^T \boldsymbol{\Delta q_i} \tag{4.11}$$

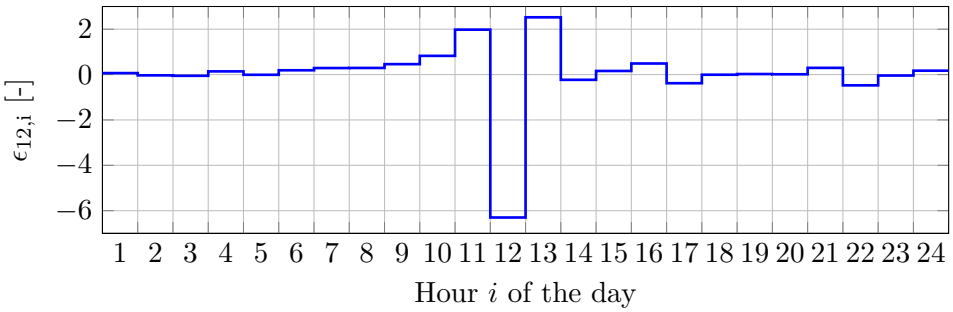

Fig. 4.6: Price elasticities of electric demand at hour 12 for a neighbourhood of 70 houses during a winter weekday

Since we applied (4.5) on each p^k, the matrix $\boldsymbol{\Delta p}$ has only $N-1$ independent rows. The classical linear model cannot be applied to matrices less than full row rank N [73], because $\boldsymbol{\Delta p}^T \boldsymbol{\Delta p}$ from (4.11) is then singular. We can bypass this problem by using the Moore-Penrose pseudo inverse [74]:

$$\boldsymbol{\Delta p}^+ = VS^+U^T \tag{4.12}$$

with $\boldsymbol{\Delta p} = USV^T$ the singular value decomposition of $\boldsymbol{\Delta p}$. The estimator $\hat{\boldsymbol{\epsilon}}_{\boldsymbol{i}}$ is then:

$$\hat{\boldsymbol{\epsilon}}_{\boldsymbol{i}} = \boldsymbol{\Delta p}^+ \boldsymbol{\Delta q}_{\boldsymbol{i}} \tag{4.13}$$

An example of $\hat{\boldsymbol{\epsilon}}_{\boldsymbol{i}}$ calculated for $i = 12$ for a specific neighbourhood of 70 houses during a winter weekday is given in Fig. 4.6. It can be clearly noticed that the own-price elasticity $\epsilon_{12,12}$ is negative and has the most influence. The values $\epsilon_{12,13}$ and $\epsilon_{12,11}$ are both positive and still fairly big, meaning that if the price is high in these adjacent hours, electricity consumption at hour 12 will rise. The other values of $\epsilon_{12,i}$ further away from hour 12 are smaller, so less important. This confirms our intuition that the electricity consumption at an hour i is only influenced by prices close to this hour i.

In a linear regression, the coefficient of determination R^2 would be a good indicator of the quality of the fit. Here, however, this is not the case since we are performing a regression without intercept[4] [75]. The R^2 value is quite meaningless then, so other indicators have to be used. A general test that can be performed to check if the linear regression is meaningful, is the test of significance. This is a statistical test that checks if all coefficients of the multiple linear regression (4.10) are significant. The null hypothesis is then defined as:

$$H_0: \quad \epsilon_{i1} = \epsilon_{i2} = \ldots = \epsilon_{iN} = 0$$

[4]Equation (4.1) does not have an intercept. If Δp is zero, Δq should also be zero, since this is the reference scenario.

This results in the following *F-statistic* [75]:

$$F = \frac{MSreg}{MSerr} = \frac{SSreg/N}{SSerr/(n-N)} = \frac{\sum_{k=1}^{n} (\Delta\hat{q}_i^k - \Delta\bar{q}_i^k)^2/N}{\sum_{k=1}^{n} (err^k)^2/(n-N)} \tag{4.14}$$

with $MSreg$ the *mean sum of squares* of the regression model, $MSerr$ the *mean sum of squares* of the error, $SSreg$ the sum of squares of the model, $SSerr$ the sum of squares of the errors, $\Delta\hat{q}_i$ the calculated Δq_i^k according to the regression.

This F-statistic has an *F-distribution* with N and $(n-N)$ degrees of freedom. This is also written as: $F \sim F(N, n-N)$. The *p-value* is then defined as the significance level or the probability that the null hypothesis H_0 is true. Applying (4.14) to our regression (4.13) results in *p-values* of approximately zero for every Δq_i, meaning that we can reject H_0 with a very strong presumption. Hence, we can conclude that the linear regression is indeed meaningful.

Selective Regression

As can be seen in Fig. 4.6, not every hour contributes the same to the resultant Δq_i. We would obtain a better[5] model if we could exclude the hours that do not contribute to Δq_i, and only retain the hours that are really significant. The result would be interesting, as it allows to determine the time span of prices around the middle value that have an influence on the electricity consumption. This can be done formally by performing a *selective regression*, in which only the variables that are statistically relevant are taken into account. This results in a reduced linear model $\epsilon_{N\times N}^{sel}$. Since the full matrix $\epsilon_{N\times N}^{full}$ from (4.13) contains all coefficients $\epsilon_{ij}, j = 1, \ldots, N$, the matrix $\epsilon_{N\times N}^{sel}$ can be thought of as a linear model 'nested' inside the full linear model $\epsilon_{N\times N}^{full}$.

A statistical *F-test* can be used to determine if a full model (with more coefficients) really fits the data better than the nested model (with less coefficients). Let ϵ_{sub} be the vector of all ϵ_{ij} that are zero in the nested model. The hypothesis test is then:

$$H_0: \quad \epsilon_{sub} = 0 \qquad \text{against} \qquad H_1: \quad \epsilon_{sub} \neq 0 \tag{4.15}$$

This results in an F-statistic with $p_2 - p_1$ and $n - p_2$ degrees of freedom [76]:

$$F = \frac{(SSerr_1 - SSerr_2)/(p_2 - p_1)}{SSerr_2/(n - p_2)} \tag{4.16}$$

with $SSerr_1$ and $SSerr_2$ the sum of squares of the errors of the nested model 1 and the full model 2 respectively, p_1 and p_2 the number of coefficients of model 1 and 2, so that $p_2 > p_1$.

Of course it is desired that the full model ϵ_i^{full} does not fit the data better than the reduced model ϵ_i^{sel}. A high p-value of (4.16) is then needed, in order not to reject the null hypothesis (4.15). In that case there is no reason to keep using the full model, and the reduced model can be used instead.

[5] The model would become 'better' in the way that it has almost the same predictive power with less coefficients needed.

Conventional Forward Selection A general method to perform this selection, is the stepwise selection technique [77]. The result of performing the conventional forward selection procedure is displayed in Fig. 4.7. As desired, a selection is made and only the values ϵ_{ij} that are statistically significant are retained. However, one can see that the remaining values ϵ_{ij} are not as centred around the middle values ϵ_{ii} as one would expect. Also many values ϵ_{ij} are present that are far from this middle value ϵ_{ii}. This can be explained by the fact that this selection method does not know that we really are looking for the relevant values ϵ_{ij} centred around ϵ_{ii}. It assumes a-priori equality of importance of every value ϵ_{ij}, while we actually want a model that assumes that values close to the middle values are more important.

The p-values of the hypothesis test (4.16) are shown in Fig. 4.8. They are always greater than 0.05[6] so there is no need to reject the null hypothesis H_0 (4.16), meaning that the full model ϵ_i^{full} is not a better fit than the reduced model ϵ_i^{sel}. The values of coefficients that are common to both models are all quite similar. The selective regression does thus not really change the values, but just eliminates the ones that are not necessary.

Adapted Selection Procedure What we really want is a matrix $\epsilon_{N\times N}^{sel}$ with only the statistically relevant coefficients ϵ_{ij} centred around the middle value ϵ_{ii} of each row i. Of course the model $\epsilon_{N\times N}^{sel}$ should be as good as the full model $\epsilon_{N\times N}^{full}$. We adapt the forward selection procedure to better follow this reasoning. The adapted procedure is as follows.

We know that the own elasticity ϵ_{ii} is the most important coefficient for each hour, so we start by performing a regression with only this coefficient. We assume that the importance of coefficients decreases when moving away from ϵ_{ii}. So the first step will be adding the coefficient $\epsilon_{i,i+1}$ to the right. Determining if this added coefficient is significant can be done by applying (4.16), where model 1 is the model with only ϵ_{ii} and model 2 the model with the two coefficients ϵ_{ii} and $\epsilon_{i,i+1}$. If the p-value is lower than 0.05, the added coefficient $\epsilon_{i,i+1}$ is said to be significant, because we then have to reject the null hypothesis H_0 (4.15), meaning that the added coefficient is not equal to zero. If this is the case, the model is extended with $\epsilon_{i,i+1}$, and if this is not the case the model is kept as it was (now only with ϵ_{ii}). Subsequently, we add the coefficient to the left $\epsilon_{i,i-1}$. The same test is done, and if this coefficient is significant it is kept in the model. Next a new coefficient to the right $\epsilon_{i,i+2}$ is investigated and added if significant and so on. These steps are repeated until we can be sure that the new model ϵ_i^{sel} is as good as the full model ϵ_i^{full}. This can be tested by performing (4.16) every time, with the full model as reference. The algorithm is then stopped once (4.16) with ϵ_i^{full} as reference gives a p-value greater than 0.05.

The final model $\epsilon_{N\times N}^{sel}$ is displayed in Fig. 4.7, by the blue circles. One can clearly notice that the values are much more centred around the middle value ϵ_{ii}. The influence of prices is clearly limited to less than $i \pm 12$. This means that we can work with only one day ($N = 24$) as time horizon, since only the influence of prices

[6]Since the p-value is defined as the probability that the null hypothesis is true, a p-value lower than 0.05 would mean that one can reject the null hypothesis with a probability of 95 %.

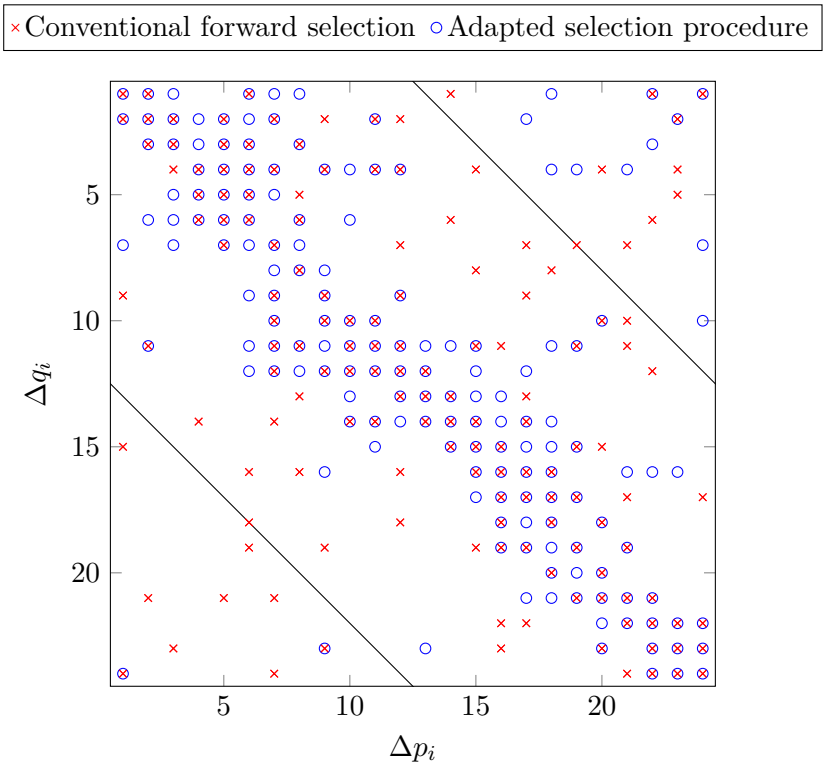

Fig. 4.7: Elasticity matrix for one day (N=24), with the conventional forward selection procedure and the adapted selection procedure. The black lines denote the values $i \pm 12$. Neighbourhood of 70 houses in a winter weekday.

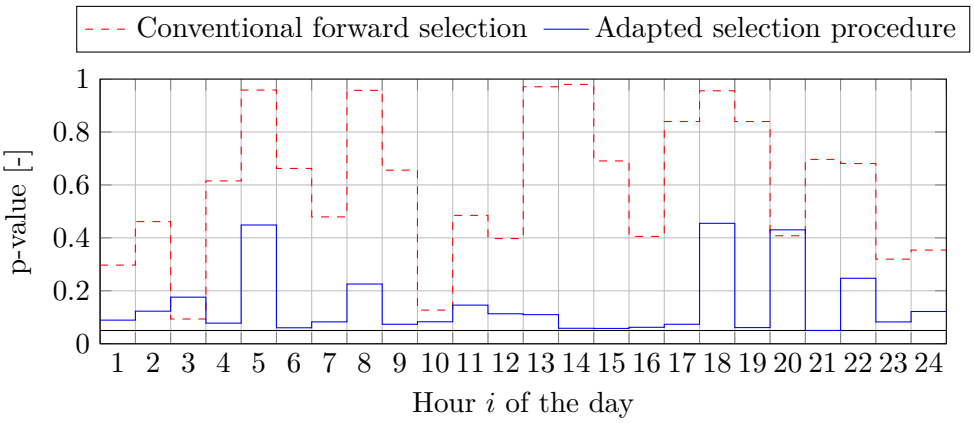

Fig. 4.8: P-values of (4.16) for the conventional forward selection and the adapted selection procedure, when compared to the full model ϵ_i^{full} (4.13). The lower black line denotes a p-value of 0.05.

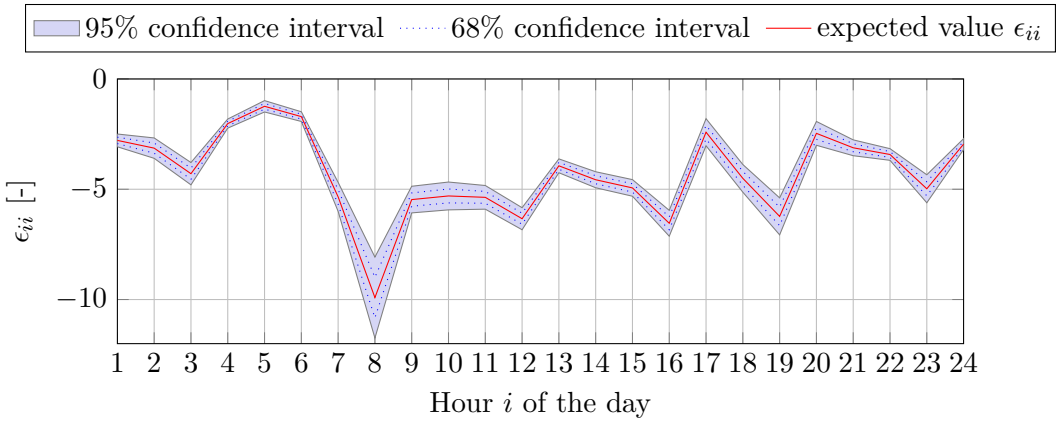

Fig. 4.9: Own elasticities ϵ_{ii} and their confidence intervals, from (4.17)

at hours $j > i + 12$ or $j < i - 12$ are statistically relevant. This is an important result, as it gives insight in the time interval in which electricity use is shifted. The p-values (Fig. 4.8) for every hour are higher than 0.05. so one can say that this model is also as good as the full model, and there is no need to take neither the full model nor the model from the conventional forwards selection.

Standard Error Because of the singularity of $\boldsymbol{\Delta p^T \Delta p}$, it was not possible to calculate the error on the estimates of the simple least squares regression. The selective regression does allow this, and one can calculate the covariance matrix of the coefficients $\boldsymbol{\epsilon_i}$:

$$Cov(\boldsymbol{\epsilon_i}) = \sigma^2(\boldsymbol{\Delta p^T \Delta p})^{-1} \tag{4.17}$$

with

$$\sigma^2 = \frac{SSerr}{n-p} = \frac{err_i^T err_i}{n-p} \tag{4.18}$$

the error variance of the estimate $\boldsymbol{\Delta q_i}$, n being the sample size and p the number of coefficients taken into account in hour i [73]. The diagonal of the covariance matrix $Cov(\boldsymbol{\epsilon_i})$ gives then the variance and thus also the standard error of the calculated coefficients: $diag(Cov(\boldsymbol{\epsilon_i})) = (\sigma^2_{\epsilon_{i1}}, \ldots, \sigma^2_{\epsilon_{iN}})$. This is a useful metric since it allows to calculate confidence intervals for the estimates ϵ_{ij}. A confidence interval is given by $\epsilon_{ij} \pm p \cdot \sigma_{\epsilon_{ij}}$, with $p = 1$ for a 68% confidence interval and $p = 2$ for a 95% confidence interval. A plot of the own elasticities ϵ_{ii} (the diagonal of $\epsilon_{N\times N}$) and their confidence intervals is illustrated in Fig. 4.9, for the same neighbourhood as described above. Notice the very low value of the own elasticity at hour 8. This can be explained by looking at Fig. 4.3b, where one can see that q_{ref} is low at hour 8, but there is a lot of potential to shift more electricity consumption to that hour. The confidence interval is the largest in hour 8, meaning that the estimate is least good there. This is probably because of the high amount of outliers at that hour, which can be seen in Fig. 4.3b and Fig. 4.4. However, this value $\sigma_{\epsilon_{8,8}} = 0.91$ is still fairly small when compared to the absolute value of the elasticity itself ($\epsilon_{8,8} = -9.91$).

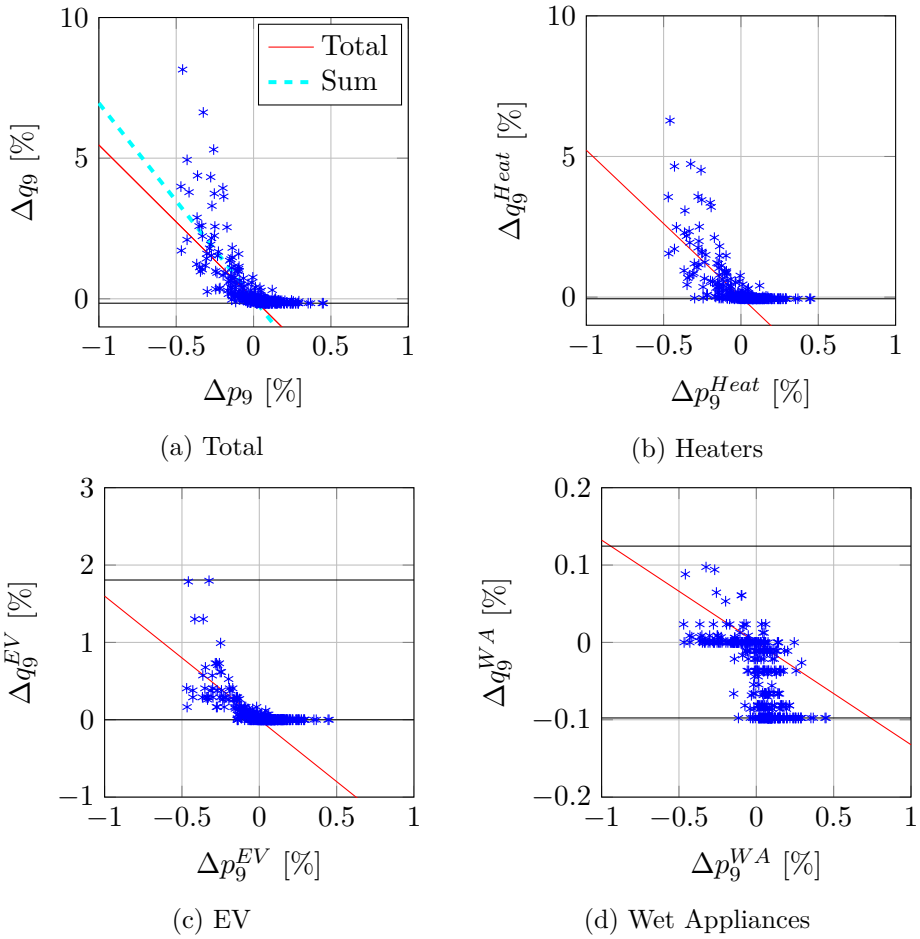

(a) Total

(b) Heaters

(c) EV

(d) Wet Appliances

Fig. 4.10: Scatter plots of Δq_9 against Δp_9 and the linear regression line through the origin, for all devices together (a), only heating devices (b), EVs (c) and wet appliances (d). The blue dotted line in (a) has a slope that is the sum of the slopes of the lines in (b), (c) and (d). The black lines denote the $\Delta q_{min,9}$ and $\Delta q_{max,9}$ limits.

Since this is the largest standard deviation, this means that our estimates ϵ_{ii} are all quite good (within 10 %).

4.2.3 Elasticity of Separate Devices

In order to be able to tell the influence of the three different types of flexible devices discussed (wet appliances, EVs and heaters), it is possible to calculate the elasticity matrix $\epsilon_{N\times N}$ for each type of device separately. This can be seen when considering following equation:

$$\epsilon_{N\times N}\cdot\Delta p=\Delta q=\frac{q-q_{ref}}{q_{ref}}=\frac{q^{WA}-q^{WA}_{ref}}{q_{ref}}+\frac{q^{EV}-q^{EV}_{ref}}{q_{ref}}+\frac{q^{Heat}-q^{Heat}_{ref}}{q_{ref}}$$
$$=\epsilon^{WA}_{N\times N}\cdot\Delta p+\epsilon^{EV}_{N\times N}\cdot\Delta p+\epsilon^{Heat}_{N\times N}\cdot\Delta p, \qquad (4.19)$$

where q^{WA}, q^{EV} and q^{Heat} is the electricity use of the wet appliances, EVs and heaters respectively. The elasticity matrix can thus be split up into 3 'sub-matrices', one for each device, which are expected to sum up to the total matrix $\epsilon_{N\times N}$.

This means three separate linear regressions can be performed, in the same way as explained in section 4.2.2, but with Δq each time calculated as indicated in (4.19). The results of these regressions are shown in Fig 4.10, for hour 9 and the same neighbourhood as used previously. The results for the other hours are given later in section 5.4.3, after a Monte Carlo simulation has been performed on them.

Fig. 4.10 shows a scatter plot Δq_9 against Δp_9 for each device separately, as indicated in (4.19), and also one for all devices together. All plots give the linear regression curve through the origin, so the slope indicates every time the own elasticity $\epsilon_{9,9}$. The dotted blue line in Fig. 4.10a has a slope $\epsilon^{sum}_{9,9}$ that is the sum of the slopes of the other elasticities: $\epsilon^{sum}_{9,9}=\epsilon^{Heat}_{9,9}+\epsilon^{EV}_{9,9}+\epsilon^{WA}_{9,9}$, as designated by (4.19). One can see that this sum does not fully coincides with the elasticity determined by the regression on Δq_9 of all devices together. This is caused by the the tail in Fig. 4.10a (the tail are the lower right values that are close to the lower limit $\Delta q_{min,9}$). In Fig. 4.10b, Fig. 4.10c and Fig. 4.10d, these values reaching $\Delta q_{min,9}$ are eliminated from the regression so they have no influence. In Fig. 4.10a , however, not all values in the tail are eliminated since e.g. values in the tail reaching $\Delta q^{EV}_{min,9}$ from Fig. 4.10c are not necessarily also reaching $\Delta q_{min,9}$ in Fig. 4.10a. This is because when looking at the whole neighbourhood it can for example occur that the EVs are all at their lowest energy consumption, but there is still one wet appliance that can be turned off. The neighbourhood as a whole is thus not at its minimum and the values that are actually belonging to this tail are not eliminated. Hence, they influence the linear regression. This leads to a lower slope or a less negative value of the own elasticity than expected when calculating the sum of the elasticities of the different devices (4.19).

4.2.4 Intermezzo: Logistic Regression

When looking at the scatter plots of Fig. 4.10, one can see that the $(\Delta p, \Delta q)$ points do not have a completely linear character, but rather follow a logistic function [78]. One can perform a transformation on the data in order to obtain a new linear relationship:

$$\log\left[\frac{(\Delta q-\Delta q_{min})\cdot\Delta q_{max}}{(\Delta q_{max}-\Delta q)\cdot(-\Delta q_{min})}\right]=\sum_{i=1}^{N}\alpha_i\Delta p_i. \qquad (4.20)$$

We observe indeed that this transformation makes our data points behave more linearly and this regression gives a better overall result. A fitted logistic curve through

the data points of Fig. 4.10a is displayed in Fig. 4.11. This clearly gives a good fit and a good description of the Δp–Δq behaviour of a residential neighbourhood with flexible demand. However, a major drawback of using (4.20) is that it is not a linear equation. Since one of the objectives of this thesis is to find a quantification of the residential flexibility in a linear way, the logistic curve as it is cannot be used.

It would be possible though to use tangents in specific points which would result in a first order approximation of the logistic curve. These tangents are linear equations and a good approximation of the logistic curve close to the tangent point. One can take this slope as an estimate for the elasticity ϵ_{ij}, which would also be in accordance to the definition (4.4). As example, two of these tangents are plotted in Fig. 4.11. Although the tangents are a good approximation close to the tangent point, further away from this point the approximation becomes quickly very coarse. Take for instance the tangent in the origin $(0, 0)$. The slope of this line is very small, which would result in very small elasticities, indicating little flexibility. However, one can see that there is quite some flexibility available in this hour, just not around the point (0,0), which would be the reference scenario. Using this slope as estimation for the elasticity would therefore result in a serious underestimation of the flexibility.

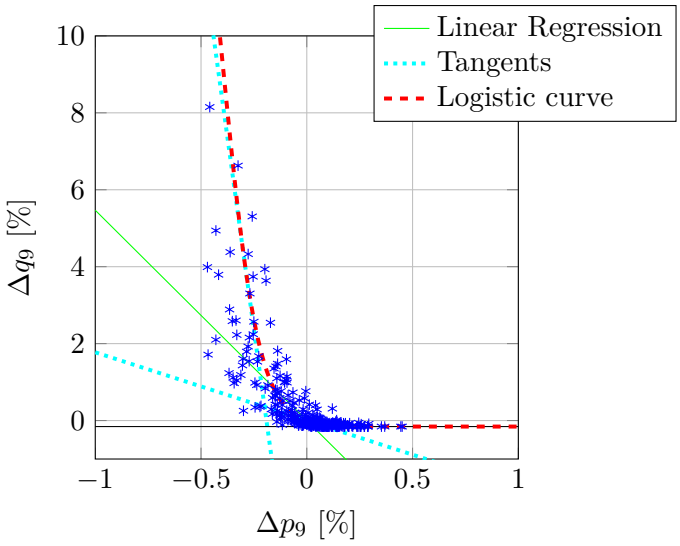

Fig. 4.11: Fit of a logistic curve through the data points and the origin at hour 9, according to (4.20). The blue lines are the tangents in the points (0,0) and (-0.30,4.36). The green solid line is the line of the linear regression as determined before.

When looking at the tangent in the point (-0.30,4.36), one can see the opposite behaviour. The slope of this tangent indicates a very big elasticity, thus very much flexibility, more than in reality is available. The slopes of the tangent lines of this logistic curve are thus not good estimators of the available flexibility *over the whole range*. The estimate made by the purely linear regression might not be the best curve to fit through the data points. However, as a linear approximation it gives

a balanced estimate of the flexibility over the whole range, in between the more extreme values one obtains when considering first order approximations of the logistic curve. We can conclude that the logistic curve is a more appropriate fit to estimate the price-demand curves that result from our simulations. However, as a linear estimate of the flexibility, the linear regression as explained in section 4.2.2 is a good compromise and we thus choose to keep on using this approach.

4.3 Monte Carlo

4.3.1 Overview of the Monte Carlo Methodology

The Monte Carlo technique is essentially a methodology that uses sample means to estimate population means [79]. Since population means can be described by integrals, the Monte Carlo method can also be used to evaluate an integral. Consider the function $z(x)$, which depends on a stochastic variable x with a probability density function (PDF) $f(x)$. Its mean, or expected value is then:

$$\langle z \rangle = \int_a^b z(x) f(x) dx, \tag{4.21}$$

where $f(x)dx$ is the probability the random variable has a value within dx about x, and the values x are in the range $[a, b]$. In the Monte Carlo method this integral is approximated by the *sample mean* of z:

$$\bar{z} = \frac{1}{N_m} \sum_{i=1}^{N_m} z(x_i), \tag{4.22}$$

where x_i are N_m randomly sampled values of the variable x according to its PDF $f(x)$. It can be shown then that $\lim_{N_m \to \infty} \bar{z} = \langle z \rangle$ [79].

A difference has to be made between the *Monte Carlo method* and a *Monte Carlo simulation*. In the former, the problem is explicitly stated as an integral (4.21), in the latter this formulation is hidden or unspecified. The simulation approach can really be seen as a stochastic simulation of some kind of physical process or mathematical model with a source of randomness. The result of a simulation is then a value $z(x_i)$, which is used in (4.22) to estimate the population mean $\langle z \rangle$. In fact, all Monte Carlo problems can be seen as a simulation or stated as an integral (4.21) but due to the distinct approach of the problem this differentiation makes sense.

Besides an estimate for the expected value $\langle z \rangle$ of the function $z(x)$, it is useful to have some information about the variance of the distribution of this value $z(x)$. This population variance $\sigma^2(z)$ depends on the unknown $\langle z \rangle$, but can be estimated by using the sample variance s^2:

$$s^2 = \frac{1}{N_m - 1} \sum_{i=1}^{N_m} [z(x_i) - \bar{z}]^2 = \frac{N_m}{N_m - 1} (\overline{z^2} - \bar{z}^2), \tag{4.23}$$

with $\bar{z}$ as in (4.22) and $\overline{z^2} = (1/N_m) \sum_{i=1}^{N_m} z(x_i)^2$. The sample standard deviation is then $s(z) = \sqrt{s^2(z)}$.

In order to have an idea of how good the estimate (4.22) of $\langle z \rangle$ is, the variance $\sigma(\bar{z})^2$ of $\bar{z}$ is needed. The standard deviation $\sigma(\bar{z})$ can be estimated by [80]:

$$\sigma(\bar{z}) \approx \frac{s(z)}{\sqrt{N_m}} \approx \sqrt{\frac{\overline{z^2} - \bar{z}^2}{N_m}}, \tag{4.24}$$

with $\bar{z}$ as in (4.22) and $\overline{z^2} = (1/N_m) \sum_{i=1}^{N_m} z(x_i)^2$. This variance is a measure for the goodness of the estimate and converges to zero with a rate $\sim \sqrt{1/N_m}$.

The *central limit theorem* tells us that $\bar{z}$ is asymptotically distributed as a normal distribution with a mean $\langle z \rangle$. The confidence intervals of the Monte Carlo estimate $\bar{z}$ of $\langle z \rangle$ can then be defined as:

$$\text{Prob}\left[\bar{z} - \lambda\sigma(\bar{z}) \leq \langle z \rangle \leq \bar{z} + \lambda\sigma(\bar{z})\right] = P, \tag{4.25}$$

where $P = 68\%$ for $\lambda = 1$ and $P = 95\%$ for $\lambda = 2$.

4.3.2 Applying Monte Carlo

The model of a house described in chapter 3 contains a lot of stochastic elements. These are summarized in table 4.1. Since we combine these houses into a neighbourhood, each neighbourhood is different and so will be the elasticity matrix from section 4.2. The whole process can be thought of as a simulation with stochastic variables x. To be able to make conclusions for a whole region consisting of a lot of different neighbourhoods, the average behaviour of these neighbourhoods has to be known. This can be found by applying a Monte Carlo simulation as explained in section 4.3.1. The stochastic variables x are then the ones listed in table 4.1. The results from the simulation — namely the elasticity matrix $\epsilon_{N\times N}$, the minimum and maximum electricity use P_{min}^{NH} and P_{max}^{NH} and the reference electricity use q_{ref} — are then the dependent values $z(x)$.

House	Number inhabitants	EV	Penetration
	Occupancy		Energy needed
	Non flexible loads		Time to charge
Wet appliances	Penetrations	DHW	Hot water demand
	Load cycle	SH	Type house
	Start & stop times	PV	Penetration & size

Table 4.1: Stochastic elements in the model

We want to get an estimate of all the averages of the values stated above. These values are obtained by performing the regressions of section 4.2 on a particular neighbourhood. By performing the same simulation for different neighbourhoods, one can obtain different samples $z(x_i)$ of these values. Applying equation (4.22) on these values gives a Monte Carlo estimate of the real average value we are looking for. In order to obtain a good estimate, a sufficient amount of neighbourhoods has to be created. However, performing the regression on a neighbourhood is

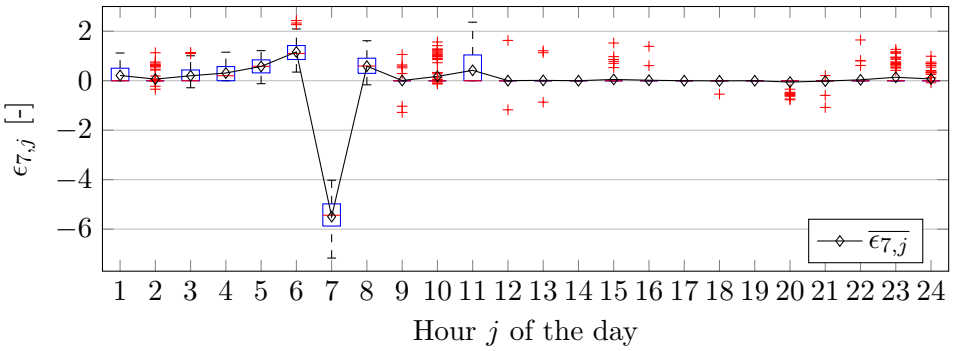

(a) Values $\epsilon_{7,j}$ from the Monte Carlo simulation

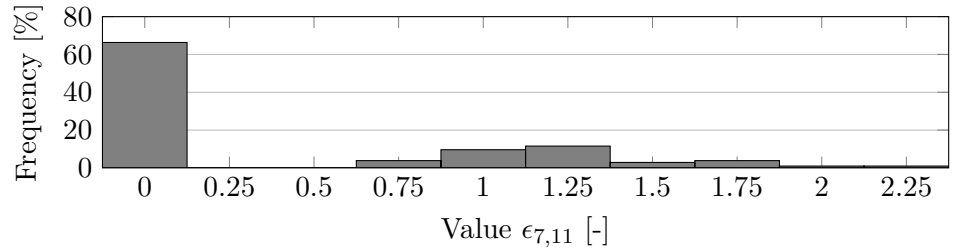

(b) Histogram

Fig. 4.12: Box plot of the elasticity values $\epsilon_{7,j}$ from 104 neighbourhoods and the Monte Carlo estimate of the mean $\overline{\epsilon_{7,j}}$ (a) and a histogram of all the values of $\epsilon_{7,11}$ (b)

already computationally very expensive, so again a compromise has to be made. If we perform at least $N_m = 100$ simulations then the standard error of the mean $\sigma(\bar{z}) \approx s(z)/\sqrt{100} = 0.10 \cdot s(z)$ is brought down to 10 % of its variance. Since the estimate of an elasticity ϵ_{ij} from the regression (section 4.2.2) has a standard deviance (4.17) of at maximum $\sigma_{\epsilon_{ij}} \leq 0.1$, there is no need to perform more than $N_m = 100$ simulations to reduce this error (4.23) further.

As an example, this is done for 104 neighbourhoods on a winter weekday. A Monte Carlo estimate $\overline{\epsilon_{7,j}}$ of the values $\epsilon_{7,j}$ according to (4.22) is denoted by the black line in Fig. 4.12a. The box plots depict the distribution of the obtained values from the 104 simulations each hour. Special attention has to be paid to hours with a zero median. Take for example hour 11. A detailed histogram is given in Fig. 4.12b. The median is indeed zero, since more than 65 % of the values are zero. These are the times this hour is insignificant, according to the selective regression explained in section 4.2.2. Since every time a new neighbourhood is used, it is possible that in some cases these values are indeed significant, and thus have a value different from zero. Since the mean is influenced by these values, in contrary to the median, the mean value is also different from zero although in the majority of the cases the values are not significant. If the mean value is retained for the overall elasticity matrix, one would obtain a matrix with very little zero values, and thus undo the effect of the selective regression, which is unwanted. Therefore, we use following approach: if in

more than half of the neighbourhoods, the elasticity ϵ_{ij} is zero — meaning that in more than half of the neighbourhoods this hour is not relevant — we say that in the overall elasticity matrix $\epsilon_{N\times N}$, this value is also not relevant, thus set to zero. If the median is not zero, this value is relevant and we take the sample mean $\overline{\epsilon_{ij}}$ from (4.22) as an estimate of the real average value $\langle\epsilon_{ij}\rangle$ of the overall elasticity matrix $\epsilon_{N\times N}$.

It is also possible to get the confidence intervals of the estimate $\overline{\epsilon_{ij}}$ by applying equation (4.25). The biggest standard deviation $\sigma_{\overline{\epsilon_{ij}}} = 0.21$ occurs at a value of $\epsilon_{ij} = -5.75$, which is an error of 3 %. The Monte Carlo estimates of the mean are thus quite good and there is indeed no need to simulate more than $N_m = 100$ neighbourhoods. If we plot a histogram of all samples of a certain value, it is even possible to get an idea of the distribution of this value over all the neighbourhoods. An example of the distribution of the own elasticity $\epsilon_{7,7}$ is given in Fig. 4.13.

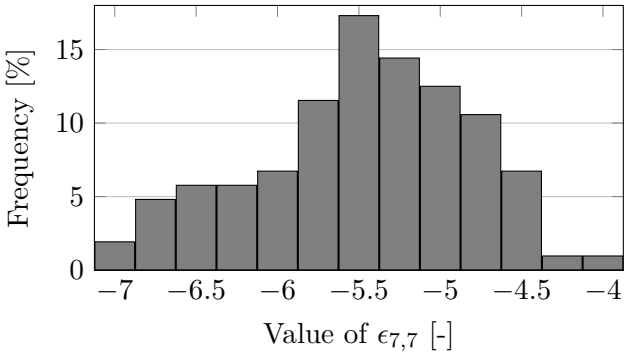

Fig. 4.13: Histogram of $\epsilon_{7,7}$

4.4 Conclusion

In this chapter, we have explained the methodology for obtaining the price elasticity matrices. This is done in two parts. First, a linear regression needs to be performed that relates an applied price signal to a corresponding electricity consumption vector for a specific neighbourhood, in a linear way. By performing a selective regression, we are able to retain only those elements of the elasticity matrix that are significant. This allows to determine the time span of prices that influence the electricity consumption at a certain hour. This time span is always well below 24 hours, which led us to the conclusion that an elasticity matrix for one day (24×24) is sufficient.

In order to make a compromise between computational cost and a better estimation of the regression coefficients, the regression is performed on 350 samples. By performing an F-test, we were able to prove that the obtained regression coefficients are statistically relevant. The error variance of the coefficients could also be determined, and gives standard deviations smaller than 10 %. We can thus say that the estimate of the obtained coefficients is quite good.

By calculating the separate elasticities of the three different types of appliances, the influence of each type on the total can be determined. Also, a logistic regression

is discussed, which gives a better fit for the price-demand curves. However, this does not result in a linear equation. A first order approximation of the logistic regression, gives quickly an over- or under-estimation of the elasticities and the related flexibility. The regular linear regression gives a good compromise and is thus kept as an estimator of the elasticities.

In a second part, we explained the Monte Carlo simulation. This is used to obtain an estimation of average values over all possible neighbourhoods, since every neighbourhood is different. A sample size of at least 100 neighbourhoods is needed to reduce the error on the estimates sufficiently. The outcomes of the Monte Carlo simulation are an estimate of the average and the statistical variance of the values of the elasticity matrix, the minimum and maximum electricity use and the electricity use at a certain reference price. The error on these estimates is always smaller than 10 %. The Monte Carlo method also allows to get an idea of the distribution of the obtained values over the different neighbourhoods.

The results of the Monte Carlo simulations will be discussed in detail in the next chapter, for different weather conditions, weekdays and weekend days.

Chapter 5

Results and Discussion

5.1 Introduction

In chapter 4 we explained the Monte Carlo simulation, which allows to obtain an estimation of the average values for the elasticity matrix, the reference electricity consumption resulting from the reference price and a maximum and minimum possible electricity consumption for each hour. The values resulting from such a Monte Carlo simulation thus represent the average neighbourhood, consisting of 70 households. We performed this Monte Carlo simulation for an average day of each season for both a weekday and a weekend day.

This chapter discusses the main results of these Monte Carlo simulations. First, we discuss the electricity consumption resulting from the reference price, as determined in chapter 4. The average electricity consumption of one neighbourhood will be scaled up to get an estimate of the residential electricity consumption for the whole of Belgium. We will put these results into its proper context and compare them to the current consumption. Furthermore, we will point out the consequences of having a fully electrified residential energy consumption.

Subsequently, we consider the elasticity matrices and we quantify the amount of available flexibility at each hour. We assess the influence of the different seasons on these values and quantify the contribution to the elasticities of the separate devices. Furthermore, we compare our results to the existing literature in this research field and point out some differences.

Then, we discuss the minimum and maximum possible electricity consumption. These are the values that can be reached in extreme circumstances. Also, the factors that limit this minimum and maximum will be indicated.

Finally, we perform a sensitivity analysis in section 5.6. The penetration of EVs is varied in a particular neighbourhood from 0 % to 100 % and we check the influence on the values of the elasticity matrices.

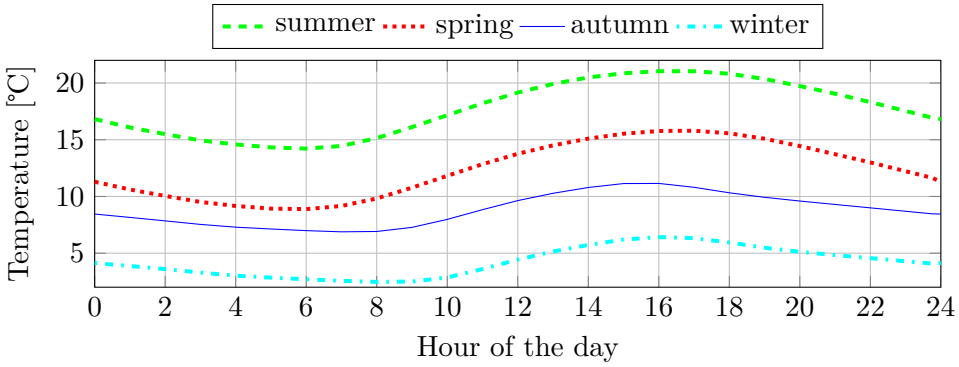

Fig. 5.1: Ambient temperatures used of the average days of the four seasons

5.2 Intermezzo: Seasonal Influence

As indicated in the introduction, the Monte Carlo simulations are performed for an average day[1] of each season, as this is an important factor that influences the energy consumption. The main difference between the seasons is the ambient temperature and the amount of solar radiation. In our model, heating is responsible for a main part of the flexible residential electricity consumption and the ambient temperature is a very determining factor when considering the amount of heating needed. The available flexibility and energy consumption from these heaters will thus be depending on the ambient temperature. Fig. 5.1 shows the average temperature profiles of the four seasons that we used.

For each season a different simulation is performed for a weekday and a weekend day. This difference is made because people tend to be more at home in weekends and this might have an impact on the available flexibility.

5.3 Electricity Consumption with Reference Price

In this section we will discuss the average reference electricity consumption $\overline{q_{ref}}$ occurring when neighbourhoods are subjected to the reference price p_{ref} (shown in Fig. 4.3a), which is determined in section 4.2.1. This average is obtained by performing a Monte Carlo simulation on the reference electricity consumption q_{ref} for at least 100 neighbourhoods, as explained in section 4.3.2.

Since this is an estimate of the average of all neighbourhoods, this can be scaled up to the level of a country. We will do this for Belgium. To put this in context, we compare these results with the present ones in terms of average annual energy consumption and peak power consumption. This will give some insight in the consequences of having a fully electrified residential energy consumption subject to a real time pricing scheme.

[1] We calculated the average day as the average of all days of a season.

5.3.1 Scaling Up

As mentioned in section 3.2, we assume that there will be 4 606 544 private households in 2050. We can then scale up the reference electricity consumption to a Belgian level as follows. The Monte Carlo simulation with 100 neighbourhoods gives a good estimate of the average q_{ref}. Since each neighbourhood consists of 70 households, we can simply multiply this average reference electricity consumption $\overline{q_{ref}}$ by a factor 4 606 544/70. As indicated before, this is performed for an average weekend and weekday of each season.

Fig. 5.2 shows the reference electricity consumption in Belgium for all seasons on a weekday. The contribution of each type of device is also shown. One can clearly see the big contribution of the heaters, especially in winter and autumn. Also notice that almost all EVs are charged during the night and that the wet appliances only contribute little, mostly in the late afternoon. The electricity consumption in this figure does not include PV production. We do this to be able to compare to the current electricity consumption profile.

Fig. 5.2 shows the same trends for all seasons: a big peak in consumption at hour 5, little consumption during noon and some smaller peaks in the evening. This is of course because the price signal p_{ref} used here is the same for all seasons and is low during these peak hours (see Fig. 4.3a). The peak in the summer amounts to approximately 14 GW whereas in autumn and winter a maximum power of around 25 GW is consumed. In spring this peak is somewhat lower, about 22 GW. The difference in peak power consumption between the seasons is clearly due to differences in heating. The contributions of other devices are almost the same in every season.

Appendix B.1 repeats the same plots for a weekend day. The consumption in the weekend is always a few GWh higher, which can be related to the fact that more people are at home in the weekends. Hence, more electricity is used in general, specifically for the non-flexible appliances (light,TV,etc.) and electric heating.

The peak loads observed here are much higher than the ones that we experience nowadays on the Belgian network and even higher than the current total installed capacity. However, we have to put these results into its proper perspective. Residential electricity consumption amounted to 20 210 GWh in 2012 as pointed out earlier (section 3.2). With 4 606 544 private households, this leads to an average yearly energy consumption of 4 387 kWh per household. It is important to recognize that in this number no EVs are included. Besides, today 83.3 % of the residential energy consumption in Flanders consists of space heating and DHW heating. Most of the space heating and part of DHW heating in Belgium is provided by non-electric boilers [23]. In our model, however, heating is completely electrified and is, together with the EVs, responsible for a big part of the yearly energy demand as we will show below. As can be seen, these two additional electric loads are almost exclusively responsible for the high peaks observed.

To get more insight in this increase in energy consumption, we compared the average annual electricity consumption and the peak power consumption resulting from our model with the ones we observe today.

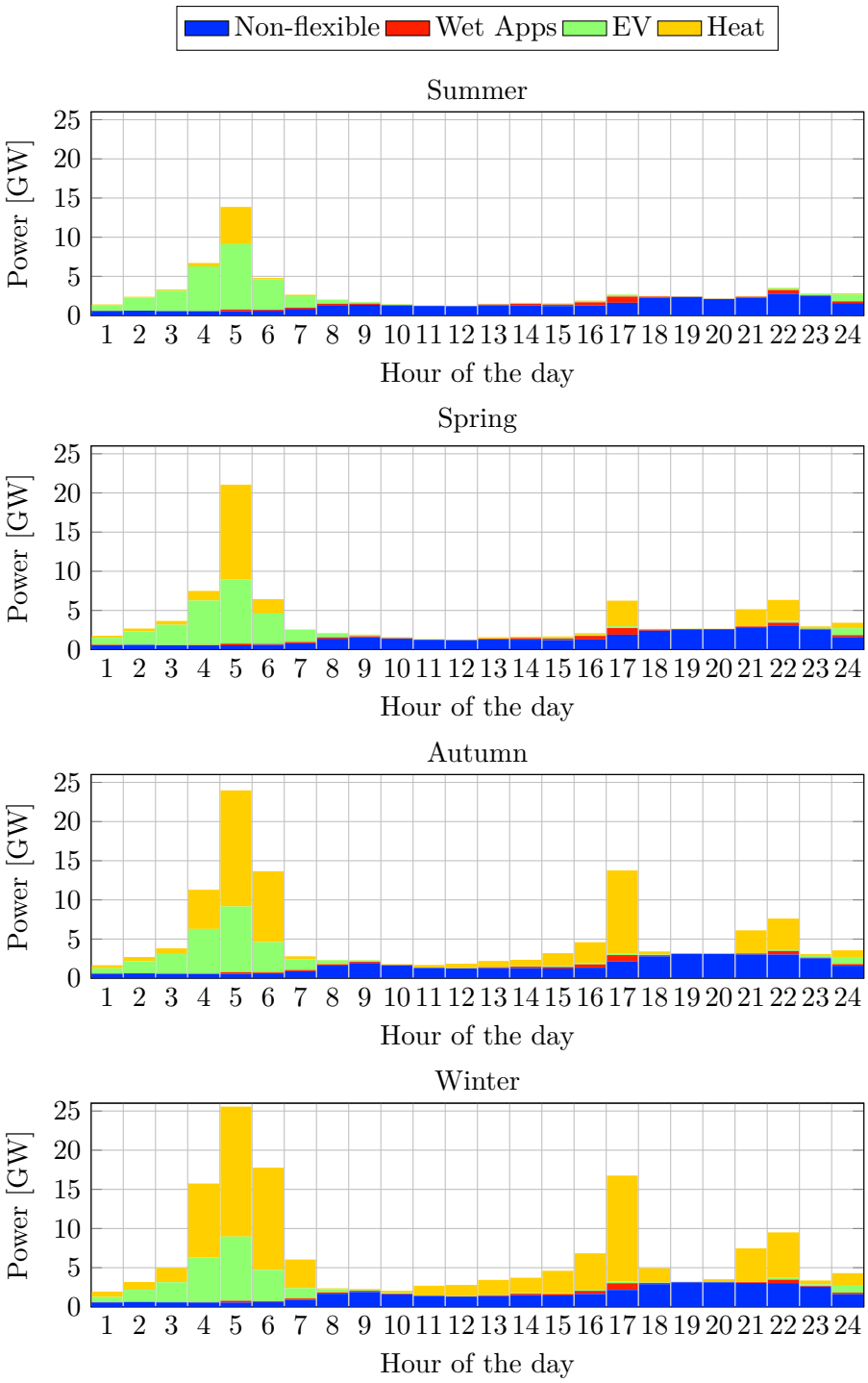

Fig. 5.2: Reference residential electricity consumption scaled up towards a Belgian level in summer, spring, autumn and winter.

Average Annual Electricity Consumption As explained earlier, we performed a Monte Carlo simulation to obtain an estimate of the average electricity consumption over all neighbourhoods. We did this for an average day of each season, and for both a weekday and a weekend day.

The non-flexible demand was calibrated as stated in section 3.2. The energy consumed by electric heaters (heat pumps and auxiliary heaters) depends strongly on the time of the year. When solar radiation and ambient temperatures are higher, it is obvious that less heating is required. Also, the occupancy of a house, and consequently the required temperature in the house, depends on whether it is weekend or a weekday. Hence, to obtain the average annual electricity consumption of a neighbourhood, these influences have to be taken into account. To obtain the average annual consumption for a household, this number is then divided by 70.

The energy consumption of EVs depends on the driving patterns, as described in section 3.3.2. These driving patterns are provided for each day and consequently also depend on time of the year. One can imagine for instance that an EV in winter will drive more than in summer. Hence, to obtain the average annual consumption of EVs we proceed in the same way as with the electric heaters. A similar reasoning could be applied to the usage of wet appliances (e.g. the tumble dryer is less often used in the summer). However, the data in our model did not include the dependence on time of the year for wet appliances.

An overview of the average annual energy consumption of the different household devices for one household subject to the reference price is shown in table 5.1.

Type of Demand	Energy consumption [kWh/year]
Non-Flexible	3 091
Electric Heating	3 587
Electric Vehicle	2 146
Wet appliances	304
Total	**9 128**

Table 5.1: Breakdown of the average annual residential electricity consumption for one household subject to the reference price.

Comparing this average total household consumption of 9 128 kWh to the one that we observe today (4 387 kWh), we see that residential electricity demand more than doubles due to the electrification. From this higher energy consumption, it follows that power demand will be much higher in our model than it is now.

One might expect that the average electricity demand would rise by more than a factor two as all heating is electrified and EVs are an important new electric load. The fact that this is not the case could be explained by:

- Heat pumps are much more energy efficient than the current gas boilers. The average COP for space heating is 3.89 and for DHW 2.24. These numbers are to be compared with the efficiencies of the most modern condensing boilers (around 98 % thermal efficiency [81]). This implies that heat pumps for space

heating are almost four times more efficient than classical boilers and for space heating double as efficient. As space heating represents the most important part we can assume that there will be around four times less energy consumed for space heating than we do nowadays.

- A second important fact is that the dwellings in our model are all newly built. They are better isolated than the average building nowadays in reality and will therefore consume even less heat.

The total annual residential electricity consumption for the whole of Belgium in our model can be obtained by scaling up the average consumption of a household as explained above, and results in 42 048.5 GWh.

Peak Power Consumption Although the total yearly electricity consumption will only double, the peak power demand in our reference scenario increases much more. It is thus also interesting to compare the instantaneous *power* consumption. First thing needed to compare are the residential load curves of the current situation. As residential customers are not yet equipped with smart meters, their consumption is not exactly known. However, today *synthetic load profiles* (SLP) are used in order to have an estimate of the consumption profile. We took the SLP for a residential customer from [82] of 2014 and averaged them for each season. The averaged SLP can be found in appendix B.2. For each time step, the SLP gives the fraction of yearly electricity demand consumed. Multiplying these average SLP by the annual electricity demand results in the power consumption curves for the average days of each season as they are nowadays. These demand profiles are presented in appendix B.3. The current peak power consumption and the one obtained in our model are compared in table 5.2 below.

	SLP [GW]	Model [GW]	Model/SLP [-]
Summer	2.57	13.87	5.39
Spring	2.82	22.12	7.84
Autumn	3.75	25.06	6.68
Winter	4.15	25.56	6.15

Table 5.2: Residential peak power consumption as it is nowadays and the one obtained in our model.

A first thing that strikes us is the big difference between the current peak power consumption and the one obtained in our model. Although the *average energy* consumption in our model is only twice as much as the current one, the ratio between the *peak power* consumption in our model and the current one varies between 5 and 8. This can be explained by the fact that in our model, we use an RTP strategy with automatic demand response, whereas currently there is only a day and night tariff. Due to this strategy, flexible demand will massively shift to the moments where electricity is cheapest. The bulk of this flexible demand consists of

heat pumps and EVs as mentioned previously. As these loads are not yet present in the current load curve (or to a very small extent), they do not appear in the peak now. Hence, the presence of these new loads and the RTP strategy combined cause the peak to be much higher in our model.

While nowadays, the residential peak in power consumption can be observed around 19h00 (see appendix B.3), the peak resulting from our model occurs between 4h00 and 5h00 in the reference scenario because:

- The reference price is at its cheapest then (see Fig. 4.3a).
- Most EVs leave a few hours later, charging of these EVs is thus shifted to the cheapest hours before their departure times.
- Most of the occupants wake up a few hours later. Space heating is turned on a few hours earlier and houses are heated up more than necessary in the fifth hour such that the temperature is still high enough when occupants awake (and when prices are higher).

5.3.2 Remarks

The results from our model have to be put in the right perspective. We do *not* want to state that the electricity grid will have to be dimensioned based on the peak power demand as obtained in the sections above. The goal of this thesis was to obtain a quantification of the potential residential flexibility in 2050, not to obtain an estimate for the absolute power profiles. Certain assumptions we made during this thesis will also influence the absolute power demand:

- We have assumed that our load shifting does not influence the price. However, for such a massive shift in demand this assumption will not hold. Production would be rescheduled and this rescheduling would have its influence on the price. The price profile would become more smooth than the one shown in Fig. 4.3a. The households would react differently to this new price profile, leading to peaks that will probably not be as high as shown in Fig. 5.2.
- We assumed a real time pricing program that incorporates *automatic* demand response. All devices thus react automatically on a change in price, creating an electricity consumption profile that is very sensitive to the price signal, as will also be demonstrated below.
- Since in this reference scenario, all users respond to the same price signal, a huge amount of load syncing can be seen. This is a desired consequence, as power is cheap and more consumption is needed. However, grid constraints are not taken into account as not to overload the model, but they will limit these peaks. This could be implemented by adding specialized distributed algorithms [72].
- We assumed the willingness of consumers to participate in a DR program to be 100%. However, it is likely that not every consumer is willing to do this.

A decreased participation willingness will reduce the power peaks, and so the available flexibility.

- Other (non-electric) technologies like for instance solar boilers were not considered in this thesis. It is possible that part of the energy demand we considered to be electric will be provided by such technologies.

5.4 Price Elasticities

In this section we will discuss the values of the price elasticities obtained from the Monte Carlo simulation, as described in section 4.3.2. First, we shortly repeat the general interpretation of these elasticities. Then, we discuss the values for the different seasons in more detail. Finally, we take a look at the absolute shift in power consumption resulting from these elasticities.

5.4.1 Monte Carlo Results

Interpretation In this thesis we have derived own-price elasticities ϵ_{ii} and cross-price elasticities ϵ_{ij} as:

$$\epsilon_{ii} \cdot \Delta p_i = \Delta q_i, \qquad \epsilon_{ij} \cdot \Delta p_j = \Delta q_i, \tag{5.1}$$

with $\Delta p_i = (p_i - p_{ref,i})/p_{ref,i}$ the relative difference in price with regard to a reference price and $\Delta q_i = (q_i - q_{ref,i})/q_{ref,i}$ the relative difference in electricity consumption with regard to a corresponding reference electricity consumption.

These elasticities thus define a linear relationship between the deviation of a price at a certain hour j from a reference price and the deviation of the associated electricity consumption at the hour i. E.g. an own elasticity of $\epsilon_{ii} = -3$ means that an increase in price of 1% at hour i leads to a decreased electricity consumption of 3 % at that same hour i. A cross-price elasticity of $\epsilon_{ij} = 3$ means that an increase in price of 1 % at hour j leads to an increase in electricity consumption of 3 % in hour i. As explained in section 2.4.3, own-price elasticities are expected to be negative and cross-price elasticities to be positive.

The own- and cross-price elasticities can be grouped into an elasticity matrix $\epsilon_{24\times24}$ for one day, as explained in chapter 4. Each row i of this matrix contains the elasticities that determine the electricity consumption at the hour i. A column j of this matrix expresses the amount of influence a price at hour j has on all hourly electricity consumptions. As demonstrated in section 4.2.2, most of the cross elasticities ϵ_{ij} further away from the diagonal are zero, meaning that a price change at the hour j has no influence on the electricity consumption at hour i.

Discussion In order to get a good estimate of the average elasticity values, a Monte Carlo simulation is performed on the elasticity matrices of at least 100 different neighbourhoods. Fig. 5.3 shows a heat map of the resulting average elasticity matrices for an average weekday in all four seasons. In appendix C the

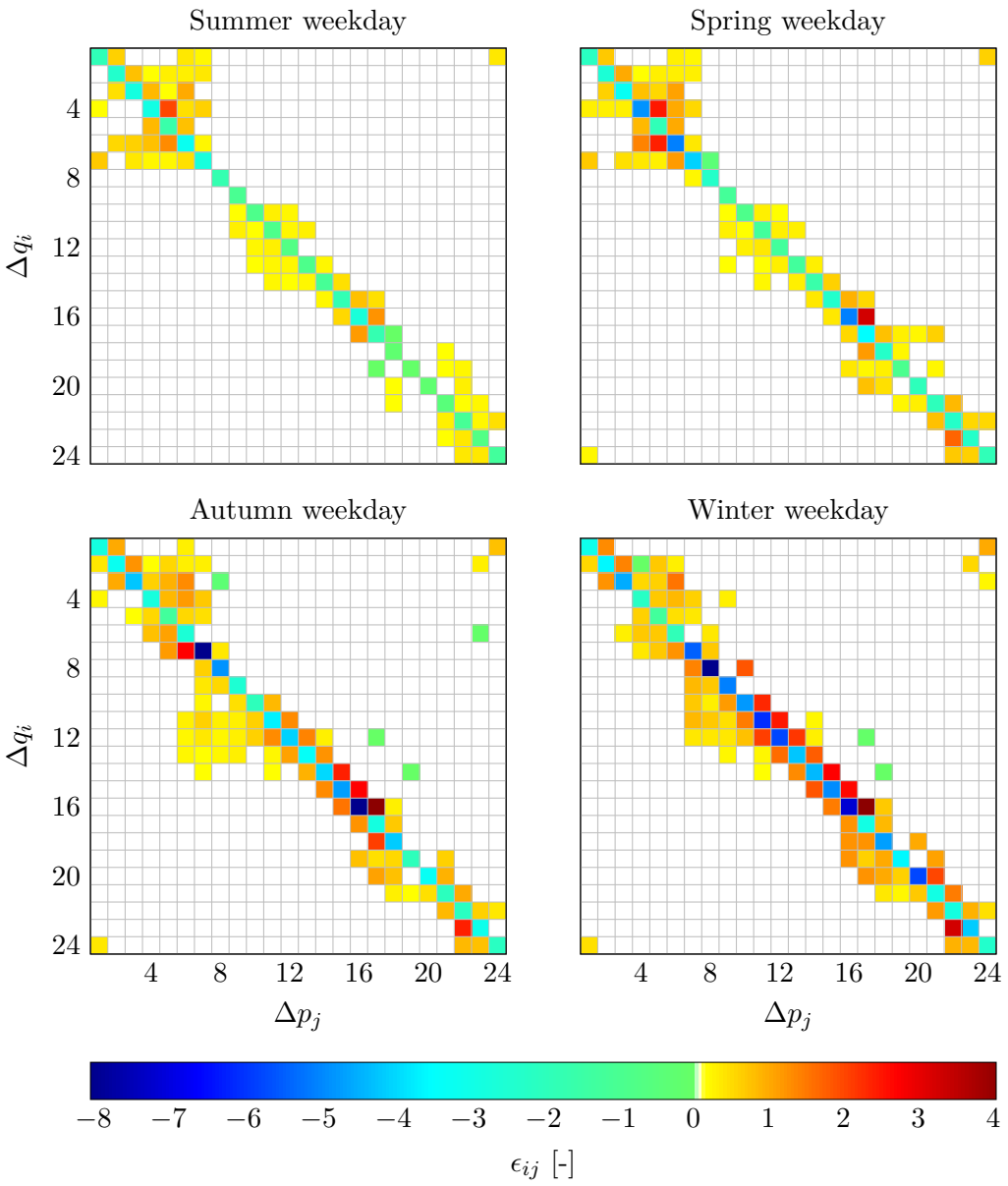

Fig. 5.3: Values of the Monte Carlo estimates of the mean price elasticity matrices for a weekday in the winter, autumn, spring and summer

numeric values of all the resulting matrices are tabulated. One can see that in each matrix the diagonal is indeed negative, and most of the off-diagonal values are positive. Only a few off-diagonal values are negative. As these are all further away from the diagonal itself, and are close to zero, they do not contribute much.

The most extreme values are found in winter, both positive and negative. This is caused by the heat pumps and electric heaters that are operating then and that provide a lot of flexibility. The smallest values are found in summer, since almost no

space heating can be used here. All available flexibility is then provided by EVs and wet appliances. In spring and autumn, the values lie in between the ones in summer and winter with in autumn greater values than in spring (positive and negative). This can again be explained by looking at the temperature profiles in Fig. 5.1. The average temperature in spring is little higher, so less heating is required. The values of the elasticity matrix are thus highly influenced by the weather conditions, specifically the ambient temperature and solar heat gains. A clear trend can be seen: when temperatures and solar irradiance decrease, elasticities are bigger (in absolute value). For a same difference in electricity price, more electricity consumption will be shifted when temperatures are colder. Hence, more flexibility is available. This can indeed be explained by the amount of electric heaters that are operating more when temperatures are lower.

The own-price elasticities are the biggest and thus the most influential. However, the cross elasticities are also important. They allow to determine how much and how far in time the electricity consumption could be displaced. Take for example an increase in electricity price of 1% at hour 7 on a winter weekday. This increase in price will lead to a decrease in electricity consumption at hour 7 of 5.49% ($\epsilon_{7,7} = -5.49$), but also to an increase in electricity consumption at hour 8 of 1.32% ($\epsilon_{8,7} = 1.32$), at hour 9 of 0.80% and so on until hour 12 where the electricity consumption will raise by 0.29%. Also, more electricity will be consumed in the hours before, at hour 3 and 4, as these cross-price elasticities are also positive. It is thus possible to obtain an idea of the time interval in which a price change has an influence on the demand. The furthest shift in demand in reaction to a price change is 7 hours, from hour 7 to hour 14 on an autumn weekday.

It can be seen that in all seasons, generally electricity consumption can be displaced from the early morning (hours 4–6) towards the first hours of the night (hours 1–4) but a price change in the first hours of the night does not lead to an equal demand change in the early morning. In other words, the PEMs are not symmetric. Electricity consumption at hour 8 is almost only determined by its own-price elasticity, and a few cross-price elasticities in winter and autumn, meaning that not much electricity can be shifted to this point in time. This can be explained by the fact that most people start their day around this time. Hence, the house needs to be at the right temperature and the EVs need to be charged. These two big sources of flexibility will thus not be available any longer. There are a lot of cross-price elasticity values to the left hours 10–14, meaning that it is possible to shift electricity towards these hours from the earlier morning.

The own-price elasticities are the most negative at hour 7,8 and hour 16, especially in the winter and the autumn. However, this does not allow to conclude that these are the hours with the most or the cheapest flexibility available. Care has to be taken when interpreting these elasticities, since they are depending on a reference electricity consumption $q_{ref,i}$. A small elasticity value with a high reference electricity consumption might still lead to a relatively large absolute difference in electricity consumption Δq_i, and a large elasticity with a small reference consumption might lead to only a small absolute difference Δq_i. These absolute shifts in consumption will be investigated in the next paragraph.

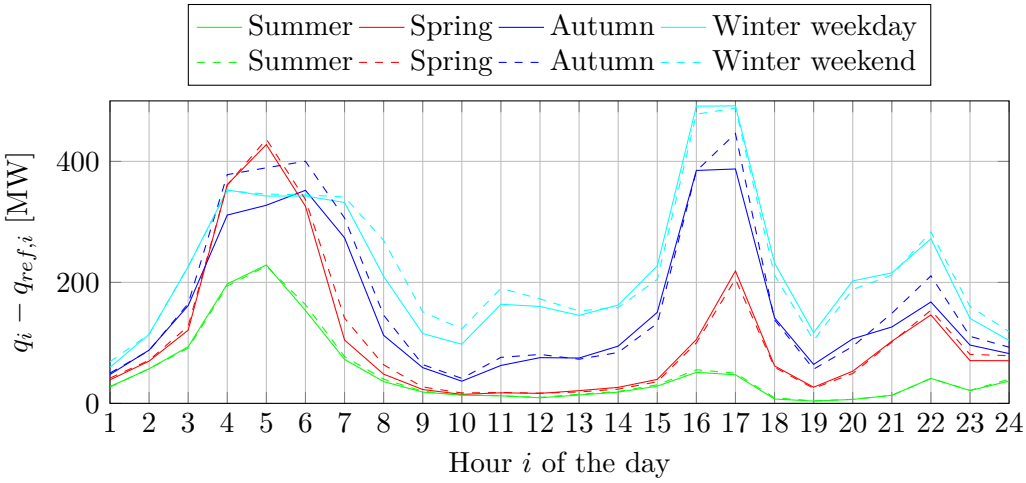

Fig. 5.4: Absolute shift in electricity consumption $q_i - q_{ref,i}$ with a price decrease of $\Delta p_i = -1\%$, at every hour i and for the four seasons, on a weekday and a weekend day. The numbers are scaled up to a Belgian level.

Absolute Demand Shift The flexibility that is independent of the reference electricity consumption will allow a better comparison between the different hours. The absolute shift in electricity demand is calculated as $q_i - q_{ref,i} = (\epsilon_{ij}\Delta p_j) \cdot q_{ref,i}$. Since the own-price elasticities are the most influential we will look at the absolute increase in electricity consumption $q_i - q_{ref,i}$ with a relative decrease of 1% of the electricity price Δp_i at the same hour. Fig. 5.4 illustrates the absolute shift in electricity demand for this case. The numbers in this figure are scaled up to a Belgian level, representing 4 606 544 households (see section 5.3).

This figure allows to draw different conclusions. First, one can see that there is indeed very little difference between a weekday and a weekend day. At most hours, the shift in electricity consumption is only slightly greater in the weekend than during the weekdays. This can be explained by the fact that more people are at home in the weekends and thus more devices might be available for shifting. However, the difference is rather small and thus can be neglected.

The trend noticed before is also visible here: for a same difference in electricity price, the difference in electricity consumption will be the biggest in winter and the smallest in summer. More flexibility is available in the winter as explained earlier. This difference in shifting possibilities between summer and winter can amount to more than 200 MW in power.

In all four seasons one can notice two main peaks: one during the night, around hour 5, and one in the afternoon, around hour 17. The highest peak at night occurs in spring, which might be counter-intuitive (we could have expected this for winter). This can be explained by the fact that in winter during the night, a lot of heat pumps are already powered on to reach the desired temperature. Hence, when prices decrease, less additional heating can be added. This is in contrary to spring, when less heaters are active during the night, and thus more can be powered on when the

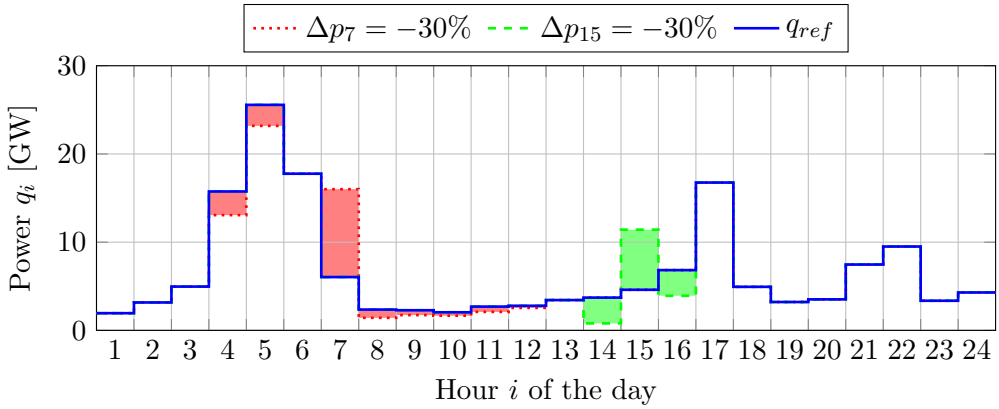

Fig. 5.5: New electricity consumption q_i with a price change of -30 % at hour 7, and at hour 15, and the reference electricity consumption q_{ref}, for the average winter weekday. The numbers are scaled up to a Belgian level.

price decreases.

The peak in the afternoon can be explained by the fact that the houses need to be heated up by the evening, when people are returning home. Hence, a lot of flexible heaters are available just before the evening, in the afternoon. A smaller peak can be noticed around hour 22 in the evening. During the day — between hour 9 and hour 15 — relatively little flexibility is available.

The values of Fig. 5.4 are in general quite big, since this represents the absolute difference in electricity with a difference in price of only 1 %. A small difference in electricity price will thus already result in a big difference in residential electricity consumption in our model. This can also be seen by the big values of the elasticities from Fig. 5.3. A price vector used in this real time pricing scheme shall thus have to be designed very carefully. Demand subject to a real RTP scheme as implemented in our model is thus found to be very sensitive to price changes. This could mean that the flexibility resulting from such a scheme is rather cheap.

A remark should be made about the fact that the elasticities obtained in this thesis are designed for *day-ahead forecasts* of the flexibility. They are thus not designed to predict sudden changes in electricity prices, or to compensate for forecast errors of e.g. wind production as a primary or secondary reserve.

Influence of Cross Elasticities To get insight in the influence of the cross elasticities in absolute demand shift, we have simulated two price signals. One has a decrease of $\Delta p_7 = -30\,\%$ at hour 7, and the other the same decrease of $\Delta p_{15} = -30\,\%$ at hour 15, with regard to the reference price. The resulting electricity demand for a winter weekday, obtained by multiplication with the elasticity matrix, is given in Fig. 5.5. One can clearly see the influence of the cross elasticities. A price decrease at hour 7, with a lot of cross elasticities $\epsilon_{i,7}$, leads to a decrease in electricity consumption at hour 4 and 5 but also to some smaller decreases at hours 8–12. One can thus say that electricity consumption of hours 4 and 5 and hours 8–12 is being

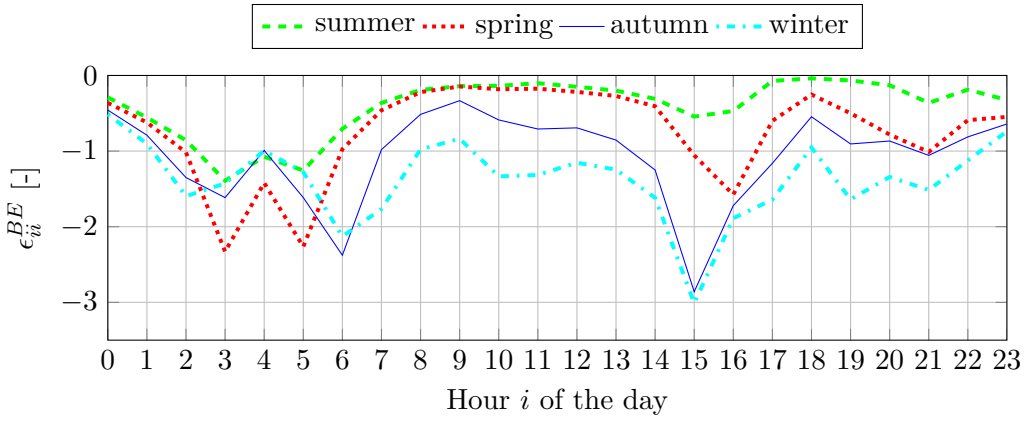

Fig. 5.6: Own-price elasticities of the whole Belgian electricity demand with only residential demand flexible, according to (5.2).

shifted towards hour 7. A price decrease at hour 15 has less influence. It leads only to a decrease in electricity consumption at hours 14 and 16.

5.4.2 Comparison with Literature

The elasticities obtained from the Monte Carlo simulations can be compared with price elasticities from the literature. De Jonghe [12] gives an overview of cross- and own-price elasticities, both on long-term and short-term. In the literature, there exists a lot of variation in the obtained short-term own-price elasticities. They range from -0.02 to -0.83, depending on the study. This variance is caused by the differences in model specification, data source and design of the experiment. Some studies focus on historical data from residential time-of-use (TOU) pricing experiments: [83] obtains values of -0.30 to -0.47 while the values in [84] range from -0.76 to -0.83 for short-term own-price elasticities. The time-of-use pricing relates slightly to the real time pricing scheme that we have considered, so could be a good base for comparison. However, the values in the literature are all rather low, especially compared to the values we obtained (see Fig. 5.3). This is because in the literature the elasticities describe *behavioural changes* of customers, e.g. doing the laundry at night because of the cheaper night tariff, while we are describing potential *automatic* demand response, where the customer behaviour is not changing. Since customer behaviour will only react slowly and automatic demand response will result in a direct change with only a small price variation, this explains partly the big difference. Another part is the fact that our model includes a lot devices that can react to price fluctuations. In fact, more than half of the residential electricity consumption is made flexible.

One should also notice that the elasticities we obtained are pure residential elasticities, they describe the change in residential electricity consumption *only*. One can transform these values to a full Belgian level by adding the non-residential electricity consumption to the reference consumption from (5.1). The elasticities for the total Belgium electricity consumption are then:

$$\Delta q_i^{BE} = \epsilon_{ij}^{BE} \Delta p_j = \left(\frac{q_{ref,i}}{q_{ref,i}^{BE}} \epsilon_{ij} \right) \Delta p_j, \tag{5.2}$$

where the superscript ^{BE} denotes the values for Belgium. The elasticities have thus to be scaled with a factor $q_{ref,i}/q_{ref,i}^{BE}$, where $q_{ref,i}$ is the reference residential electricity use of Belgium as discussed in section 5.3. $q_{ref,i}^{BE}$ is the total reference electricity use of Belgium, thus the same residential electricity use plus the non-residential electricity use as given by [85] and projected to 2050 by use of [42]. The resulting own elasticities are plotted in Fig. 5.6. The values are smaller, and peaks as previously noted at e.g. hour 8 in the winter have disappeared. The reason is that this peak was rather caused by a small reference electricity consumption than by a high flexibility. Since in (5.2) the whole Belgian electricity consumption is taken as a reference, a fairly big base load is added to all hours, eliminating the effect of low residential reference consumption.

The elasticities from (5.2) have to be interpreted with care. They are rather indicative than real elasticities for the whole of Belgium, since they describe only the residential flexible electricity demand. It is indeed assumed in (5.2) that the rest of the Belgian electricity consumption is not reacting to a variable price and behaves as a non-flexible load. Also, in (5.2) the residential sector is assumed to be completely electrified while the rest is not, leading to a higher ratio of residential electricity consumption to total electricity consumption than would the real case.

5.4.3 Influence of Different Devices

To get an idea of the contribution of the different types of devices on the flexibility, the elasticity matrix $\epsilon_{24\times24}$ can be split up into three separate matrices $\epsilon_{24\times24}^{WA}$, $\epsilon_{24\times24}^{EV}$ and $\epsilon_{24\times24}^{Heat}$, for the wet appliances, EVs and heaters respectively. This can be done according to (4.19), as explained in section 4.2.3. We have performed the same Monte Carlo simulation as described in section 4.3.2 on these matrices. Since summer and winter are the most extreme seasons, we will only discuss the results of those two seasons here. The difference between a weekday and a weekend day has been shown to be minimal, so only a weekday will be considered. Since the own elasticities are the most crucial ones, only these will be examined in order to be able to make an easy comparison and draw some clear conclusions.

A plot with the own elasticities for the three types of devices is shown in Fig. 5.7 for both summer and winter. The reason that the sum of the different elasticities does not always coincide with the elasticities from the total matrix is explained in section 4.2.3.

Fig. 5.7 is an interesting plot since it allows to determine the separate influences of the three different types of devices on the flexibility. One can see that the heaters are the ones that determine the flexibility almost completely during winter. During the night the EVs also contribute to the flexibility, but during the day their elasticity is almost zero. The wet appliances have a relatively small influence in winter. The

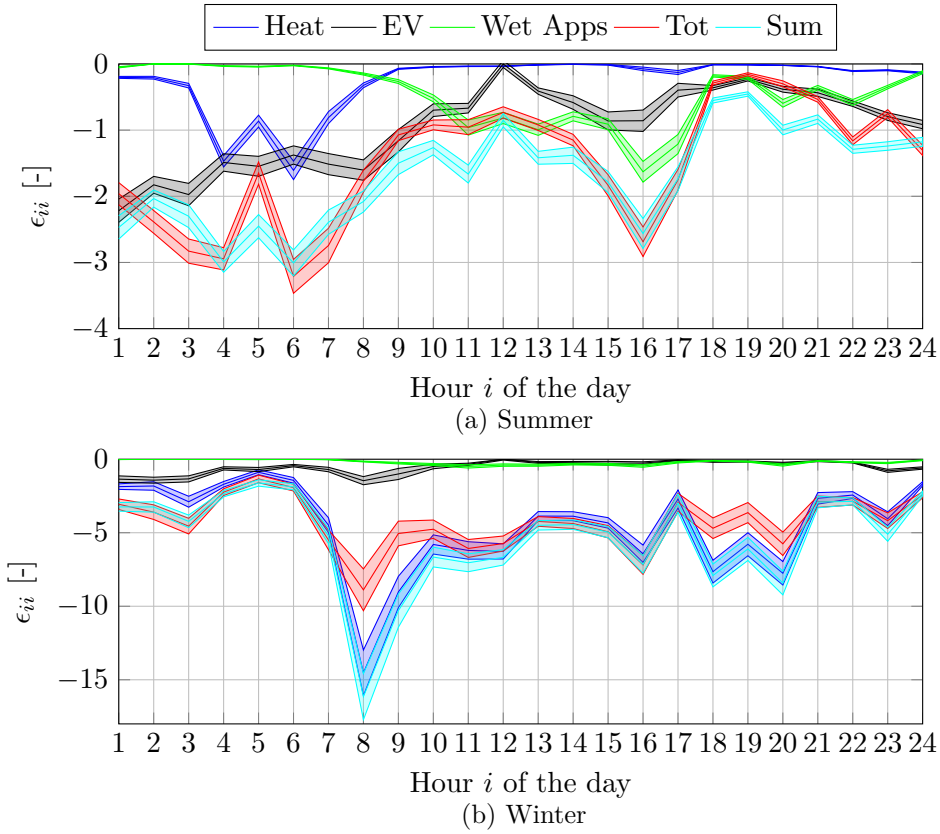

(a) Summer

(b) Winter

Fig. 5.7: Own elasticities of the different devices, their sum and the own elasticities of all appliances together (4.19), for a summer and winter weekday. The bands designate the 95% confidence interval.

large negative peak around hour 7 is mostly due to the low value of the reference electricity consumption at that moment.

In the summer time, the contribution of the heaters is brought down to almost zero during the day. Only around hours 3–6, they still contribute and have own elasticity values around -1. Nevertheless, this is less negative the values in winter. Since the heaters were responsible for the major part of the flexibility in winter, far less flexibility is available in summer. This means the relative contribution of the EVs and the wet appliances is much higher in summer. The EVs mainly determine the flexibility during the night but also provide some flexibility around noon. The own elasticities of the wet appliances are still very close to zero during the night, but in daytime they are really significant and contribute a lot.

These results confirm our previous observations and assumptions: the heaters determine the major part of the flexibility, the EVs are mostly important during the night and the contribution of the wet appliances is relatively small.

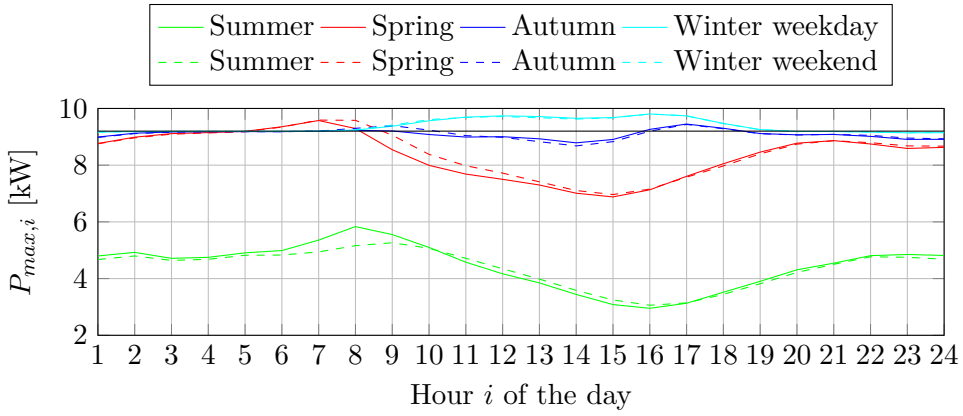

(a) Maximum electricity consumption

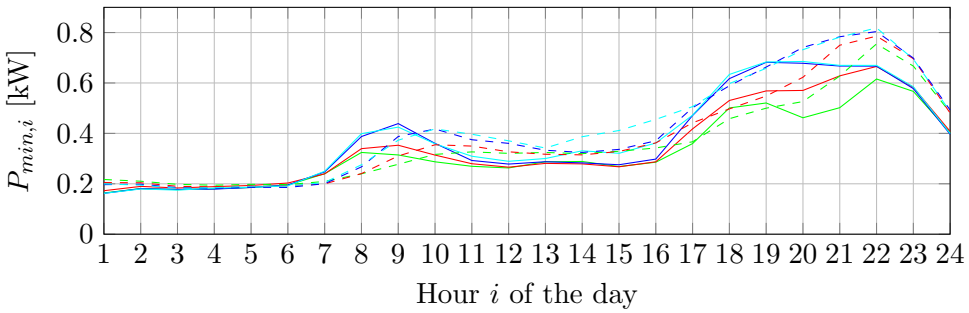

(b) Minimum electricity consumption

Fig. 5.8: Average maximum (a) and minimum (b) electricity consumption for 1 household. The black line in (a) denotes the household limit of 9.2kW

5.5 Minimum and Maximum Power Consumption

In section 3.6.1 it is explained how the minimum and maximum amount of power P_{min}^{NH} and P_{max}^{NH} that can be consumed every hour, can be determined for a single neighbourhood. By performing a Monte Carlo simulation (section 4.3) on this data, we obtain an estimate of the mean values over the different neighbourhoods. The resulting average $\overline{P_{min}}$ and $\overline{P_{max}}$ is given in Fig. 5.8, for one household. The minimum amount of power $P_{min,i}^{NH}$ is often reached with the price vectors we imposed on the neighbourhoods (see also the boxplot of Fig. 4.4). The upper value $P_{max,i}^{NH}$, however, is in reality almost never reached. This can be explained by looking at the price profile that is applied in order to calculated $P_{max,i}^{NH}$ (Fig. 3.8), which has a value that is zero on the hour i. The heaters will therefore heat up the house until the maximum allowed temperature during that hour, which is very unlikely to happen with realistic price profiles. The maximum amount of power $P_{max,i}$ can thus be rather seen as some kind of theoretical maximum power that can be consumed during one hour i in rare, extreme circumstances, when price profiles are like Fig. 3.8b.

It should be noticed that during noon in winter and around hour 7 during spring, $P_{max,i}$ can be higher than the household limit of 9.2 kW (Fig. 5.8a). This is caused

by the PV installations. These are integrated in our model in such a way that if a house consumes its own PV production, this is not a part of the household limit of 9.2 kW that it can draw from the distribution grid. During the evening and the night, thus at moments without PV electricity production, $P_{max,i}$ is restricted by the household limit of 9.2 kW. It might thus be that when increasing this limit, an even higher $P_{max,i}$ can be obtained.

From Fig. 5.8a, it is clear that the maximum amount of power $P_{max,i}$ that can be consumed is the highest in winter and the lowest in summer, with spring and autumn in between. This can again be related to the amount of electric heating that can be turned on, and thus to the weather conditions. This also explains why $P_{max,i}$ is lower during the day in the autumn, spring and summer: the ambient temperature is higher around noon, thus less electric heating is available.

The minimum amount of power that has to be consumed $P_{min,i}$ is plotted in Fig. 5.8b. This is almost entirely determined by the non-flexible load. Only during the night it is slightly higher, as a certain amount of EVs has to charge the whole night in order to be completely charge in the morning. The difference in $P_{min,i}$ between the seasons is thus not really big, since the non-flexible load is only slightly influenced by the season.

5.6 Sensitivity Analysis

In this section, we perform a sensitivity analysis to investigate the dependence of the elasticities on a change of appliance penetration rates. Due to the high computational cost of a full Monte Carlo simulation, this sensitivity analysis was only performed for one neighbourhood. We investigated the influence of a changing penetration rate of EVs on the price elasticities.

Fig. 5.9 shows the own-price elasticities for penetration rates of EVs ranging between 0 % and 100 % with steps of 20 % in the summer and the winter. From these figures we can conclude that a variation in the share of EVs has a negligible influence on the values of the elasticities, as they have more or less the same values for different penetration rates in all hours of the day. A reason is that the elasticities determine the *relative* increase in electricity consumption with a relative increase in price. With less EVs available, one has less flexibility available in general. However, the reference electricity consumption will also be lower with a lower penetration degree of EVs. The effect of less flexibility will thus mainly be cancelled by the effect of having a lower reference electricity consumption.

Only in the summer with no EVs present, one can notice some deviant behaviour in the fourth and the sixth. This can be explained by the very low reference electricity consumption caused by the zero amount of EVs, while there is still a lot of possibility for shifting, coming from the heaters that are scheduled at hour 4 in the reference scenario. Looking back at the definition of price elasticities (4.4), this results in high (in absolute value) own-price elasticities.

It is not because the difference in price elasticities is small with different penetration rates of EVs, that the difference in absolute electricity shift is also small.

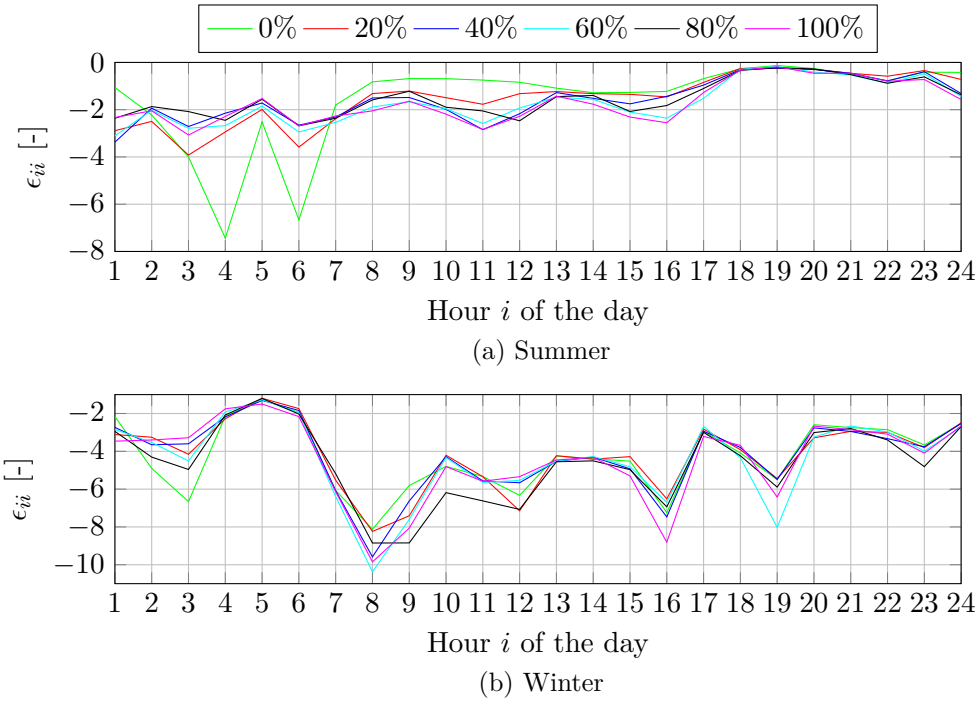

(a) Summer

(b) Winter

Fig. 5.9: Own-price price elasticities of a neighbourhood in (a) summer and (b) winter for different penetration rates of EVs

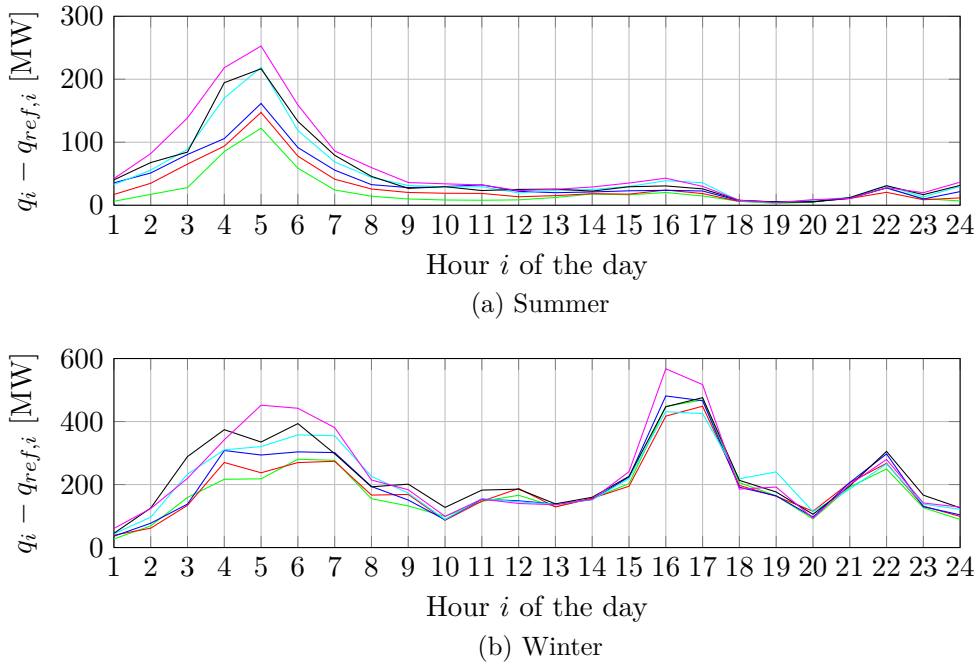

(a) Summer

(b) Winter

Fig. 5.10: Absolute shift in electricity consumption $q_i - q_{ref,i}$ of all devices, with a price decrease of $\Delta p_i = -1\%$, at every hour i for (a) summer and (b) winter for different EV penetration rates.

This can be seen in Fig. 5.9b. It shows the absolute difference in electricity demand $q_i - q_{ref,i}$ with a price decrease of $\Delta p_i = -1\,\%$, for different EV penetration rates in summer and winter. As in summer the power consumption of heating devices is far less than in winter, one can clearly see the effect of the penetration rate of EVs on the absolute demand shift. An increasing EV penetration rate leads to a greater absolute demand shift, which makes sense since more EVs can be charged when prices are cheaper. Since most of the EVs are charged at night, the difference between the distinct penetration degrees is the biggest at these moments. During the other hours of the day the curves are almost all coincident, since in all cases almost no EVs are available to charge at these hours.

5.7 Conclusions

In this chapter, the results of the Monte Carlo simulation are discussed and scaled up to a level Belgian level. This simulation has three main outcomes, namely the scaled up reference electricity consumption, the price elasticity matrices and the minimum and maximum possible power consumption.

The first outcome, the scaled up reference electricity consumption resulting from our model, was discussed in section 5.3 for all four seasons. To put this result in context, two resulting parameters were compared to the current electricity consumption, namely the average annual *energy* consumption and the instant peak *power* consumption. Due to the electrification in our model, the annual residential energy consumption in our model is slightly more than double compared to that of 2012. Electrified space heating and EVs are the devices that contribute the most to this result. Although the annual energy consumption only doubles, the residential peak power consumption resulting from our model is a factor 5 to 8 higher than the residential peak power consumed today. This enormous rise in power consumption must be put in its proper context. The RTP strategy leads to load syncing of different devices. This happens in the fifth hour in every season as most EVs have to be charged and the houses heated up a few hours later. Hence, the RTP strategy in combination with these new electric loads explains the big rise in peak power consumption.

The second and most important outcome of the Monte Carlo simulation and this thesis are the price elasticity matrices. The results of these matrices were described in section 5.4 for the four seasons. Different conclusions can be drawn from these PEM:

- The own-price elasticities are all negative and the cross-price elasticities are mostly positive as expected.
- The PEMs are different for each season, as they are influenced by the weather conditions. The most extreme values (both positive and negative) are found in winter while the values in summer are smaller in absolute value. This is a consequence of the higher flexibility provided by the heat pumps and electric heaters when it's colder.

- The maximum time length over which demand is shifted from the reference scenario in reaction to a price change is 7 hours. Outside this range of influence, all cross-price elasticities are zero.
- The absolute shift in demand at a certain hour in reaction to a price change at the same hour reveals that during the night and in the late afternoon there are a lot of shifting possibilities. During noon, not much flexibility is available. Again, the ambient temperature influences this absolute shift in demand as in winter more flexibility is provided by the electric heaters.
- The elasticity values obtained are relatively big, meaning that the RTP scheme we considered is very sensitive to the price signal. This price signal should be thus carefully designed in order to reach the expected response. This could be partly due to the fact that the elasticities we obtained are representing day-ahead forecasts of the flexibility, and cannot be used to predict the response on sudden price changes.
- When comparing the results with the literature, we find that our elasticities have a much bigger value. This is because in the literature, elasticities describe the behavioural reaction to a changing price, while we are investigating automatic demand response with a lot more flexible devices available.
- The influence of the three different type of devices on the flexibility is investigated. The heaters offer the most flexibility in all seasons but the summer. The EVs are mainly available for load shifting during the night. The wet appliances have only a small contribution, mainly during the day.

The third outcome of the Monte Carlo simulation is the minimum power that must be consumed and the maximum amount of power that could be consumed. The minimum amount of power is largely determined by the non-flexible load, in all seasons. Except during the night, when a part of the EVs always has to charge. The maximum amount of power that could be consumed is mostly restricted by the household limit of 9.2 kW and related to the weather conditions, since when the ambient temperature is higher, less heaters can be turned on.

A sensitivity analysis was performed to assess the influence of the penetration rate of EVs on the values of the price elasticity matrices. From this, we can conclude that the price elasticities are quite insensitive to a changing penetration rate of EVs.

Chapter 6

General Conclusions

This chapter summarizes all conclusions that were drawn throughout this thesis and revisits the research questions as posed in section 1.3. We approach the results in a critical way and point out possible flaws in our modelling approach. Finally, some possible topics for further research are discussed.

6.1 Summary and Recapitulation

This thesis has investigated and quantified the potential flexibility of residential electricity demand in 2050 through price elasticities, which are grouped into price elasticity matrices. These price elasticities of residential demand were determined following a bottom-up approach, taking into account the technical characteristics and constraints of different devices. First, we performed an extensive literature study from which we synthesized important information to build our own model upon.

The total residential electricity demand consists partly of non-flexible and partly of flexible demand. The non-flexible demand was modelled following the approach of Richardson et al. [52]. A lot of different potentially flexible loads exist, as pointed out in section 2.3. In our model, three types of flexible devices are implemented: heating devices (heat pumps and back-up electric heaters), electric vehicles and wet appliances. We implemented these three devices since they seem the most probable to be used for demand response, and could have considerable impact in Belgium (see chapter 2 for a more detailed explanation). This answers the question of the types of devices that we can consider to be flexible, or the first sub question of section 1.3.

Different demand response programs exist in smart grids. We chose to implement a real time pricing scheme, since it is believed to be the most efficient and most advanced price based program that can free up the most flexibility (see section 2.2). The term 'flexibility' is quite vague and can be represented in different manners (section 2.4). Price elasticities are considered a good method as they make up a linear relationship between a price change and a change in electricity demand. This addresses the second sub question of section 1.3: in which way to represent the flexibility.

All devices are grouped together in houses according to their penetration rates. Subsequently, houses are grouped together in neighbourhoods in order to represent a correct population structure. Each house is subject to the same real time price and optimizes its flexible electricity consumption towards minimal electricity cost. Examples for a single house and an entire neighbourhood were discussed in chapter 3. From these examples it can be seen that flexible devices shift their consumption to the cheapest moment, which causes enormous peaks in the power consumption. This is called *load syncing* and might be a desired consequence, as power is cheap and more consumption is needed. However, the grid should be able to bear such high peaks. In our model only a maximum amount of power for a house is incorporated while other grid constraints are neglected. This is a major flaw in our model, and can be improved by implementing specialised distributed algorithms. A question arises thus about the grid strength in the future. Hence, our result can be seen as the maximum potential, as if a future grid has been designed to facilitate these flows.

A variety of prices are passed on to a neighbourhood yielding corresponding electricity consumption patterns. A linear relationship between the applied prices and electricity consumption is sought, in the form of elasticities. Since price elasticities are defined in a certain reference point, in this thesis the reference price is chosen to be the average of all price signals applied, but of course other reference prices can be applied.

A selective linear regression is then performed which relates the changes in price to the changes in electricity consumption, relative to this reference point. This yields the required elasticity matrix for the examined neighbourhood. The selective regression allows to assess the length of the time interval in which a price change still influences a change in demand in a statistical manner. The error variance of the obtained coefficients gives standard deviations smaller than 10 %.

We found that a (higher-order) logistic regression gives a better fit to the absolute price-demand points, but this is not a linear model, and the first-order approximation of this curve quickly over- or underestimates the elasticities. The regular linear regression was found to be a good compromise.

Since each neighbourhood comprises a number of stochastic elements and is thus different, a Monte Carlo simulation was performed on 100 neighbourhoods, in order to give an estimate of average the desired results. Since these are averages over all possible neighbourhoods, this allows scaling up the results to the level of a whole country. This Monte Carlo simulation was repeated for each season and both weekend and weekdays in order to assess their influence on the flexibility.

The outcomes of this Monte Carlo simulation are an estimate of the average and the statistical variance of the values of the elasticity matrix, the minimum and maximum electricity use and the electricity use at the applied reference price. The results are discussed in chapter 5. All results are scaled up towards a Belgian level. The main conclusions are:

- The annual residential electricity consumption more or less doubles w.r.t. the one we experience today. The peak power demand increases by a factor 5 to 8. This is due to the electrification of residential energy demand and the load

syncing that occurs when all households schedule day-ahead to the same RTP signal, which they are assumed not to influence.

- The price elasticity matrices (and thus flexibility) are strongly influenced by weather conditions. A higher flexibility is available in winter (because more heating appliances are available), the least flexibility is available in summer. There is little difference between weekdays and weekends. This is an answer to the influences on the amount of flexibility available, the third sub question.
- The elasticity values are quite large, meaning that a RTP scheme is very sensitive to the price signal applied, when implementing automatic demand response. This means that this price signal, which results from a day-ahead forecast, should be carefully designed.
- The maximum shift in time of (a part of) the electricity demand to another hour from the reference scenario is found to be 7 hours. This differs for every season and can be read from the obtained elasticity matrices from the Monte Carlo simulation. This provides an answer to sub question 5 regarding the time interval demand is shifted.
- The absolute minimum of electricity consumption is almost completely defined be the non-flexible load except during the night, when a part of the EVs has to charge no matter what. This is found to be true for all seasons.
- The absolute maximum electricity consumption possible is found to be limited by the households' power limit rather than the appliances', except for the summer, when heaters cannot be turned on. This defines the absolute maximum amount of flexibility, sub question 4.
- Heaters provide the most flexibility in each season but the summer. EVs in this residential context are mainly available for load shifting during the night and wet appliances only contribute little to the overall flexibility during the day. This is explained in section 5.4.3 and addresses the sixth sub question: the separate influence of each devices.
- A sensitivity analysis assessing the influence of EVs concludes that the price elasticities are quite insensitive to a changing penetration rate, which addresses the final sub question.

6.2 Further Research

The methodology and results of this study could be used in further research to improve the estimation of the flexibility. Possible adaptations and enhancements to our model would be:

- A better estimation of parameters that are inputs in our model, like penetration and cycles of wet appliances or EVs, or a better estimation of the building stock with related building models.

- Design and integration of non-considered devices and applications, for instance air conditioning, V2G or solar boilers.
- Application of the model to other regions in Europe.
- The incorporation of distributed algorithms such as in [72]. These algorithms can be applied to the level of a neighbourhood, in order to take into account hard grid constraints, for instance the distribution transformer limit, voltage limits etc.
- This can be elaborated into a real nodal pricing algorithm, in which for instance losses or grid reinforcements due to DER are appropriately priced.
- Quantification of the flexibility for industrial and commercial electricity demand, and possible incorporation of a medium voltage (MV) grid. The residential neighbourhoods can also be integrated in the MV grid by sampling neighbourhoods from the distributions resulting from the Monte Carlo simulations, and allocating them in the MV grid. This would then allow taking into account its constraints and limitations.
- A better estimation of the price elasticities via more elaborate regression methods.
- Combination with a unit commitment model that can manage price elasticity matrices in order to calculate a new price that incorporates the flexible demand. This could flatten the power peaks we now observe.

Appendices

Appendix A

Household Level Optimization

In this appendix the structure of the optimization problem of section 3.5 as it is solved in MATLAB is elaborated in further detail. The optimization problem was stated in (3.12) as follows:

$$\begin{aligned} \min_{x} \quad & \mathbf{c}^T \cdot \mathbf{x} \\ \text{subject to} \quad & \mathbf{A} \cdot \mathbf{x} = \mathbf{b}_{eq} \\ & \mathbf{H} \cdot \mathbf{x} \leq \mathbf{b}_{ineq} \\ & \mathbf{x}_l \leq \mathbf{x} \leq \mathbf{x}_u \end{aligned} \tag{A.1}$$

The structure of the vectors is explained here for optimizing one day. When optimizing multiple days in a row, this structure is simply repeated. We assume that one day is split up in N time steps. The price vector $\mathbf{p}^T$ for a particular day can then be written as $\mathbf{p}^T = (p_1, ..., p_N)$.

The vector $\mathbf{x}$ and $\mathbf{c}$ in this equation can be further divided in variables for wet appliances (WA), space heating (SH), domestic hot water (DHW) and EVs respectively:

$$\mathbf{x} = (\mathbf{x}_{WA}^T | \mathbf{x}_{SH}^T | \mathbf{x}_{DHW}^T | \mathbf{x}_{EV}^T) \tag{A.2}$$

$$\mathbf{c} = (\mathbf{c}_{WA}^T | \mathbf{c}_{SH}^T | \mathbf{c}_{DHW}^T | \mathbf{c}_{EV}^T) \tag{A.3}$$

The equality constraints could now be written in matrix form as:

$$\begin{pmatrix} \mathbf{A}_{WA} & \mathbf{0} & \mathbf{0} & \mathbf{0} \\ \mathbf{0} & \mathbf{A}_{SH} & \mathbf{0} & \mathbf{0} \\ \mathbf{0} & \mathbf{0} & \mathbf{A}_{DHW} & \mathbf{0} \\ \mathbf{0} & \mathbf{0} & \mathbf{0} & \mathbf{A}_{EV} \end{pmatrix} \cdot \mathbf{x} = \begin{pmatrix} \mathbf{b}_{WA} \\ \mathbf{b}_{SH} \\ \mathbf{b}_{DHW} \\ \mathbf{b}_{EV} \end{pmatrix} \tag{A.4}$$

Similarly, for the inequality constraints:

$$\begin{pmatrix} \mathbf{0} & \mathbf{A}_{ineq,SH} & \mathbf{0} & \mathbf{0} \\ \mathbf{0} & \mathbf{H}_{SH} & \mathbf{H}_{DHW} & \mathbf{0} \\ \mathbf{0} & \mathbf{0} & \mathbf{A}_{ineq,DHW} & \mathbf{0} \\ \mathbf{H}_{WA,max} & \mathbf{H}_{SH,max} & \mathbf{H}_{DHW,max} & \mathbf{H}_{EV,max} \end{pmatrix} \cdot \mathbf{x} \leq \begin{pmatrix} \mathbf{b}_{ineq,SH} \\ \mathbf{b}_{ineq,SH,DHW} \\ \mathbf{b}_{ineq,DHW} \\ \mathbf{b}_{overall,max} \end{pmatrix} \tag{A.5}$$

Finally, the upper and lower boundaries in vector form can be noted as:

$$\begin{pmatrix} \mathbf{x}_{l,WA} \\ \mathbf{x}_{l,SH} \\ \mathbf{x}_{l,DHW} \\ \mathbf{x}_{l,EV} \end{pmatrix} \leq \begin{pmatrix} \mathbf{x}_{WA} \\ \mathbf{x}_{SH} \\ \mathbf{x}_{DHW} \\ \mathbf{x}_{EV} \end{pmatrix} \leq \begin{pmatrix} \mathbf{x}_{u,WA} \\ \mathbf{x}_{u,SH} \\ \mathbf{x}_{u,DHW} \\ \mathbf{x}_{u,EV} \end{pmatrix} \tag{A.6}$$

A.1 Wet Appliances

The vector $\mathbf{x}_{WA}$ can be further split up in variables for a washing machine (WM), a dishwasher (DW) and a tumble dryer (TD) if present and running on that particular day:

$$\mathbf{x}_{WA} = (\mathbf{x}_{WM}^T | \mathbf{x}_{DW}^T | \mathbf{x}_{TD}^T). \tag{A.7}$$

These are binary variables which equal 1 when a machine is running and zero when not running. This is included in the boundaries of (A.6). For each device there are as many variables as timesteps where the cycle is possible to shift to (see (3.13)). In other words, the variables of the wet appliances represent each possible start time of the appliance. The same breakdown can be used on the coefficient vector $\mathbf{c}_{WA}$. In order to obtain the coefficients, the start of the power cycle of the appliance is placed at each possible start time and each time subsequently multiplied by the price vector and summed up. Each wet appliance can only run one time a day. This constraint is included in the equality matrices $\mathbf{A}_{WA}$ and $\mathbf{b}_{WA}$ by saying that $\sum_j x_{WM,j} = 1$, $\sum_j x_{DW,j} = 1$ and $\sum_j x_{TD,j} = 1$.

A.2 Space Heating and Domestic Hot Water

The vector for space heating $\mathbf{x}_{SH}^T$ consists of N times the same variable structure repeated $(\mathbf{x}_{SH,1}^T, ..., \mathbf{x}_{SH,N}^T)$ because there are N time steps. For time step j, $\mathbf{x}_{SH,j}^T$ consists of the vector $\mathbf{T}_j$ stated in (3.2), the vector $\mathbf{U}_j^{SH} = (\dot{Q}_j^{HP,SH}, \dot{Q}_j^{AUX1,SH}, \dot{Q}_j^{AUX2,SH})$ and the binary variable for space heating x_j^{SH}:

$$\mathbf{x}_{SH,j}^T = (\mathbf{T}_j, \mathbf{U}_j^{SH}, x_j^{SH})^T. \tag{A.8}$$

The variable vector for domestic hot water is made up in an analogous way. For time step j, $\mathbf{x}_{DHW,j}$ is built up as follows:

$$\mathbf{x}_{DHW,j}^T = (T_j^{tank}, \dot{Q}_j^{HP,DHW}, \dot{Q}_j^{AUX1,DHW}, \dot{Q}_j^{AUX2,DHW}, x_j^{DHW})^T \tag{A.9}$$

and this structure is again repeated N times in $\mathbf{x}_{DHW}$. The coefficient vectors for space heating and domestic hot water respectively can be written as:

$$\mathbf{c}_{SH}^T = (0_{1\times 9}, \frac{p_1}{COP_j^{HP,SH}}, \frac{p_1}{\eta^{AUX1}}, \frac{p_1}{\eta^{AUX2}}, ..., 0_{1\times 9}, \frac{p_N}{COP_N^{HP,SH}}, \frac{p_N}{\eta^{AUX1}}, \frac{p_N}{\eta^{AUX2}}, 0_{1\times 9})^T \tag{A.10}$$

$$\mathbf{c}_{DHW}^T = (0, \frac{p_1}{COP_j^{HP,DHW}}, \frac{p_1}{\eta^{AUX1}}, \frac{p_1}{\eta^{AUX2}}, 0, ..., 0, \frac{p_N}{COP_j^{HP,DHW}}, \frac{p_1}{\eta^{AUX1}}, \frac{p_N}{\eta^{AUX2}}, 0)^T \tag{A.11}$$

- The matrices $\mathbf{A}_{SH}$ and $\mathbf{b}_{SH}$ in (A.4) contain the thermal dynamic behaviour of the building as described by (3.1). The matrices $\mathbf{A}_{eq,DHW}$ and $\mathbf{b}_{eq,DHW}$ hold the dynamic behaviour of the tank as described by (3.8).
- The first line in the inequality matrix of (A.5) holds equations (3.14), (3.15) and (3.16) for each time step. The second line holds the maximimum constraints on the electric heating devices (3.19) by adding the contributions of the space heating and domestic hot water. The third line represents (3.18).
- The minimum constraint on the power output (3.21) and the minimum temperature constraints are taken care of in the lower boundaries in (A.6). Furthermore, the boundaries $\mathbf{x}_{l,DHW}$ and $\mathbf{x}_{u,DHW}$ set the minimum and maximum temperature in the storage tank and assure that $\dot{Q}^{AUX2,DHW} = 0$ at all time steps as this heater cannot heat up the water in the tank.

A.3 EVs

The variable vector of the EV $\mathbf{x}_{EV}$ contains two variables for each time step. The variable vector and the coefficient vector $\mathbf{c}_{EV}$ in vector form are:

$$\mathbf{x}_{EV}^T = (SOC_1, P_1^{charge}, ..., SOC_N, P_N^{charge})^T \tag{A.12}$$

$$\mathbf{c}_{EV}^T = (0, 1, ..., 0, 1)^T \tag{A.13}$$

- The evolution of the SOC in time governed by (3.9) is contained in the matrix $\mathbf{A}_{EV}$ of equation A.4.
- The upper and lower limits on the SOC (3.22) and the charging power P^{charge} (3.23) are taken care of in the boundaries $\mathbf{x}_{u,EV}$ and $\mathbf{x}_{l,EV}$.

A.4 Overall Power Constraint

The overall power constraint of (3.24) is handled in the last line of the inequality matrix in (A.5) where all contributing *electric* powers are added for each time step.

Appendix B

Electricity Consumption in Belgium

In this appendix, we show some figures that help to interpret the total electricity use as obtained in our model. We refer to section 5.3 for the related interpretations of the figures shown below. Appendix B.1 shows the electricity consumption at the reference price for each season in the weekend. The same figure is presented in the text for weekdays. In appendix B.2 we show modified synthetic load profiles for each season, which represent the fraction of yearly energy consumed on an average seasonal day as it is nowadays. With these modified profiles we can obtain the absolute residential electricity demand for an average day in a certain season. We used these absolute demand profiles as a base to compare the electricity demand obtained by our model with. The residential electricity demand profiles as they are nowadays are plotted in appendix B.3.

B.1 Weekend Consumption

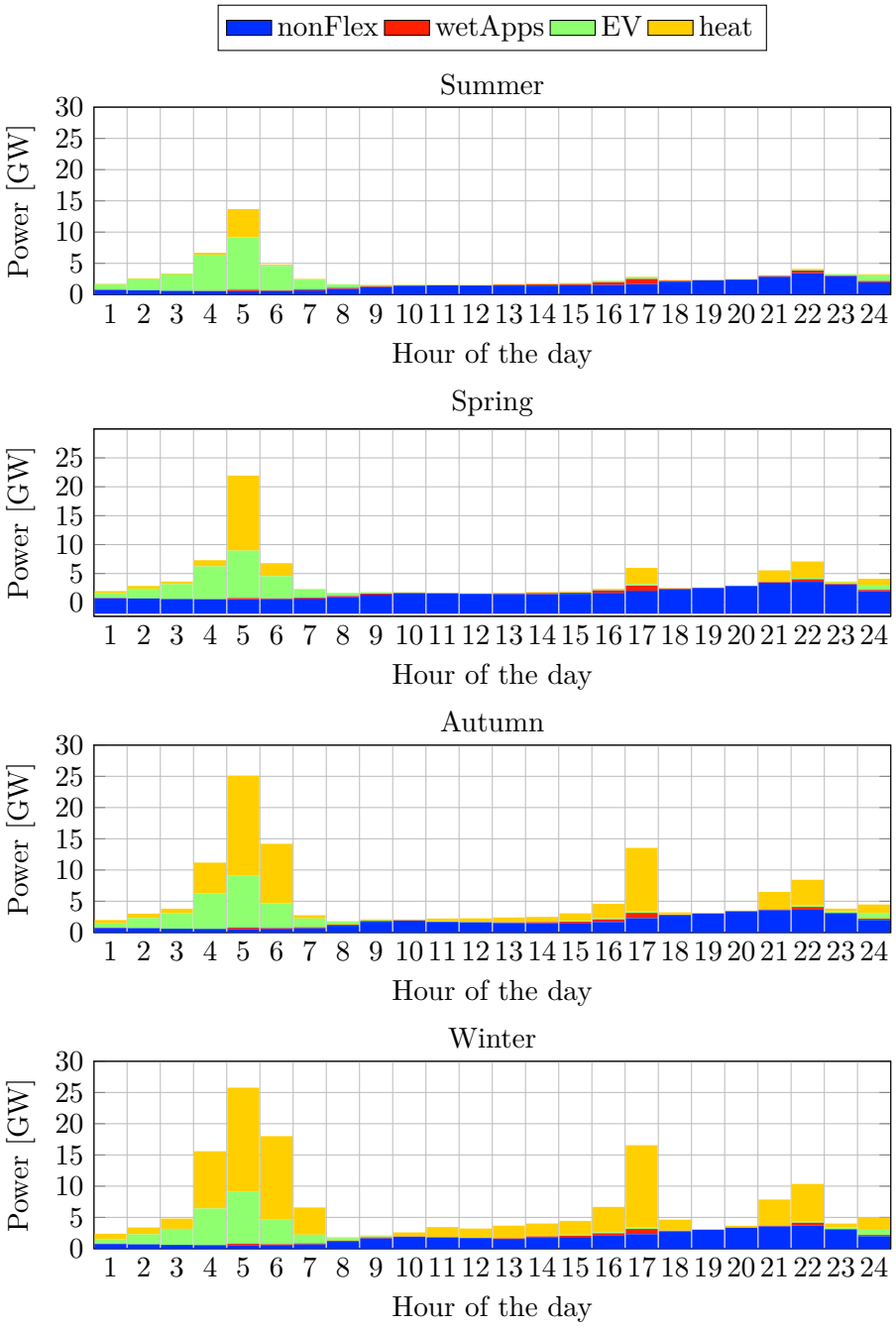

Fig. B.1: Reference residential electricity consumption scaled up towards a Belgian level in summer, spring, autumn and winter for a weekend day.

B.2 Modified SLP

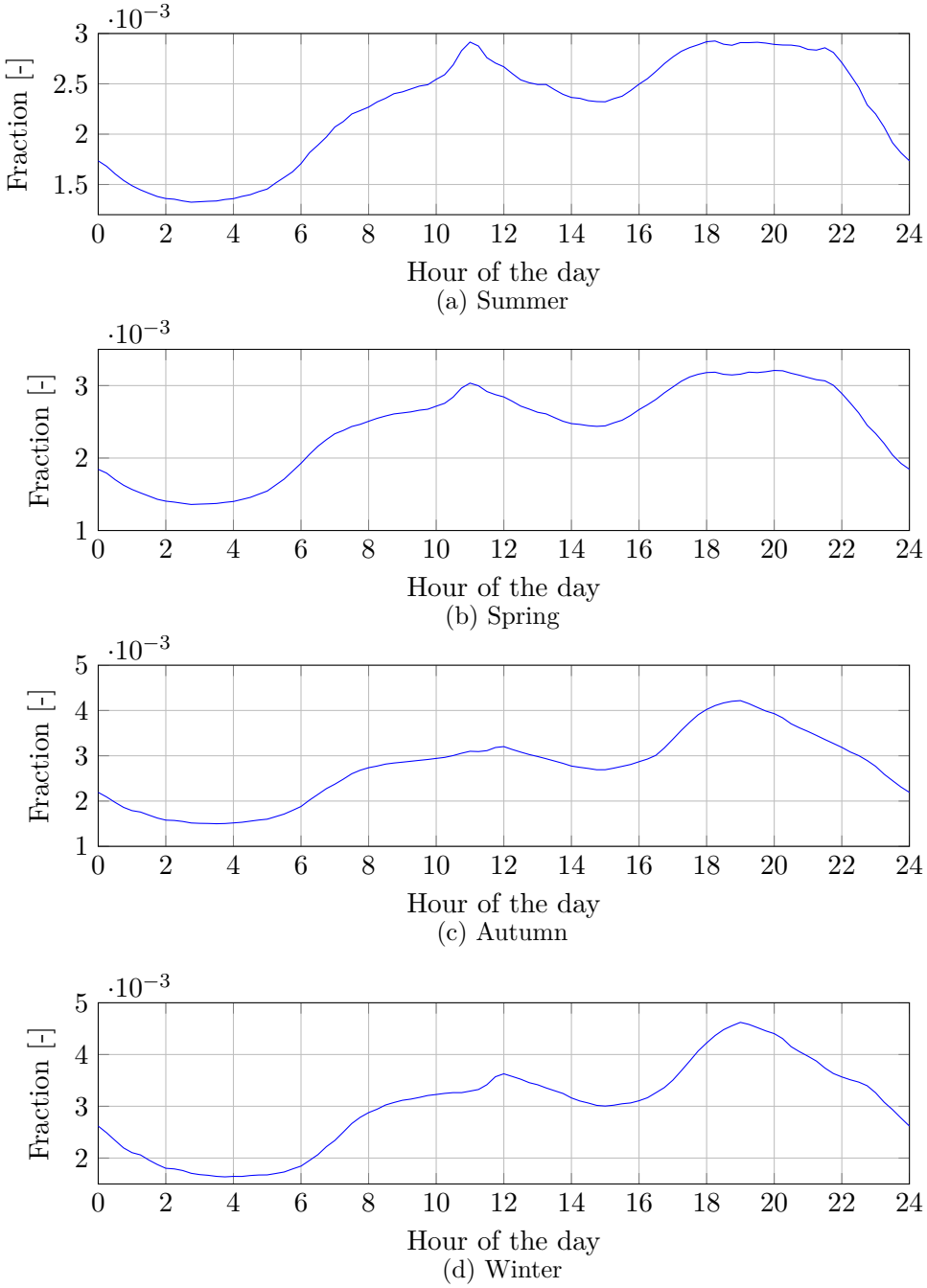

Fig. B.2: Synthetic load profiles showing the fraction of yearly electricity demand for the average day in (a) summer (b) spring (c) autumn (d) winter

B.3 Absolute Demand Profiles 2014

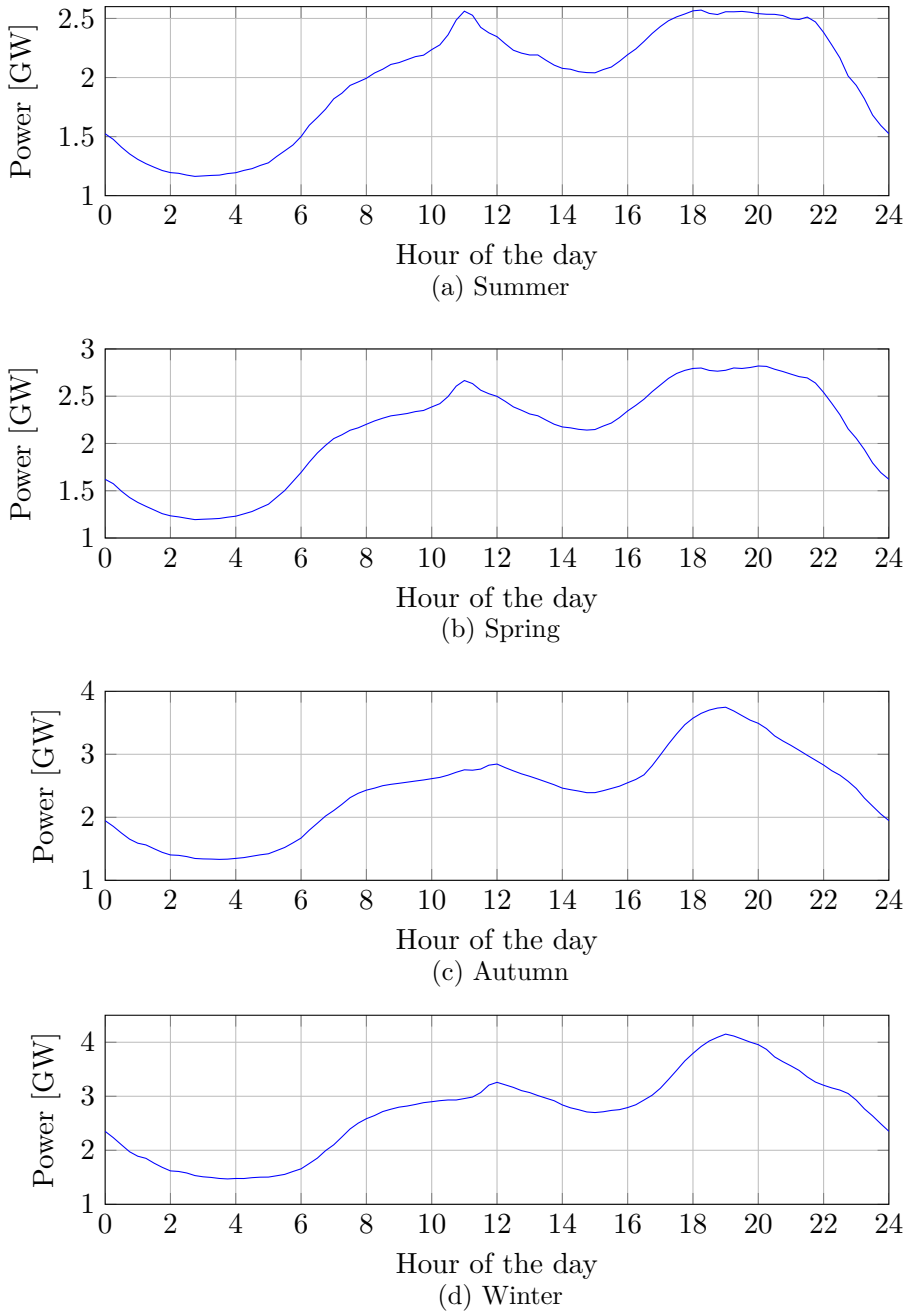

Fig. B.3: Absolute power demand in 2014 for the average day in (a) spring (b) summer (c) autumn (d) winter

Appendix C

Price Elasticity Matrices

In this appendix, the values of the resulting price elasticity matrices are shown in tables, two each season: a weekday and a weekend day.

-2.0	0.5	0.0	0.0	0.0	0.3	0.2	0.0	0.0	0.0	0.0	0.0	0.0	0.0	0.0	0.0	0.0	0.0	0.0	0.0	0.0	0.0	0.0	0.3
0.0	-2.4	0.7	0.1	0.2	0.3	0.3	0.0	0.0	0.0	0.0	0.0	0.0	0.0	0.0	0.0	0.0	0.0	0.0	0.0	0.0	0.0	0.0	0.0
0.0	0.4	-2.8	0.8	0.1	0.9	0.0	0.0	0.0	0.0	0.0	0.0	0.0	0.0	0.0	0.0	0.0	0.0	0.0	0.0	0.0	0.0	0.0	0.0
0.1	0.0	0.0	-2.9	1.9	0.4	0.5	0.0	0.0	0.0	0.0	0.0	0.0	0.0	0.0	0.0	0.0	0.0	0.0	0.0	0.0	0.0	0.0	0.0
0.0	0.0	0.0	0.7	-1.6	0.7	0.0	0.0	0.0	0.0	0.0	0.0	0.0	0.0	0.0	0.0	0.0	0.0	0.0	0.0	0.0	0.0	0.0	0.0
0.0	0.4	0.5	0.7	1.3	-3.2	0.1	0.0	0.0	0.0	0.0	0.0	0.0	0.0	0.0	0.0	0.0	0.0	0.0	0.0	0.0	0.0	0.0	0.0
0.6	0.0	0.3	0.2	0.2	0.4	-2.7	-0.0	0.0	0.0	0.0	0.0	0.0	0.0	0.0	0.0	0.0	0.0	0.0	0.0	0.0	0.0	0.0	0.0
0.0	0.0	0.0	0.0	0.0	0.0	0.0	-1.8	0.0	0.0	0.0	0.0	0.0	0.0	0.0	0.0	0.0	0.0	0.0	0.0	0.0	0.0	0.0	0.0
0.0	0.0	0.0	0.0	0.0	0.0	0.0	0.0	-1.1	0.0	0.0	0.0	0.0	0.0	0.0	0.0	0.0	0.0	0.0	0.0	0.0	0.0	0.0	0.0
0.0	0.0	0.0	0.0	0.0	0.0	0.0	0.0	0.1	-0.9	0.2	0.1	0.0	0.0	0.0	0.0	0.0	0.0	0.0	0.0	0.0	0.0	0.0	0.0
0.0	0.0	0.0	0.0	0.0	0.0	0.0	0.0	0.2	0.1	-1.0	0.2	0.2	0.0	0.0	0.0	0.0	0.0	0.0	0.0	0.0	0.0	0.0	0.0
0.0	0.0	0.0	0.0	0.0	0.0	0.0	0.0	0.0	0.2	0.2	-0.7	0.0	0.0	0.0	0.0	0.0	0.0	0.0	0.0	0.0	0.0	0.0	0.0
0.0	0.0	0.0	0.0	0.0	0.0	0.0	0.0	0.0	0.1	0.1	0.1	-0.9	0.2	0.0	0.0	0.0	0.0	0.0	0.0	0.0	0.0	0.0	0.0
0.0	0.0	0.0	0.0	0.0	0.0	0.0	0.0	0.0	0.0	0.1	0.1	0.1	-1.2	0.4	0.0	0.0	0.0	0.0	0.0	0.0	0.0	0.0	0.0
0.0	0.0	0.0	0.0	0.0	0.0	0.0	0.0	0.0	0.0	0.0	0.0	0.0	0.2	-1.8	0.7	0.4	0.0	0.0	0.0	0.0	0.0	0.0	0.0
0.0	0.0	0.0	0.0	0.0	0.0	0.0	0.0	0.0	0.0	0.0	0.0	0.0	0.5	-2.7	1.2	0.0	0.0	0.0	0.0	0.0	0.0	0.0	0.0
0.0	0.0	0.0	0.0	0.0	0.0	0.0	0.0	0.0	0.0	0.0	0.0	0.0	0.0	1.0	-1.8	-0.1	0.0	0.0	0.0	0.0	0.0	0.0	0.0
0.0	0.0	0.0	0.0	0.0	0.0	0.0	0.0	0.0	0.0	0.0	0.0	0.0	0.0	0.0	0.0	-0.3	0.0	0.0	0.1	0.0	0.0	0.0	0.0
0.0	0.0	0.0	0.0	0.0	0.0	0.0	0.0	0.0	0.0	0.0	0.0	0.0	0.0	0.0	0.0	-0.1	0.0	-0.2	0.0	0.0	0.1	0.0	0.0
0.0	0.0	0.0	0.0	0.0	0.0	0.0	0.0	0.0	0.0	0.0	0.0	0.0	0.0	0.0	0.0	0.1	0.0	-0.3	0.0	0.2	0.0	0.0	0.0
0.0	0.0	0.0	0.0	0.0	0.0	0.0	0.0	0.0	0.0	0.0	0.0	0.0	0.0	0.0	0.0	0.1	0.0	0.0	-0.5	0.1	0.2	0.0	0.0
0.0	0.0	0.0	0.0	0.0	0.0	0.0	0.0	0.0	0.0	0.0	0.0	0.0	0.0	0.0	0.0	0.0	0.0	0.0	0.2	-1.2	0.2	0.4	0.0
0.0	0.0	0.0	0.0	0.0	0.0	0.0	0.0	0.0	0.0	0.0	0.0	0.0	0.0	0.0	0.0	0.0	0.0	0.0	0.1	0.3	-0.7	0.0	0.0
0.0	0.0	0.0	0.0	0.0	0.0	0.0	0.0	0.0	0.0	0.0	0.0	0.0	0.0	0.0	0.0	0.0	0.0	0.0	0.0	0.3	0.3	-1.3	0.0

Table C.1: Price elasticity matrix of the average summer weekday

-1.6	0.5	0.0	0.0	0.0	0.2	0.0	0.0	0.0	0.0	0.0	0.0	0.0	0.0	0.0	0.0	0.0	0.0	0.0	0.0	0.0	0.0	0.0	0.2
0.0	-2.2	0.7	0.1	0.2	0.2	0.2	0.0	0.0	0.0	0.0	0.0	0.0	0.0	0.0	0.0	0.0	0.0	0.0	0.0	0.0	0.0	0.0	0.0
0.0	0.3	-2.7	0.7	0.1	0.9	0.0	0.0	0.0	0.0	0.0	0.0	0.0	0.0	0.0	0.0	0.0	0.0	0.0	0.0	0.0	0.0	0.0	0.0
0.1	0.0	0.0	-2.9	1.9	0.4	0.6	0.0	0.0	0.0	0.0	0.0	0.0	0.0	0.0	0.0	0.0	0.0	0.0	0.0	0.0	0.0	0.0	0.0
0.0	0.0	0.0	0.7	-1.7	0.8	0.0	0.0	0.0	0.0	0.0	0.0	0.0	0.0	0.0	0.0	0.0	0.0	0.0	0.0	0.0	0.0	0.0	0.0
0.0	0.0	0.4	0.8	1.3	-3.4	0.2	0.0	0.0	0.0	0.0	0.0	0.0	0.0	0.0	0.0	0.0	0.0	0.0	0.0	0.0	0.0	0.0	0.0
0.6	0.0	0.3	0.3	0.2	0.5	-3.1	0.0	0.0	0.0	0.0	0.0	0.0	0.0	0.0	0.0	0.0	0.0	0.0	0.0	0.0	0.0	0.0	0.0
0.0	0.0	0.0	0.0	0.0	0.0	0.0	-2.4	0.0	0.0	0.0	0.0	0.0	0.0	0.0	0.0	0.0	0.0	0.0	0.0	0.0	0.0	0.0	0.0
0.0	0.0	0.0	0.0	0.0	0.0	0.0	0.0	-1.3	0.0	0.0	0.0	0.0	0.0	0.0	-0.2	0.0	0.0	0.0	0.0	0.0	0.0	0.0	0.0
0.0	0.0	0.0	0.0	0.0	0.0	0.0	0.0	0.1	-0.9	0.2	0.1	0.0	0.0	0.0	0.0	0.0	0.0	0.0	0.0	0.0	0.0	0.0	0.0
0.0	0.0	0.0	0.0	0.0	0.0	0.0	0.0	0.1	0.1	-0.8	0.1	0.2	0.0	0.0	0.0	0.0	0.0	0.0	0.0	0.0	0.0	0.0	0.0
0.0	0.0	0.0	0.0	0.0	0.0	0.0	0.0	0.0	0.1	0.2	-0.6	0.0	0.0	0.0	0.0	0.0	0.0	0.0	0.0	0.0	0.0	0.0	0.0
0.0	0.0	0.0	0.0	0.0	0.0	0.0	0.0	0.0	0.1	0.1	0.1	-0.9	0.1	0.0	0.0	0.0	0.0	0.0	0.0	0.0	0.0	0.0	0.0
0.0	0.0	0.0	0.0	0.0	0.0	0.0	0.0	0.0	0.0	0.2	0.0	0.1	-1.1	0.4	0.0	0.0	0.0	0.0	0.0	0.0	0.0	0.0	0.0
0.0	0.0	0.0	0.0	0.0	0.0	0.0	0.0	0.0	0.0	0.0	0.0	0.0	0.2	-1.7	0.6	0.4	0.0	0.0	0.0	0.0	0.0	0.0	0.0
0.0	0.0	0.0	0.0	0.0	0.0	0.0	0.0	0.0	0.0	0.0	0.0	0.0	0.0	0.4	-2.5	1.1	0.0	0.0	0.0	0.0	0.0	0.0	0.0
0.0	0.0	0.0	0.0	0.0	0.0	0.0	0.0	0.0	0.0	0.0	0.0	0.0	0.0	0.0	1.0	-1.7	-0.1	0.0	0.0	0.0	0.0	0.0	0.0
0.0	0.0	0.0	0.0	0.0	0.0	0.0	0.0	0.0	0.0	0.0	0.0	0.0	0.0	0.0	0.0	0.0	-0.4	0.0	0.0	0.1	0.0	0.0	0.0
0.0	0.0	0.0	0.0	0.0	0.0	0.0	0.0	0.0	0.0	0.0	0.0	0.0	0.0	0.0	-0.0	-0.0	0.0	-0.2	0.0	0.0	0.1	0.0	0.0
0.0	0.0	0.0	0.0	0.0	0.0	0.0	0.0	0.0	0.0	0.0	0.0	0.0	0.0	0.0	0.0	0.0	0.1	0.0	-0.3	0.0	0.2	0.0	0.0
0.0	0.0	0.0	0.0	0.0	0.0	0.0	0.0	0.0	0.0	0.0	0.0	0.0	0.0	0.0	0.0	0.0	0.1	0.0	0.0	-0.4	0.1	0.1	0.0
0.0	0.0	0.0	0.0	0.0	0.0	0.0	0.0	0.0	0.0	0.0	0.0	0.0	0.0	0.0	0.0	0.0	0.0	0.0	0.0	0.2	-1.0	0.1	0.3
0.0	0.0	0.0	0.0	0.0	0.0	0.0	0.0	0.0	0.0	0.0	0.0	0.0	0.0	0.0	0.0	0.0	0.0	0.0	0.0	0.3	-0.7	0.0	
0.0	0.0	0.0	0.0	0.0	0.0	0.0	0.0	0.0	0.0	0.0	0.0	0.0	0.0	0.0	0.0	0.0	0.0	0.0	0.0	0.3	0.3	-1.2	

Table C.2: Price elasticity matrix of the average summer weekend day

-2.2	0.6	0.0	0.0	0.0	0.3	0.2	0.0	0.0	0.0	0.0	0.0	0.0	0.0	0.0	0.0	0.0	0.0	0.0	0.0	0.0	0.0	0.0	0.5
0.0	-2.6	0.9	0.1	0.2	0.2	0.3	0.0	0.0	0.0	0.0	0.0	0.0	0.0	0.0	0.0	0.0	0.0	0.0	0.0	0.0	0.0	0.0	0.0
0.0	0.5	-3.3	0.7	0.4	1.0	0.0	0.0	0.0	0.0	0.0	0.0	0.0	0.0	0.0	0.0	0.0	0.0	0.0	0.0	0.0	0.0	0.0	0.0
0.2	0.2	0.2	-4.8	2.4	0.9	0.5	0.0	0.0	0.0	0.0	0.0	0.0	0.0	0.0	0.0	0.0	0.0	0.0	0.0	0.0	0.0	0.0	0.0
0.0	0.0	0.0	0.7	-1.9	0.9	0.0	0.0	0.0	0.0	0.0	0.0	0.0	0.0	0.0	0.0	0.0	0.0	0.0	0.0	0.0	0.0	0.0	0.0
0.0	0.0	0.0	1.3	2.3	-5.1	0.3	0.0	0.0	0.0	0.0	0.0	0.0	0.0	0.0	0.0	0.0	0.0	0.0	0.0	0.0	0.0	0.0	0.0
0.6	0.0	0.4	0.3	0.2	1.1	-4.1	-0.5	0.0	0.0	0.0	0.0	0.0	0.0	0.0	0.0	0.0	0.0	0.0	0.0	0.0	0.0	0.0	0.0
0.0	0.0	0.0	0.0	0.0	0.0	0.1	-2.3	0.0	0.0	0.0	0.0	0.0	0.0	0.0	0.0	0.0	0.0	0.0	0.0	0.0	0.0	0.0	0.0
0.0	0.0	0.0	0.0	0.0	0.0	0.0	0.0	-1.2	0.0	0.0	0.0	0.0	0.0	0.0	0.0	0.0	0.0	0.0	0.0	0.0	0.0	0.0	0.0
0.0	0.0	0.0	0.0	0.0	0.0	0.0	0.0	0.1	-0.9	0.2	0.1	0.0	0.0	0.0	0.0	0.0	0.0	0.0	0.0	0.0	0.0	0.0	0.0
0.0	0.0	0.0	0.0	0.0	0.0	0.0	0.0	0.2	0.1	-1.3	0.2	0.2	0.0	0.0	0.0	0.0	0.0	0.0	0.0	0.0	0.0	0.0	0.0
0.0	0.0	0.0	0.0	0.0	0.0	0.0	0.0	0.0	0.2	0.3	-1.3	0.0	0.0	0.0	0.0	0.0	0.0	0.0	0.0	0.0	0.0	0.0	0.0
0.0	0.0	0.0	0.0	0.0	0.0	0.0	0.0	0.1	0.0	0.1	0.2	-1.3	0.2	0.0	0.0	0.0	0.0	0.0	0.0	0.0	0.0	0.0	0.0
0.0	0.0	0.0	0.0	0.0	0.0	0.0	0.0	0.0	0.0	0.2	0.0	0.2	-1.6	0.6	0.0	0.0	0.0	0.0	0.0	0.0	0.0	0.0	0.0
0.0	0.0	0.0	0.0	0.0	0.0	0.0	0.0	0.0	0.0	0.0	0.0	0.0	0.3	-2.4	0.9	0.4	0.0	0.0	0.0	0.0	0.0	0.0	0.0
0.0	0.0	0.0	0.0	0.0	0.0	0.0	0.0	0.0	0.0	0.0	0.0	0.0	0.0	0.3	-5.1	3.2	0.0	0.0	0.0	0.0	0.0	0.0	0.0
0.0	0.0	0.0	0.0	0.0	0.0	0.0	0.0	0.0	0.0	0.0	0.0	0.0	0.0	0.0	0.5	-3.5	0.7	0.3	0.1	0.5	0.0	0.0	0.0
0.0	0.0	0.0	0.0	0.0	0.0	0.0	0.0	0.0	0.0	0.0	0.0	0.0	0.0	0.0	0.0	1.0	-2.3	0.2	0.0	0.0	0.0	0.0	0.0
0.0	0.0	0.0	0.0	0.0	0.0	0.0	0.0	0.0	0.0	0.0	0.0	0.0	0.0	0.0	0.3	0.2	0.2	-1.0	0.0	0.2	0.0	0.0	0.0
0.0	0.0	0.0	0.0	0.0	0.0	0.0	0.0	0.0	0.0	0.0	0.0	0.0	0.0	0.0	0.0	0.7	0.4	0.0	-2.0	0.0	0.0	0.0	0.0
0.0	0.0	0.0	0.0	0.0	0.0	0.0	0.0	0.0	0.0	0.0	0.0	0.0	0.0	0.0	0.0	0.0	0.0	0.1	0.3	-2.0	0.8	0.0	0.0
0.0	0.0	0.0	0.0	0.0	0.0	0.0	0.0	0.0	0.0	0.0	0.0	0.0	0.0	0.0	0.0	0.0	0.0	0.0	0.0	0.7	-2.3	0.4	0.4
0.0	0.0	0.0	0.0	0.0	0.0	0.0	0.0	0.0	0.0	0.0	0.0	0.0	0.0	0.0	0.0	0.0	0.0	0.0	0.0	0.0	1.6	-2.3	0.0
0.2	0.0	0.0	0.0	0.0	0.0	0.0	0.0	0.0	0.0	0.0	0.0	0.0	0.0	0.0	0.0	0.0	0.0	0.0	0.0	0.0	0.6	0.6	-2.0

Table C.3: Price elasticity matrix of the average spring weekday

-2.1	0.7	0.0	0.0	0.0	0.2	0.0	0.0	0.0	0.0	0.0	0.0	0.0	0.0	0.0	0.0	0.0	0.0	0.0	0.0	0.0	0.0	0.0	0.6
0.3	-2.5	0.8	0.1	0.2	0.2	0.2	0.0	0.0	0.0	0.0	0.0	0.0	0.0	0.0	0.0	0.0	0.0	0.0	0.0	0.0	0.0	0.0	0.0
0.0	0.7	-3.5	0.8	0.4	1.0	0.0	0.0	0.0	0.0	0.0	0.0	0.0	0.0	0.0	0.0	0.0	0.0	0.0	0.0	0.0	0.0	0.0	0.0
0.3	0.0	0.3	-4.9	2.5	0.9	0.5	0.0	0.0	0.0	0.0	0.0	0.0	0.0	0.0	0.0	0.0	0.0	0.0	0.0	0.0	0.0	0.0	0.0
0.0	0.0	0.0	0.7	-2.0	0.9	0.0	0.0	0.0	0.0	0.0	0.0	0.0	0.0	0.0	0.0	0.0	0.0	0.0	0.0	0.0	0.0	0.0	0.0
0.0	0.0	0.0	1.2	2.3	-5.0	0.4	0.0	0.0	0.0	0.0	0.0	0.0	0.0	0.0	0.0	0.0	0.0	0.0	0.0	0.0	0.0	0.0	0.0
0.8	0.0	0.5	0.5	0.4	1.8	-6.0	0.1	0.0	0.0	0.0	0.0	0.0	0.0	0.0	0.0	0.0	0.0	0.0	0.0	0.0	0.0	0.0	0.0
0.0	0.0	0.0	0.0	0.0	0.0	0.5	-3.8	0.0	0.0	0.0	0.0	0.0	0.0	0.0	0.0	0.0	0.0	0.0	0.0	0.0	0.0	0.0	0.0
0.0	0.0	0.0	0.0	0.0	0.0	0.2	0.0	-1.5	0.0	0.0	0.0	0.0	0.0	0.0	0.0	0.0	0.0	0.0	0.0	0.0	0.0	0.0	0.0
0.0	0.0	0.0	0.0	0.0	0.0	0.0	0.0	0.1	-1.0	0.3	0.1	0.0	0.0	0.0	0.0	0.0	0.0	0.0	0.0	0.0	0.0	0.0	0.0
0.0	0.0	0.0	0.0	0.0	0.0	0.0	0.0	0.2	0.1	-1.1	0.1	0.2	0.0	0.0	0.0	0.0	0.0	0.0	0.0	0.0	0.0	0.0	0.0
0.0	0.0	0.0	0.0	0.0	0.0	0.0	0.0	0.0	0.2	0.3	-1.1	0.0	0.0	0.0	0.0	0.0	0.0	0.0	0.0	0.0	0.0	0.0	0.0
0.0	0.0	0.0	0.0	0.0	0.0	0.0	0.0	0.1	0.1	0.1	0.2	-1.1	0.2	0.0	0.0	0.0	0.0	0.0	0.0	0.0	0.0	0.0	0.0
0.0	0.0	0.0	0.0	0.0	0.0	0.0	0.0	0.0	0.0	0.1	0.0	0.2	-1.3	0.4	0.0	0.0	0.0	0.0	0.0	0.0	0.0	0.0	0.0
0.0	0.0	0.0	0.0	0.0	0.0	0.0	0.0	0.0	0.0	0.0	0.0	0.0	0.2	-1.9	0.7	0.4	0.0	0.0	0.0	0.0	0.0	0.0	0.0
0.0	0.0	0.0	0.0	0.0	0.0	0.0	0.0	0.0	0.0	0.0	0.0	0.0	0.0	0.2	-4.2	2.6	0.0	0.0	0.0	0.0	0.0	0.0	0.0
0.0	0.0	0.0	0.0	0.0	0.0	0.0	0.0	0.0	0.0	0.0	0.0	0.0	0.0	0.0	0.0	-3.4	0.6	0.3	0.1	0.6	0.0	0.0	0.0
0.0	0.0	0.0	0.0	0.0	0.0	0.0	0.0	0.0	0.0	0.0	0.0	0.0	0.0	0.0	0.0	1.0	-2.4	0.2	0.0	0.0	0.0	0.0	0.0
0.0	0.0	0.0	0.0	0.0	0.0	0.0	0.0	0.0	0.0	0.0	0.0	0.0	0.0	0.0	0.0	0.2	0.2	-1.0	0.0	0.2	0.0	0.0	0.0
0.0	0.0	0.0	0.0	0.0	0.0	0.0	0.0	0.0	0.0	0.0	0.0	0.0	0.0	0.0	0.0	0.4	0.4	0.0	-1.7	0.0	0.0	0.0	0.0
0.0	0.0	0.0	0.0	0.0	0.0	0.0	0.0	0.0	0.0	0.0	0.0	0.0	0.0	0.0	0.0	0.0	0.0	0.1	0.2	-1.8	0.8	0.0	0.0
0.0	0.0	0.0	0.0	0.0	0.0	0.0	0.0	0.0	0.0	0.0	0.0	0.0	0.0	0.0	0.0	0.0	0.0	0.0	0.0	0.6	-2.2	0.4	0.4
0.0	0.0	0.0	0.0	0.0	0.0	0.0	0.0	0.0	0.0	0.0	0.0	0.0	0.0	0.0	0.0	0.0	0.0	0.0	0.0	0.0	1.5	-2.2	0.0
0.2	0.0	0.0	0.0	0.0	0.0	0.0	0.0	0.0	0.0	0.0	0.0	0.0	0.0	0.0	0.0	0.0	0.0	0.0	0.0	0.0	0.6	0.5	-1.9

Table C.4: Price elasticity matrix of the average spring weekend day

-2.8	0.9	0.0	0.0	0.0	0.2	0.0	0.0	0.0	0.0	0.0	0.0	0.0	0.0	0.0	0.0	0.0	0.0	0.0	0.0	0.0	0.0	0.0	0.7
0.3	-3.2	1.2	0.1	0.4	0.2	0.2	0.0	0.0	0.0	0.0	0.0	0.0	0.0	0.0	0.0	0.0	0.0	0.0	0.0	0.0	0.0	0.2	0.0
0.0	0.9	-4.2	0.6	0.8	1.2	0.0	-0.4	0.0	0.0	0.0	0.0	0.0	0.0	0.0	0.0	0.0	0.0	0.0	0.0	0.0	0.0	0.0	0.0
0.2	0.0	0.0	-2.8	0.8	1.1	0.6	0.0	0.0	0.0	0.0	0.0	0.0	0.0	0.0	0.0	0.0	0.0	0.0	0.0	0.0	0.0	0.0	0.0
0.0	0.0	0.1	0.5	-1.3	0.4	0.3	0.0	0.0	0.0	0.0	0.0	0.0	0.0	0.0	0.0	0.0	0.0	0.0	0.0	0.0	0.0	0.0	0.0
0.0	0.0	0.0	0.7	1.0	-2.6	0.0	0.0	0.0	0.0	0.0	0.0	0.0	0.0	0.0	0.0	0.0	0.0	0.0	0.0	0.0	0.0	-0.2	0.0
0.0	0.0	0.0	0.0	1.1	2.6	-9.8	0.3	0.0	0.0	0.0	0.0	0.0	0.0	0.0	0.0	0.0	0.0	0.0	0.0	0.0	0.0	0.0	0.0
0.0	0.0	0.0	0.0	0.0	0.0	0.5	-4.8	0.0	0.0	0.0	0.0	0.0	0.0	0.0	0.0	0.0	0.0	0.0	0.0	0.0	0.0	0.0	0.0
0.0	0.0	0.0	0.0	0.0	0.0	0.3	0.5	-2.6	0.0	0.0	0.0	0.0	0.0	0.0	0.0	0.0	0.0	0.0	0.0	0.0	0.0	0.0	0.0
0.0	0.0	0.0	0.0	0.0	0.0	0.2	0.0	0.4	-2.0	0.8	0.0	0.0	0.0	0.0	0.0	0.0	0.0	0.0	0.0	0.0	0.0	0.0	0.0
0.0	0.0	0.0	0.0	0.0	0.2	0.6	0.3	0.2	0.6	-3.7	1.2	0.0	0.0	0.0	0.0	0.0	0.0	0.0	0.0	0.0	0.0	0.0	0.0
0.0	0.0	0.0	0.0	0.0	0.2	0.3	0.1	0.2	0.5	1.2	-4.1	1.3	0.2	0.0	0.0	-0.1	0.0	0.0	0.0	0.0	0.0	0.0	0.0
0.0	0.0	0.0	0.0	0.0	0.2	0.1	0.1	0.2	0.0	0.2	1.0	-3.4	1.2	0.0	0.0	0.0	0.0	0.0	-0.0	0.0	0.0	0.0	0.0
0.0	0.0	0.0	0.0	0.0	0.0	0.1	0.0	0.0	0.0	0.1	0.0	0.8	-4.0	2.3	0.0	0.0	0.0	-0.1	0.0	0.0	0.0	0.0	0.0
0.0	0.0	0.0	0.0	0.0	0.0	0.0	0.0	0.0	0.0	0.0	0.0	0.0	1.2	-4.7	2.6	0.0	0.0	0.0	0.0	0.0	0.0	0.0	0.0
0.0	0.0	0.0	0.0	0.0	0.0	0.0	0.0	0.0	0.0	0.0	0.0	0.0	0.0	1.5	-8.4	5.4	0.3	0.0	0.0	0.0	0.0	0.0	0.0
0.0	0.0	0.0	0.0	0.0	0.0	0.0	0.0	0.0	0.0	0.0	0.0	0.0	0.0	0.0	1.2	-2.8	0.6	0.0	0.0	0.0	0.0	0.0	0.0
0.0	0.0	0.0	0.0	0.0	0.0	0.0	0.0	0.0	0.0	0.0	0.0	0.0	0.0	0.0	0.0	2.0	-4.1	0.0	0.0	0.0	0.0	0.0	0.0
0.0	0.0	0.0	0.0	0.0	0.0	0.0	0.0	0.0	0.0	0.0	0.0	0.0	0.0	0.0	0.7	0.4	0.4	-2.0	0.0	0.5	0.0	0.0	0.0
0.0	0.0	0.0	0.0	0.0	0.0	0.0	0.0	0.0	0.0	0.0	0.0	0.0	0.0	0.0	0.0	1.0	0.7	0.0	-3.3	0.8	0.0	0.0	0.0
0.0	0.0	0.0	0.0	0.0	0.0	0.0	0.0	0.0	0.0	0.0	0.0	0.0	0.0	0.0	0.0	0.0	0.2	0.1	0.4	-2.1	0.9	0.0	0.0
0.0	0.0	0.0	0.0	0.0	0.0	0.0	0.0	0.0	0.0	0.0	0.0	0.0	0.0	0.0	0.0	0.0	0.0	0.0	0.0	0.7	-2.2	0.5	0.3
0.0	0.0	0.0	0.0	0.0	0.0	0.0	0.0	0.0	0.0	0.0	0.0	0.0	0.0	0.0	0.0	0.0	0.0	0.0	0.0	0.0	2.3	-3.1	0.0
0.3	0.0	0.0	0.0	0.0	0.0	0.0	0.0	0.0	0.0	0.0	0.0	0.0	0.0	0.0	0.0	0.0	0.0	0.0	0.0	0.0	0.7	0.7	-2.2

Table C.5: Price elasticity matrix of the average autumn weekday

-2.5	1.0	0.0	0.0	0.0	0.0	0.0	0.0	0.0	0.0	0.0	0.0	0.0	0.0	0.0	0.0	0.0	0.0	0.0	0.0	0.0	0.0	0.0	0.8
0.4	-2.9	1.0	0.0	0.3	0.2	0.2	0.0	0.0	0.0	0.0	0.0	0.0	0.0	0.0	0.0	0.0	0.0	0.0	0.0	0.0	0.0	0.0	0.0
0.0	1.0	-4.3	0.5	0.9	1.2	0.0	0.0	0.0	0.0	0.0	0.0	0.0	0.0	0.0	0.0	0.0	0.0	0.0	0.0	0.0	0.0	0.0	0.0
0.1	0.0	0.0	-3.4	0.9	1.3	0.7	0.0	0.0	0.0	0.0	0.0	0.0	0.0	0.0	0.0	0.0	0.0	0.0	0.0	0.0	0.0	0.0	0.0
0.0	0.0	0.0	0.6	-1.6	0.5	0.5	0.0	0.0	0.0	0.0	0.0	0.0	0.0	0.0	0.0	0.0	0.0	0.0	0.0	0.0	0.0	0.0	0.0
0.0	0.0	0.0	0.9	1.1	-2.8	0.0	0.5	0.0	0.0	0.0	0.0	0.0	0.0	0.0	0.0	0.0	0.0	0.0	0.0	0.0	0.0	0.0	0.0
0.0	0.0	0.0	0.0	1.5	3.0	-11.1	0.5	0.0	0.0	0.0	0.0	0.0	0.0	0.0	0.0	0.0	0.0	0.0	0.0	0.0	0.0	0.0	0.0
0.0	0.0	0.0	0.0	0.0	0.0	1.2	-8.1	0.0	0.0	0.0	0.0	0.0	0.0	0.0	0.0	0.0	0.0	0.0	0.0	0.0	0.0	0.0	0.0
0.0	0.0	0.0	0.0	0.0	0.0	0.5	0.5	-3.1	0.0	0.0	0.0	0.0	0.0	0.0	0.0	0.0	0.0	0.0	0.0	0.0	0.0	0.0	0.0
0.0	0.0	0.0	0.0	0.0	0.0	0.2	0.0	0.4	-2.0	0.8	0.0	0.0	0.0	0.0	0.0	0.0	0.0	0.0	0.0	0.0	0.0	0.0	0.0
0.0	0.0	0.0	0.0	0.0	0.1	0.5	0.2	0.2	0.6	-3.4	1.2	0.0	0.0	0.0	0.0	0.0	0.0	0.0	0.0	0.0	0.0	0.0	0.0
0.0	0.0	0.0	0.0	0.0	0.0	0.3	0.1	0.1	0.4	1.2	-3.6	1.1	0.0	0.0	0.0	-0.1	0.0	0.0	0.0	0.0	0.0	0.0	0.0
0.0	0.0	0.0	0.0	0.0	0.0	0.0	0.1	0.2	0.0	0.2	1.0	-3.0	1.0	0.0	0.0	0.0	0.0	0.0	0.0	0.0	0.0	0.0	0.0
0.0	0.0	0.0	0.0	0.0	0.0	0.0	0.0	0.0	0.0	0.1	0.0	0.7	-3.4	1.9	0.0	0.0	0.0	-0.1	-0.1	0.0	0.0	0.0	0.0
0.0	0.0	0.0	0.0	0.0	0.0	0.0	0.0	0.0	0.0	0.0	0.0	0.0	1.1	-4.3	2.4	0.0	0.0	0.0	0.0	0.0	0.0	0.0	0.0
0.0	0.0	0.0	0.0	0.0	0.0	0.0	0.0	0.0	0.0	0.0	0.0	0.0	0.0	1.3	-8.4	5.6	0.3	0.0	0.0	0.0	0.0	0.0	0.0
0.0	0.0	0.0	0.0	0.0	0.0	0.0	0.0	0.0	0.0	0.0	0.0	0.0	0.0	0.0	1.3	-3.3	0.7	0.0	0.0	0.0	0.0	0.0	0.0
0.0	0.0	0.0	0.0	0.0	0.0	0.0	0.0	0.0	0.0	0.0	0.0	0.0	0.0	0.0	0.0	2.1	-4.3	0.0	0.0	0.0	0.0	0.0	0.0
0.0	0.0	0.0	0.0	0.0	0.0	0.0	0.0	0.0	0.0	0.0	0.0	0.0	0.0	0.0	0.8	0.3	0.4	-1.8	0.0	0.4	0.0	0.0	0.0
0.0	0.0	0.0	0.0	0.0	0.0	0.0	0.0	0.0	0.0	0.0	0.0	0.0	0.0	0.0	0.6	0.7	-0.1	-2.7	0.6	0.0	0.0	0.0	0.0
0.0	0.0	0.0	0.0	0.0	0.0	0.0	0.0	0.0	0.0	0.0	0.0	0.0	0.0	0.0	0.0	0.2	0.1	0.4	-2.3	1.1	0.0	0.0	
0.0	0.0	0.0	0.0	0.0	0.0	0.0	0.0	0.0	0.0	0.0	0.0	0.0	0.0	0.0	0.0	0.0	0.0	0.0	0.8	-2.5	0.7	0.4	
0.0	0.0	0.0	0.0	0.0	0.0	0.0	0.0	0.0	0.0	0.0	0.0	0.0	0.0	0.0	0.0	0.0	0.0	0.0	0.0	2.1	-2.9	0.0	
0.3	0.0	0.0	0.0	0.0	0.0	0.0	0.0	0.0	0.0	0.0	0.0	0.0	0.0	0.0	0.0	0.0	0.0	0.0	0.0	0.7	0.6	-2.1	

Table C.6: Price elasticity matrix of the average autumn weekend day

-3.1	1.2	0.0	0.0	0.0	0.0	0.0	0.0	0.0	0.0	0.0	0.0	0.0	0.0	0.0	0.0	0.0	0.0	0.0	0.0	0.0	0.0	0.0	0.9
0.4	-3.6	1.3	-0.0	0.6	0.2	0.0	0.0	0.0	0.0	0.0	0.0	0.0	0.0	0.0	0.0	0.0	0.0	0.0	0.0	0.0	0.0	0.4	0.0
0.0	1.1	-4.6	0.5	0.6	1.5	0.0	0.0	0.0	0.0	0.0	0.0	0.0	0.0	0.0	0.0	0.0	0.0	0.0	0.0	0.0	0.0	0.0	0.1
0.0	0.0	0.0	-2.2	0.6	0.7	0.6	0.0	0.2	0.0	0.0	0.0	0.0	0.0	0.0	0.0	0.0	0.0	0.0	0.0	0.0	0.0	0.0	0.0
0.0	0.0	0.0	0.6	-1.3	0.4	0.3	0.0	0.0	0.0	0.0	0.0	0.0	0.0	0.0	0.0	0.0	0.0	0.0	0.0	0.0	0.0	0.0	0.0
0.0	0.0	0.2	0.6	0.6	-1.9	0.0	0.3	0.0	0.0	0.0	0.0	0.0	0.0	0.0	0.0	0.0	0.0	0.0	0.0	0.0	0.0	0.0	0.0
0.0	0.0	0.0	0.3	0.6	1.2	-5.5	0.6	0.0	0.0	0.0	0.0	0.0	0.0	0.0	0.0	0.0	0.0	0.0	0.0	0.0	0.0	0.0	0.0
0.0	0.0	0.0	0.0	0.0	0.0	1.3	-8.9	0.0	1.8	0.0	0.0	0.0	0.0	0.0	0.0	0.0	0.0	0.0	0.0	0.0	0.0	0.0	0.0
0.0	0.0	0.0	0.0	0.0	0.0	0.8	0.7	-5.1	0.0	0.0	0.0	0.0	0.0	0.0	0.0	0.0	0.0	0.0	0.0	0.0	0.0	0.0	0.0
0.0	0.0	0.0	0.0	0.0	0.0	0.6	0.2	1.1	-4.8	2.2	0.0	0.0	0.0	0.0	0.0	0.0	0.0	0.0	0.0	0.0	0.0	0.0	0.0
0.0	0.0	0.0	0.0	0.0	0.0	0.7	0.6	0.4	1.4	-6.1	2.4	0.0	0.2	0.0	0.0	0.0	0.0	0.0	0.0	0.0	0.0	0.0	0.0
0.0	0.0	0.0	0.0	0.0	0.0	0.3	0.3	0.3	0.7	2.0	-5.7	2.1	0.2	0.0	0.0	-0.1	0.0	0.0	0.0	0.0	0.0	0.0	0.0
0.0	0.0	0.0	0.0	0.0	0.0	0.0	0.0	0.2	0.0	0.2	1.5	-4.2	1.7	0.0	0.0	0.0	0.0	0.0	0.0	0.0	0.0	0.0	0.0
0.0	0.0	0.0	0.0	0.0	0.0	0.0	0.0	0.0	0.0	0.1	0.0	1.2	-4.4	2.6	0.0	0.0	-0.1	0.0	0.0	0.0	0.0	0.0	0.0
0.0	0.0	0.0	0.0	0.0	0.0	0.0	0.0	0.0	0.0	0.0	0.0	0.0	1.8	-4.9	2.6	0.0	0.0	0.0	0.0	0.0	0.0	0.0	0.0
0.0	0.0	0.0	0.0	0.0	0.0	0.0	0.0	0.0	0.0	0.0	0.0	0.0	0.0	1.4	-7.2	4.0	0.6	0.0	0.0	0.0	0.0	0.0	0.0
0.0	0.0	0.0	0.0	0.0	0.0	0.0	0.0	0.0	0.0	0.0	0.0	0.0	0.0	0.0	1.1	-2.9	0.8	0.0	0.0	0.0	0.0	0.0	0.0
0.0	0.0	0.0	0.0	0.0	0.0	0.0	0.0	0.0	0.0	0.0	0.0	0.0	0.0	0.0	1.2	1.2	-4.7	0.0	0.9	0.0	0.0	0.0	0.0
0.0	0.0	0.0	0.0	0.0	0.0	0.0	0.0	0.0	0.0	0.0	0.0	0.0	0.0	0.0	1.2	0.5	0.9	-3.6	0.0	1.0	0.0	0.0	0.0
0.0	0.0	0.0	0.0	0.0	0.0	0.0	0.0	0.0	0.0	0.0	0.0	0.0	0.0	0.0	0.0	1.1	0.9	0.6	-5.8	1.9	0.0	0.0	0.0
0.0	0.0	0.0	0.0	0.0	0.0	0.0	0.0	0.0	0.0	0.0	0.0	0.0	0.0	0.0	0.0	0.0	0.3	0.2	0.6	-2.9	1.4	0.0	0.0
0.0	0.0	0.0	0.0	0.0	0.0	0.0	0.0	0.0	0.0	0.0	0.0	0.0	0.0	0.0	0.0	0.0	0.0	0.0	0.0	1.1	-2.9	0.8	0.4
0.0	0.0	0.0	0.0	0.0	0.0	0.0	0.0	0.0	0.0	0.0	0.0	0.0	0.0	0.0	0.0	0.0	0.0	0.0	0.0	0.0	3.2	-4.2	0.0
0.4	0.0	0.0	0.0	0.0	0.0	0.0	0.0	0.0	0.0	0.0	0.0	0.0	0.0	0.0	0.0	0.0	0.0	0.0	0.0	0.8	0.8	-2.4	

Table C.7: Price elasticity matrix of the average winter weekday

-2.9	1.1	0.0	0.0	0.0	0.0	0.0	0.0	0.0	0.0	0.0	0.0	0.0	0.0	0.0	0.0	0.0	0.0	0.0	0.0	0.0	0.0	0.0	1.0
0.5	-3.4	1.1	-0.0	0.6	0.1	0.0	0.0	0.0	0.0	0.0	0.0	0.0	0.0	0.0	0.0	0.0	0.0	0.0	0.0	0.0	0.0	0.0	0.4	0.0
0.0	1.2	-4.7	0.4	0.7	1.5	0.0	0.0	0.0	0.0	0.0	0.0	0.0	0.0	0.0	0.0	0.0	0.0	0.0	0.0	0.0	0.0	0.0	0.0	0.1
0.0	0.0	0.0	-2.3	0.6	0.7	0.6	0.1	0.2	0.0	0.0	0.0	0.0	0.0	0.0	0.0	0.0	0.0	0.0	0.0	0.0	0.0	0.0	0.0	0.0
0.0	0.0	0.0	0.6	-1.3	0.4	0.3	0.0	0.0	0.0	0.0	0.0	0.0	0.0	0.0	0.0	0.0	0.0	0.0	0.0	0.0	0.0	0.0	0.0	0.0
0.0	0.0	0.2	0.6	0.6	-1.9	0.0	0.4	0.0	0.0	0.0	0.0	0.0	0.0	0.0	0.0	0.0	0.0	0.0	0.0	0.0	0.0	0.0	0.0	0.0
0.0	0.0	0.0	0.4	0.5	1.2	-5.2	0.5	0.0	0.0	0.0	0.0	0.0	0.0	0.0	0.0	0.0	0.0	0.0	0.0	0.0	0.0	0.0	0.0	0.0
0.0	0.0	0.0	0.0	0.0	0.0	2.2	-14.9	0.0	0.0	0.0	0.0	0.0	0.0	0.0	0.0	0.0	0.0	0.0	0.0	0.0	0.0	0.0	0.0	0.0
0.0	0.0	0.0	0.0	0.0	0.0	1.2	0.8	-7.2	0.0	0.0	0.0	0.0	0.0	0.0	0.0	0.0	0.0	0.0	0.0	0.0	0.0	0.0	0.0	0.0
0.0	0.0	0.0	0.0	0.0	0.0	0.6	0.3	1.2	-4.7	2.2	0.0	0.0	0.0	0.0	0.0	0.0	0.0	0.0	0.0	0.0	0.0	0.0	0.0	0.0
0.0	0.0	0.0	0.0	0.0	0.0	0.6	0.6	0.4	1.4	-5.5	2.1	0.0	0.1	0.0	0.0	0.0	0.0	0.0	0.0	0.0	0.0	0.0	0.0	0.0
0.0	0.0	0.0	0.0	0.0	0.0	0.0	0.3	0.3	0.6	2.1	-5.4	2.0	0.0	0.0	0.0	0.0	0.0	0.0	0.0	0.0	0.0	0.0	0.0	0.0
0.0	0.0	0.0	0.0	0.0	0.0	0.0	0.0	0.1	0.0	0.2	1.5	-4.2	1.8	0.0	0.0	0.0	0.0	0.0	0.0	0.0	0.0	0.0	0.0	0.0
0.0	0.0	0.0	0.0	0.0	0.0	0.0	0.0	0.0	0.0	0.1	0.0	1.2	-3.9	2.2	0.0	0.0	0.0	0.0	0.0	0.0	0.0	0.0	0.0	0.0
0.0	0.0	0.0	0.0	0.0	0.0	0.0	0.0	0.0	0.0	0.0	0.0	0.0	1.6	-4.6	2.4	0.0	0.0	0.0	0.0	0.0	0.0	0.0	0.0	0.0
0.0	0.0	0.0	0.0	0.0	0.0	0.0	0.0	0.0	0.0	0.0	0.0	0.0	0.0	1.3	-7.2	4.2	0.6	0.0	0.0	0.0	0.0	0.0	0.0	0.0
0.0	0.0	0.0	0.0	0.0	0.0	0.0	0.0	0.0	0.0	0.0	0.0	0.0	0.0	0.0	1.2	-2.9	0.8	0.0	0.0	0.0	0.0	0.0	0.0	0.0
0.0	0.0	0.0	0.0	0.0	0.0	0.0	0.0	0.0	0.0	0.0	0.0	0.0	0.0	0.0	1.1	1.1	-4.6	0.0	0.8	0.0	0.0	0.0	0.0	0.0
0.0	0.0	0.0	0.0	0.0	0.0	0.0	0.0	0.0	0.0	0.0	0.0	0.0	0.0	0.0	1.1	0.0	0.8	-3.4	0.0	0.9	0.0	0.0	0.0	0.0
0.0	0.0	0.0	0.0	0.0	0.0	0.0	0.0	0.0	0.0	0.0	0.0	0.0	0.0	0.0	0.0	1.0	0.9	0.4	-5.2	1.8	0.0	0.0	0.0	0.0
0.0	0.0	0.0	0.0	0.0	0.0	0.0	0.0	0.0	0.0	0.0	0.0	0.0	0.0	0.0	0.0	0.0	0.2	0.2	0.6	-2.7	1.2	0.0	0.0	0.0
0.0	0.0	0.0	0.0	0.0	0.0	0.0	0.0	0.0	0.0	0.0	0.0	0.0	0.0	0.0	0.0	0.0	0.0	0.0	0.0	1.0	-2.7	0.9	0.4	0.0
0.0	0.0	0.0	0.0	0.0	0.0	0.0	0.0	0.0	0.0	0.0	0.0	0.0	0.0	0.0	0.0	0.0	0.0	0.0	0.0	0.0	3.0	-4.0	0.0	0.0
0.5	0.0	0.0	0.0	0.0	0.0	0.0	0.0	0.0	0.0	0.0	0.0	0.0	0.0	0.0	0.0	0.0	0.0	0.0	0.0	0.0	0.8	0.8	-2.4	0.0

Table C.8: Price elasticity matrix of the average winter weekend day

Bibliography

[1] European Climate Foundation, "Roadmap 2050: Practical guide to a prosperous, low-carbon Europe," tech. rep., ECF, 2011.

[2] COM(2011) 885/2 from the European Commission, "Energy roadmap 2050," 2011.

[3] COM(2011) 112 from the European Commission, "A roadmap for moving to a competitive low-carbon economy in 2050," 2011.

[4] Eurelectric, "Power choices: Pathways to carbon-neutral electricity in Europe by 2050," tech. rep., Eurelectric, 2011.

[5] S. Teske, J. Muth, S. Sawyer, T. Pregger, S. Simon, T. Naegler, M. O'Sullivan, S. Schmid, J. Pagenkopf, B. Frieske, *et al.*, "Energy [r]evolution: a sustainable world energy outlook," tech. rep., Greenpeace International, EREC and GWEC, 2012.

[6] F. Comaty, "Modeling and Simulation of the European Power System using Power Nodes - Assessing the Value of Flexibility for High-Share Integration of Renewable Energies in Europe," Master's thesis, ETH Zürich, 2013.

[7] Energy institute KU Leuven, "Fundamental study of a greenhouse gas emission-free energy system." GOA study at the Energy institute of KU Leuven, 2010.

[8] Edward J. Bloustein School of Planning and Public Policy, "Assessment of customer response to real time pricing," tech. rep., Rutgers - The State University of New Jersey, June 2005.

[9] J. Wang, S. Kennedy, and J. Kirtley, "A new wholesale bidding mechanism for enhanced demand response in smart grids," in *Innovative Smart Grid Technologies (ISGT), 2010*, pp. 1–8, IEEE, 2010.

[10] S. Koch, J. L. Mathieu, and D. S. Callaway, "Modeling and control of aggregated heterogeneous thermostatically controlled loads for ancillary services," in *Proc. PSCC*, pp. 1–7, 2011.

[11] M. Alizadeh, A. Scaglione, and R. J. Thomas, "From packet to power switching: Digital direct load scheduling," *IEEE Journal on Selected Areas in Communications*, vol. 30, no. 6, pp. 1027–1036, 2012.

[12] C. De Jonghe, *Short-term demand response in electricity generation planning and scheduling*. PhD thesis, KU Leuven, 2011.

[13] Global Smart Grid Federation, "Smart grids." Online: `http://www.globalsmartgridfederation.org/smart-grids/`. Accessed: 2014-06-03.

[14] European Technology Platform for Smart Grids, "What is a smart grid?." Online: `http://www.smartgrids.eu/ETPSmartGrids`. Accessed: 2014-06-03.

[15] J. Eto, "The past, present, and future of US utility demand-side management programs," tech. rep., Lawrence Berkeley National Lab., CA (United States), 1996.

[16] M. Albadi and E. El-Saadany, "Demand response in electricity markets: An overview," in *IEEE Power Engineering Society General Meeting*, vol. 2007, pp. 1–5, 2007.

[17] C. Cuijpers and B.-J. Koops, "Smart metering and privacy in Europe: Lessons from the Dutch case," in *European data protection: coming of age*, pp. 269–293, Springer, 2013.

[18] G. Strbac, "Demand side management: Benefits and challenges," *Energy Policy*, vol. 36, pp. 4419–4426, Dec. 2008.

[19] G. Barbose, C. Goldman, and B. Neenan, "A survey of utility experience with real time pricing," tech. rep., Lawrence Berkely National Laboratory, December 2004.

[20] S. Ashok and R. Banerjee, "An optimization mode for industrial load management," *IEEE Transactions on Power Systems*, vol. 16, no. 4, pp. 879–884, 2001.

[21] M. Paulus and F. Borggrefe, "The potential of demand-side management in energy-intensive industries for electricity markets in Germany," *Applied Energy*, vol. 88, pp. 432–441, Feb. 2011.

[22] B. Kirby, M. Starke, and S. Adhikari, "NYISO Industrial Load Response Opportunities : Resource and Market Assessment – Task 2 Final Report," tech. rep., Oak Ridge National Laboratory, October 2009.

[23] J. Couder and A. Verbruggen, "Uitbreiding van de tool saver-leap voor scenario-analyses voor de huishoudens," Tech. Rep. MIRA/2008/01, Universiteit Antwerpen, onderzoeksgroep STEM, 2008. Studie uitgevoerd in opdracht van MIRA, milieurapport Vlaanderen.

[24] D. Papadaskalopoulos, P. Mancarella, and G. Strbac, "Decentralized, agent-mediated participation of flexible thermal loads in electricity markets," in *16th International Conference on Intelligent System Application to Power Systems (ISAP)*, pp. 1–6, IEEE, 2011.

[25] R. De Coninck, R. Baetens, D. Saelens, A. Woyte, and L. Helsen, "Rule-based demand-side management of domestic hot water production with heat pumps in zero energy neighbourhoods," *Journal of Building Performance Simulation*, pp. 1–18, June 2013.

[26] U.S. Department of Energy, "Energy Plus Energy Simulation Software." Online: `http://www1.eere.energy.gov/buildings/about.html`. Accessed: 2014-06-03.

[27] W. Zhang, J. Lian, C.-Y. Chang, K. Kalsi, and Y. Sun, "Reduced-order modeling of aggregated thermostatic loads with demand response," *51st IEEE Conference on Decision and Control (CDC)*, pp. 5592–5597, Dec. 2012.

[28] C. Verhelst, F. Logist, J. Van Impe, and L. Helsen, "Study of the optimal control problem formulation for modulating air-to-water heat pumps connected to a residential floor heating system," *Energy and Buildings*, vol. 45, pp. 43–53, Feb. 2012.

[29] P. Bertoldi and B. Atanasiu, "Electricity consumption and efficiency trends in the enlarged European Union," tech. rep., Institute for Environment and Sustainability, 2007.

[30] R. Stamminger and G. Broil, "Synergy potential of smart appliances," tech. rep., Smart-A, 2008.

[31] P. Delaruelle, "Using Demand Flexibility in Smart Grids for Balancing Purposes," Master's thesis, KU Leuven, 2013.

[32] C. Timpe, "Smart domestic appliances supporting the system integration of renewable energy," tech. rep., Smart-A, 2009.

[33] N. Tanaka *et al.*, "Technology roadmap: Electric and plug-in hybrid electric vehicles," *International Energy Agency, Tech. Rep*, 2011.

[34] N. Leemput, J. Van Roy, F. Geth, P. Tant, B. Claessens, and J. Driesen, "Comparative Analysis of Coordination Strategies for Electric Vehicles," in *European Electric Vehicle Congress (EEVC)*, October 2011.

[35] M. D. Galus, R. La Fauci, and G. Andersson, "Investigating PHEV wind balancing capabilities using heuristics and model predictive control," in *Power and Energy Society General Meeting*, pp. 1–8, IEEE, 2010.

[36] J. Van Roy, N. Leemput, S. De Breucker, F. Geth, P. Tant, and J. Driesen, "An Availability Analysis and Energy Consumption Model for a Flemish Fleet of Electric Vehicles," in *European Electric Vehicle congress (EEVC)*, October 2011.

[37] R. A. Verzijlbergh, Z. Lukszo, E. Veldman, J. G. Slootweg, and M. Ilic, "Deriving electric vehicle charge profiles from driving statistics," *IEEE Power and Energy Society General Meeting*, pp. 1–6, July 2011.

[38] Q. Wu, A. H. Nielsen, J. Østergaard, S. T. Cha, F. Marra, Y. Chen, and C. Træholt, "Driving pattern analysis for electric vehicle (EV) grid integration study," in *Innovative Smart Grid Technologies Conference Europe (ISGT Europe)*, IEEE, 2010.

[39] N. Leemput, F. Geth, B. Claessens, J. Van Roy, R. Ponnette, and J. Driesen, "A case study of coordinated electric vehicle charging for peak shaving on a low voltage grid," in *3rd IEEE PES International Conference and Exhibition on Innovative Smart Grid Technologies (ISGT Europe)*, pp. 1–7, IEEE, 2012.

[40] W. Labeeuw, *Characterization and modelling of residential electricity demand*. PhD thesis, KU Leuven, 2013.

[41] C. Nabe and G. Papaefthymiou, "All island renewable grid study updated to include demand side management," tech. rep., Ecofys Germany GmbH, March 2009.

[42] D. Devogelaer, J. Duerinck, D. Gusbin, Y. Marenne, W. Nijs, M. Orsini, and M. Pairon, "Towards 100 % renewable energy in Belgium by 2050," tech. rep., VITO, ICEDD, Federal Planning Bureau, April 2013.

[43] M. Alizadeh, T.-H. Chang, and A. Scaglione, "On modeling and marketing the demand flexibility of deferrable loads at the wholesale level," in *46th Hawaii International Conference on System Sciences (HICSS)*, pp. 2177–2186, IEEE, 2013.

[44] A. Scaglione, "Networks and Markets for Scheduling Energy Consumption." Unpublished presentation, 2013.

[45] T. Lambert, P. Gilman, and P. Lilienthal, *Micropower System Modeling with Homer*. John Wiley and Sons, 2006.

[46] N. Lu, D. Chassin, and S. Widergren, "Modeling uncertainties in aggregated thermostatically controlled loads using a state queueing model," *IEEE Transactions on Power Systems*, vol. 20, pp. 725–733, May 2005.

[47] S. Vandael, B. Claessens, M. Hommelberg, T. Holvoet, and G. Deconinck, "A Scalable Three-Step Approach for Demand Side Management of Plug-in Hybrid Vehicles," *IEEE Transactions on Smart Grid*, vol. 4, pp. 720–728, June 2013.

[48] D. Kirschen and G. Strbac, *Fundamentals of power system economics*. Wiley, 2004.

[49] H. Aalami, M. P. Moghaddam, and G. Yousefi, "Demand response modeling considering Interruptible/Curtailable loads and capacity market programs," *Applied Energy*, vol. 87, pp. 243–250, Jan. 2010.

[50] T. N. Taylor, P. M. Schwarz, and J. E. Cochell, "24/7 hourly response to electricity real-time pricing with up to eight summers of experience," *Journal of regulatory economics*, vol. 27, no. 3, pp. 235–262, 2005.

[51] David,A.K. and Li, Y.Z., "Consumer rationality assumptions in the real-time pricing of electricity," *Generation, Transmission and Distribution IEEE Proceedings*, vol. 139, no. 4, p. 315, 1992.

[52] I. Richardson, M. Thomson, D. Infield, and A. Delahunty, "A modelling framework for the study of highly distributed power systems and demand side management," in *International Conference on Sustainable Power Generation and Supply*, pp. 1–6, April 2009.

[53] I. Richardson, M. Thomson, and D. Infield, "A high-resolution domestic building occupancy model for energy demand simulations," *Energy and Buildings*, vol. 40, pp. 1560–1566, Jan. 2008.

[54] I. Richardson, M. Thomson, D. Infield, and A. Delahunty, "Domestic lighting: A high-resolution energy demand model," *Energy and Buildings*, vol. 41, no. 7, pp. 781–789, 2009.

[55] I. Richardson, M. Thomson, D. Infield, and C. Clifford, "Domestic electricity use: A high-resolution energy demand model," *Energy and Buildings*, vol. 42, pp. 1878–1887, Oct. 2010.

[56] IEA Statistics, "Energy statistics of oecd countries," tech. rep., International Energy Agency, 2012.

[57] FOD Economie Belgium, "Structuur van de bevolking volgens huishoudens: per jaar, gewest en grootte." Online: `http://statbel.fgov.be/nl/statistieken/cijfers/bevolking/structuur/huishoudens/jaar_gewest_grootte/`. Accessed: 2014-06-03.

[58] K. Bruninx, D. Patteeuw, E. Delarue, L. Helsen, and W. D'haeseleer, "Short-term demand response of flexible electric heating systems: the need for integrated simulations," in *10th International Conference on the European Energy Market (EEM)*, pp. 1–10, IEEE, 2013.

[59] T. Van Oevelen, "Regeling van warmtepompsystemen in woningen, implementatie van modelgebaseerde predictieve regeling (in Dutch)," Master's thesis, KU Leuven, 2008.

[60] TABULA, "Residential building typology." Online: `http://www.building-typology.eu/building-typology/country/be/`. Accessed: 2014-06-03.

[61] "Meteonorm version 6.1 - edition 2009," 2009.

[62] F. A. Peuser, K.-H. Remmers, and M. Schnauss, *Solar thermal systems: Successful planning and construction.* Beuth Verlag GmbH, 2002.

[63] D. Schalck *et al.*, "Mobiliteitsrapport van Vlaanderen," tech. rep., Mobiliteitsraad van Vlaanderen, 2009.

[64] P. Frankl and S. Nowak, "Technology roadmap: solar photovoltaic energy," tech. rep., International Energy Agency, 2010.

[65] Eandis, "Belgische distributienetbeheerder." Online: `http://www.eandis.be/eandis/klant/k_lokale_productie.htm`. Accessed: 2014-06-03.

[66] ERDF, "Panorama des installations de production raccordées." `http://www.erdfdistribution.fr/panorama_des_installations_de_production`. Accessed: 2014-06-03.

[67] Belpex, "The Belgian power exchange." `http://www.belpex.be/`. Accessed: 2014-06-03.

[68] C. Verhelst, F. Logist, J. V. Impe, and L. Helsen, "Study of the optimal control problem formulation for modulating air-to-water heat pumps connected to a residential floor heating system," *Energy & Buildings*, vol. 45, pp. 43–53, 2012.

[69] VREG, "Vlaamse regulator van de elektriciteits- en gasmarkt." Online: `http://www.vreg.be/eenvoudige-aansluiting/`. Accessed: 2014-06-03.

[70] E. Veldman, *Impacts of flexibility in future residential electricity demand on distribution network utilisation*. PhD thesis, Eindhoven University of Technology, September 2013.

[71] P. Sotkiewicz and J. Vignolo, "Nodal pricing for distribution networks: efficient pricing for efficiency enhancing dg," *IEEE Transactions on Power Systems*, vol. 21, pp. 1013–1014, May 2006.

[72] D. Alaerts and J. De Turck, "Investigation and comparison of distributed algorithms for demand-side management," Master's thesis, KU Leuven, 2013.

[73] L. Fahrmeir, K. Thomas, S. Lang, and B. Marx, *Regression. Models, Methods and Applications*. Springer, 2013.

[74] M. Diehl, *Script for Numerical Optimization Course*. KU Leuven, 2012.

[75] S. Weisberg, *Applied linear regression*, vol. 528. John Wiley & Sons, 2005.

[76] "Graphpad curve fitting guide." Online: `http://www.graphpad.com/guides/prism/6/curve-fitting/index.htm?reg_approaches_to_comparing_models.htm`. Accessed: 2014-05-09.

[77] A. C. Rencher, *Methods of Multivariate Analysis*. John Wiley & Sons, 2002.

[78] Wikipedia, "Logistic function." Online: `http://en.wikipedia.org/wiki/Logistic_function`.

[79] W. L. Dunn and J. K. Shultis, *Exploring Monte Carlo Methods*. Elsevier, 2011.

[80] C. Lemieux, *Monte Carlo and Quasi-Monte Carlo Sampling*, vol. 20. Springer, 2009.

[81] "Viessmann." Online: https://www.viessmann.com/com/en/products/Gas-fired_condensing_boilers.html. Accessed: 2014-06-03.

[82] "Synergrid, de federatie van de netbeheerders elektriciteit en aardgas in België." Online: http://www.synergrid.be/index.cfm?PageID=16896&language_code=NED. Accessed: 2014-06-03.

[83] A. Faruqui and S. Sergici, "Household response to dynamic pricing of electricity: a survey of 15 experiments," *Journal of Regulatory Economics*, vol. 38, no. 2, pp. 193–225, 2010.

[84] M. Filippini, "Short- and long-run time-of-use price elasticities in Swiss residential electricity demand," *Energy Policy*, vol. 39, no. 10, pp. 5811 – 5817, 2011.

[85] Elia, "The Belgian transmission system operator." Online: http://www.elia.be/nl/grid-data. Accessed: 2014-05-26.